9.03 Formation of the Earth's Core

DC Rubie, Universität Bayreuth, Bayreuth, Germany
F Nimmo, University of California, Santa Cruz, CA, USA
HJ Melosh, Purdue University, West Lafayette, IN, USA

9.03.1 Core Formation in the Earth and Terrestrial Planets

9.03.1.1 Introduction and Present State of Cores in Solar System Bodies

The Earth's metallic core, comprising 32% of the total mass of the planet, lies beneath a silicate mantle, with the core–mantle boundary (CMB) located at a depth of 2891 km. The differentiation of the Earth into a metallic core and silicate mantle occurred during the accretion of the planet and represents the most important differentiation event in its history. Other terrestrial planets (e.g., Mercury, Venus, and Mars) and small asteroid bodies also underwent such differentiation events during the early history of the solar system and are thus important for providing additional information that helps in understanding differentiation of the Earth.

'Core formation' implies a single event, whereas in reality, the core of the Earth most likely formed through a long series of events, over an extended time period. In this chapter, we consider the period up to which the core reached roughly 99% of its present-day mass; its later evolution is considered in the chapter by Nimmo (Chapter 9.08). Other relevant chapters in this volume are concerned with the early Earth's composition by Halliday and Wood (Chapter 9.02) and the terrestrial magma ocean by Solomatov (Chapter 9.04).

Here, we first provide a general outline of the physical processes that are likely to be involved in core formation, including a discussion of the various uncertainties that arise. The second part of this chapter is focused on observations and experimental data that place constraints on the processes that operated and the state of the core during its formation.

The ultimate reason that the Earth and planets have cores is a matter of elementary physics: Because metallic iron and its alloys are denser than silicates or ices, the most stable arrangement of a rotating, self-gravitating mass of material is an oblate spheroid with the dense iron at the center. Although the physical imperative driving core formation is simple, its realization is complicated by the usual factors of contingency and history. How the cores of the terrestrial planets came to their present configuration depends on what materials were available to make them, at what time and in what condition this material was added, and then how this mass of material evolved with time.

The origin and abundance of the elements of our solar system is now understood as the consequence of (mainly) stellar nucleosynthesis. Nuclear burning in stars created the

elements and established their abundances in our solar system. Iron, as the end product of nuclear burning, owes its large abundance to its maximal nuclear stability. However, this chapter cannot go that far back. Fortunately, there are many good reviews of current ideas about the origin of the elements in our solar system (e.g., Busso et al., 1999; Turan, 1984). But we cannot entirely ignore this aspect of solar system history, because one of the major developments in the past few years follows from the contingent circumstance that the solar system formed in conjunction with one or more nearby supernovas. These catastrophic events produced a substantial abundance of the short-lived radioactive isotopes ^{60}Fe and ^{26}Al, among many others. The consequences of this accident reverberate through our present solar system in ways that are just now becoming clear.

However, before exploring the antecedents of planetary cores in detail, we first consider what is known. All of the terrestrial planets and satellites are believed to possess a dense, probably metallic, core. This belief is founded mainly on the density and moment of inertia of each body. If the average (uncompressed) density of a planet is much larger than the density of the material at its surface, one must infer that its interior is denser. A homogeneous body has a moment of inertia ratio C/MR^2 equal to 0.400. Substantially smaller values of this ratio indicate a central mass concentration, one that usually implies a change of state or composition in the interior (we here exclude the slight decrease in this ratio due to self-compression).

The size of the Earth's core is known accurately from seismic data. The limited operating lifetime of the Apollo lunar seismic array provided tentative evidence for a lunar core (Weber et al., 2011), and as yet no seismic data exist for any other solar system object. Mercury presently possesses a small magnetic field and Mars and the Moon probably had one in the past, suggesting the presence of metallic, fluid, and electrically conducting cores in these planets. Although Venus and Mars do not have magnetic fields at the present time, spacecraft measurements of their k_2 Love number indicate a large deformation in response to solar tides, implying an at least partially liquid core; observations of lunar nutations likewise suggest a liquid lunar core. Some asteroid parent bodies also apparently developed core dynamos (e.g., Fu et al., 2012; Tarduno et al., 2012). **Table 1** summarizes our present knowledge of cores in the terrestrial planets and other bodies in the solar system.

9.03.1.2 The Relevance of Iron Meteorites

During the two centuries after meteorites were first accepted as samples of other bodies in our solar system, approximately 18 000 iron meteorites have been cataloged that, on the basis of trace element groupings, appear to have originated as the cores of approximately 100 separate bodies. These iron meteorite parent bodies were small: cooling rates estimated from Fe/Ni diffusion profiles across taenite/kamacite crystal contacts suggest parent body diameters ranging from 30 to 100 km (Chabot and Haack, 2006; Wasson, 1985). Until a few years ago, it was believed that the iron meteorite parent bodies differentiated into an iron–nickel core and mantle sometime after most of the other meteorites, principally chondrites, had formed. However, dates obtained using the extinct (9 Myr half-life) ^{182}Hf–^{182}W radioactive system have demonstrated that magmatic iron meteorites actually formed about 3 Myr *before* most chondrites (Scherstén et al., 2006). This is nearly the same age as the heretofore oldest objects in the solar system, the CAIs (calcium–aluminum inclusions) found in carbonaceous chondrites. This observation has completely changed our perception of the events in the early solar system and, in particular, the nature of the planetesimals that accumulated to form the Earth and other terrestrial planets.

Table 1 Planetary and satellite cores

Body	*Mean density ($Mg\ m^{-3}$)*	*Moment of inertia factor, C/MR^2*	*Tidal Love number, k_2*	*Mean planet radius, R_p (km)*	*Core radius (km)*	*Magnetic moment, R_p^3 (T)*	*Core mechanical state*	*Composition*
Mercury	5.427	0.346[a]	?	2440	~1600	4×10^{-7}[b]	Liquid	Fe, Ni?
Venus	5.204	~0.33	~0.25	6051.8	~3200	None at present	Liquid	Fe, Ni?
Earth	5.515	0.3308	0.299	6371	3485	6.1×10^{-5}	Liquid outer, solid inner core	Fe, Ni, FeO/FeS?
Moon	3.344	0.3935	0.026[c]	1737.53	400?	None at present	Liquid?	Fe, Ni?
Mars	3.933	0.366	~0.14	3389.9	~1700	Only local sources	Liquid?	Fe, Ni, FeO/FeS?
Io[d]	3.53	0.378	?	1821	~950	None	Liquid?	Fe, Ni, FeS?
Europa[d]	2.99	0.346	?	1565	200–700	None	Liquid?	Fe, Ni, FeS?
Ganymede[d]	1.94	0.312	?	2631	650–900	7.15×10^{-7}[d]	Liquid?	Fe, Ni, FeS?
Callisto[d]	1.83	0.355?	?	2410	None?	None	–	–

[a] Margot et al. (2012).
[b] Russell and Luhmann (1997).
[c] Goossens et al. (2011).
[d] Schubert et al. (2004).
Unless otherwise noted, data are from Yoder (1995) The '?' indicates that the values are unknown.

Previous to this revision in the age of the iron meteorites, the source of the heat necessary to differentiate the iron meteorite parent bodies was obscure: Suggestions ran the gamut from electromagnetic induction in solar flares to lightning in the solar nebula. Although the short-lived radioactive isotopes ^{26}Al (half-life 0.74 Myr) and ^{60}Fe (1.5 Myr) were known to have been present in the early solar system, it was believed that, by the time that the iron meteorite parent bodies formed, these potential heat sources had burned themselves out. However, with the new ages, a new view emerges.

The effectiveness of the heating caused by the decay of a radioactive isotope of a stable element can be gauged from the following formula that gives the maximum temperature rise ΔT occurring in a completely insulated sample of material during the time subsequent to its isolation:

$$\Delta T = \frac{f C_m E_D}{c_p} \quad [1]$$

where c_p is the heat capacity of the material, C_m is the concentration of the stable element in the material, f is the fraction of radioactive isotope at the beginning of the isolation interval, and E_D is the nuclear decay energy released into heat (we do not count the energy of neutrinos emitted during beta decay). Table 2 lists the values of this temperature rise for undifferentiated material of carbonaceous chondrite composition at the time of CAI and iron meteorite formation and at the time that the bulk of the chondrites formed, 3 million years later.

The principal implication of this finding for core formation in the Earth is that many (if not most) of the planetesimals that accumulated to form the major planets possessed metallic cores at the time of their accretion. As yet, the consequences of accretional impacts among partially molten planetesimals are not well studied. However, it is clear that if the planetesimals contributing to the growth of planetary embryos had already formed iron cores, chemical equilibration between iron and silicates initially occurred in a low-pressure regime. In addition, the iron that was added to the growing embryos might not have been in the form of small, dispersed droplets, as required for efficient equilibration.

Just how the iron core of an impacting planetesimal mixes with the existing Earth's surface is presently somewhat unclear. Even the largest meteorite impacts on the present Earth seldom preserve more than a trace of the projectile. In most cases, the projectile, if it can be identified at all, is only revealed by geochemical or isotopic tracers in the rock melted by the impact. The largest intact remnant of an impactor presently known is a 25 cm diameter fragment of LL6 chondrite discovered in the melt sheet of the ca. 70 km diameter Morokweng crater (Maier et al., 2006). The impactor that created the 170 km diameter Chicxulub crater is known only from a few millimeter-sized fragments recovered from a deep-sea core (Kyte, 1998). The projectiles that created these craters are at the low end of the size spectrum we expect for planetesimals: the diameter of the Morokweng impactor was about 4 km or more, while the Chicxulub impactor was probably about 15 km in diameter. Both objects probably impacted near the average velocity for asteroidal impactors on the Earth, about 17 km s^{-1}. Although this velocity is substantially higher than the encounter velocity of the nearly formed Earth with infalling planetesimals (less than about 10 km s^{-1}, or a factor of more than three times less energy than current asteroidal impacts), it still illustrates the fact that impacts typically disrupt the impactor, and whatever the arrangement of materials might have been in the impacting objects, this arrangement is greatly distorted during the impact event.

If we can extrapolate from these observations to the impacts of much larger objects, one would conclude that it makes little difference whether the impacting planetesimal was differentiated or not – in either case, the result of the impact is a finely dispersed mixture of melted target and projectile material. On the other hand, computer simulations of the much larger Moon-forming impact show that the core of a planet-sized impactor remains mostly together in a discrete mass during the impact and appears to merge almost *en masse* with the Earth's core (Canup, 2004). In these simulations, however, each 'particle' representing the material of the Earth and projectile is about 200 km in diameter, so that it is not possible to resolve details of how the iron mass from the projectile core really interacts with the Earth's mantle and core. It thus seems possible that the cores of large planetesimals might remain intact in homogeneous masses too large for chemical equilibration (i.e., larger than a few centimeters) with their surroundings, at least at the beginning of their descent into the Earth's mantle. This is an area needing further study from the impact perspective. Later in this chapter, we discuss the probable fate of such large masses of iron in their inexorable fall toward the Earth's core.

9.03.1.3 History of Early Ideas on Core Formation

Ideas on how the Earth's core formed have shifted dramatically over the past century. At the beginning of the twentieth century, most geophysicists believed, following Lord Kelvin, that the Earth began in a completely molten state and its subsequent history was one of secular cooling and solidification (Thomson and Tait, 1883, p. 482). As late as 1952, Jeffreys

Table 2 Temperature rise of undifferentiated carbonaceous chondrites due to radioactive decay

Radioisotope	*Half-life (Myr)*	*Fractional abundance of isotope at CAI time*, f	*Nuclear decay energy*, E_D *(J kg^{-1})*	*ΔT at CAI time (K)*	*ΔT 3 Myr later (K)*
^{26}Al	0.74	$(5–7) \times 10^{-5}$	1.16×10^{13}[a]	4170	251
^{60}Fe	1.5	4.4×10^{-6}[b]	4.43×10^{12}	2960	740

[a] Schramm et al. (1970)

[b] Quitté et al. (2005). Note that the fractional ^{60}Fe abundance has recently been reestimated as 1.1×10^{-8} (Tang and Dauphas, 2012), which would make this isotope unimportant as a heat source. Assuming the solar system abundances of Anders and Grevesse (1989) and heat capacity $c_p = 1200$ J kg^{-1}K^{-1}. Abundances of Fe and Al are assumed to be chondritic, at 18.2 and 0.865 wt%, respectively (Lodders and Fegley, 1998).

found core formation totally unproblematic, because dense iron would inevitably sink through the liquid protomantle (Jeffreys, 1952, p. 271). However, about the same time, Urey (1952) was elaborating Chamberlin's (1916) hypothesis that the planets had formed from a swarm of small, cold, mutually gravitating 'planetesimals.' In Urey's analysis, core formation becomes highly problematic. The apparent difficulty posed by Urey's view initiated much of our current thinking about how the Earth's metallic iron core originated.

In his famous book *The Planets*, Urey (1952) presented a model of planet formation that strongly appealed to physicists, although, as we shall soon see, it lacked many aspects of reality. Urey approximated the growing Earth as a spherical, homogeneous, isotropic body of radius r that grew from cold matter in space by the addition of infinitesimally thin shells of thickness dr. In this model, he equated the gravitational energy of infalling matter, $-GM(r)/r$ per unit mass, where G is Newton's gravitational constant and $M(r)$ is the mass of the nascent Earth at radius r, with the heat gained after the matter accreted to the Earth. This energy was apportioned between heating of the added mass, heat conduction into the interior, and thermal radiation to space. Because the shell of added matter is very thin, thermal radiation dominates and the planet accretes at very low temperatures.

Models of this kind led Hanks and Anderson (1969) to discover that, even if the Earth accreted in as little as 1 Myr, it would not reach the melting temperature of rock anywhere in its interior. They showed that radioactive heating would only warm the Earth's interior to the melting point much later, initiating core formation as late as 1.6 Gyr after its formation.

By the 1970s, however, study of lead isotopes in ancient crustal rocks indicated that the core had formed within a few hundred million years of the iron meteorites (Gancarz and Wasserburg, 1977) and that a problem existed with the models for thermal evolution of the Earth. Safronov (1978) and Kaula (1979) independently suggested that Urey's model, in which thin shells of infalling matter radiated most of its energy to space, is too drastic. If the impacting planetesimals were of moderate size, a few kilometers or more in diameter, some substantial, but not easily computed, fraction h of the gravitational energy would be buried in the planet. Although this solution has seemed attractive for many decades, it has one central flaw: because the gravitational energy of the planet is initially rather small, the energy added by each unit of mass, $hGM(r)/r$, increases roughly as the square of the radius of the Earth. The center of the Earth thus starts out cold, although a hotter, molten, outer shell eventually develops around it. We thus end up with an Earth that is thermally inside out: cold in the center and hot on the outside.

This apparent conundrum over the initial thermal structure of the Earth led to a series of clever examinations of the stability of a shell of molten, segregated iron in the hot outer portion of the Earth. Elsasser (1963) suggested that a shell of molten iron would push its way to the Earth's center by diapiric instabilities. Later, Stevenson (1981) showed that this instability is even stronger than Elsasser suspected and that the iron would actually fracture the cold kernel of the Earth on a timescale of hours, supposing that such a global iron layer ever had time to form. Recently, more sophisticated models of this type, investigating, for example, the effects of different rheologies, have been published (Lin et al., 2009, 2011).

In our modern era, in which a much more catastrophic view of the Earth's formation reigns (Wetherill, 1985), the problematic initial thermal profile of the Earth is ameliorated by the ability of gigantic impacts to implant heat deep into a growing planet (Melosh, 1990). Deep, strong heating and core formation can be initiated by impacts themselves, given only that they are large and late enough (Tonks and Melosh, 1992). Magma oceans are now seen as an inevitable consequence of the late accretion of planet-scale protoplanets (Tonks and Melosh, 1993). In this era, the problem is not so much how cores form as how, and under what circumstances, iron and silicate may have equilibrated chemically; and how the current inventories of chemical elements in the crusts and mantles of the Earth and planets were established.

9.03.2 Physics of Core Formation

The Earth is the end product of multiple collisions between smaller protoplanets. This process of accretion results in increased temperatures and, ultimately, melting on a planetary scale. As discussed in the succeeding text, differentiation is unavoidable once melting begins; thus, the accretion process is intimately connected to the manner in which the Earth, and its precursor bodies, underwent differentiation and core formation. In this section, our theoretical understanding of the accretion process and its consequences for core formation are discussed; in **Section 9.03.3**, observational and experimental constraints on these processes are outlined.

Earlier reviews and discussions of the processes enumerated here may be found in Stevenson (1989, 1990), Rubie et al. (2003, 2011), Walter and Tronnes (2004), and Wood et al. (2006). The collection of papers edited by Canup and Righter (2000) is also highly recommended as well as the set of papers in *Philosophical Transactions of the Royal Society A (2008) 366*.

9.03.2.1 Accretion

The basic physics of planetary accretion are now reasonably well understood, although many details remain obscure (see Chambers, 2010, for a useful review). Growth of kilometer-sized objects (planetesimals) from the initial dusty, gaseous nebula must have been a rapid process (occurring within approximately 10^3 years), because otherwise the dust grains would have been lost due to gas drag. At sizes >1 km, mutual gravitational interactions between planetesimals become important. Furthermore, because the largest bodies experience the greatest gravitational focusing, they tend to grow at the expense of smaller surrounding objects. This 'runaway growth' phase, if uninterrupted, can potentially result in the development of tens to hundreds of Mars- to Moon-sized embryos in $\sim 10^5$ years at a distance of around 1 astronomical unit (AU) from the Sun (Wetherill and Stewart, 1993). However, runaway growth slows down as the initial swarm of small bodies becomes exhausted and the velocity dispersion of the remaining larger bodies increases (Kokubo and Ida, 1998). Thus, the development of Moon- to Mars-sized embryos probably took $\sim 10^6$ years at 1 AU (Weidenschilling et al., 1997) and

involved collisions both between comparably sized embryos and between embryos and smaller, leftover planetesimals. Based on astronomical observations of dust disks (Haisch et al., 2001), the dissipation of any remaining nebular gas also takes place after a few million years; the dissipation timescale of gas has implications for the orbital evolution of the bodies (e.g., Kominami et al., 2005), their volatile inventories (e.g., Porcelli et al., 2001), and their surface temperatures (e.g., Abe, 1997) and is currently a critical unknown parameter. Noble gas isotopes, in particular those of xenon, have been used to argue for a primordial, dense, radiatively opaque terrestrial atmosphere (e.g., Halliday, 2003; Porcelli et al., 2001), but this interpretation remains controversial (see **Chapter 9.02**).

A recently recognized complication in the process of terrestrial planet formation is that the orbits of the gas giants may have evolved with time, due to scattering of planetesimals. Reorganization of the architecture of the outer solar system may have profoundly affected the inner solar system. For instance, when Jupiter and Saturn encountered the 2:1 resonance, the inner planets may have experienced a potentially prolonged period of high impact flux (Bottke et al., 2012; Gomes et al., 2005). Rapid inward-then-outward migration of Jupiter (the 'Grand Tack' scenario) may have stunted the growth of Mars (Walsh et al., 2011). Gas giant migration was certainly important in the formation of many exoplanetary systems (Chambers, 2009).

Collisional growth processes lead to a peculiar size–frequency spectrum of the accumulating bodies. At first, the runaway accretional processes produce a spectrum in which the cumulative number of objects (the number of objects equal to or greater than diameter D) is proportional to an inverse power of their diameter, generally of form $N_{\rm cum}(D) \sim D^{-b}$, where b is often approximately 2 (Melosh, 1990). One of the principal characteristics of such a distribution is that, although the smallest bodies overwhelmingly dominate in number, most of the mass and energy reside in the very largest objects. Accretional impacts are thus catastrophic in the sense that objects at the largest end of the size spectrum dominate planetary growth. Later, during oligarchic growth at the planetary embryo scale, the large bodies represent an even larger fraction of the size spectrum and giant impacts, that is, impacts between bodies of comparable size, dominate planetary growth history.

The subsequent growth of Earth-sized bodies from smaller Mars-sized embryos is slow, because the embryos grow only when mutual gravitational perturbations lead to crossing orbits. Numerical simulations show that Earth-sized bodies take 10–100 Myr to develop (e.g., Agnor et al., 1999; Chambers and Wetherill, 1998; Morbidelli et al., 2000; Morishima et al., 2010; O'Brien et al., 2006; Raymond et al., 2007) and do so through a relatively small number of collisions between objects of roughly comparable sizes. A result of great importance is that geochemical observations, notably using the Hf–W isotopic system, have been used to verify the timescales obtained theoretically through computer simulations of accretion processes (see **Section 9.03.3.1**).

It should be noted that an important implicit assumption of most late-stage accretion models is that collisions result in mergers. In fact, this assumption is unlikely to be correct (Agnor and Asphaug, 2004; Asphaug, 2010; Asphaug et al., 2006) and many collisions may involve little net transfer of material, though both transient heating and transfer of angular momentum will occur. In fact, nearly 80% of the mantle of Mercury may have been *lost* by collisional erosion after core formation, thus explaining the huge size (mass fraction) of its metallic core (Benz et al., 2007). Such disruptive collisions may also have influenced the bulk chemistry of the terrestrial planets and could explain why some elements (such as Sm–Nd; Caro et al., 2008) are not present in CI chondritic ratios (O'Neill and Palme, 2008). Incorporating incomplete accretion into N-body models represents a major computational challenge, though some progress has been made (Chambers, 2008; Dwyer et al., 2015; Kokubo and Genda, 2010; Leinhardt and Richardson, 2005). Ultimately, such studies may significantly change our picture of the timescales and physical and chemical consequences of accretion.

Figure 1(a) shows a schematic example (obtained by splicing together two different accretion simulations) of how a roughly Earth-mass ($1M_e$) body might grow. Here, the initial mass distribution consists of 11 lunar-mass embryos ($\approx 0.01M_e$) and 900 smaller ($\approx 0.001M_e$) noninteracting planetesimals centered around 1 AU. The solid line shows the increase in mass, and the crosses show the impactor–target mass ratio γ (both in log units). The early stage of growth is characterized by steady collisions with small planetesimals and occasional collisions with other comparably sized embryos (e.g., at 0.068 and 1.9 Myr). Because the planetesimals do not grow, the impactor–target mass ratio γ of colliding planetesimals declines with time; embryo–embryo collisions show up clearly, having $\gamma \sim 1$. At 2 Myr, the growing object has a mass of $0.2M_e$ and roughly half of this mass has been delivered by large impacts. The late stage of growth consists entirely of large impacts, between embryos of comparable masses ($\gamma \sim 0.5$). This final stage takes place over a more extended timescale – in this case, the last significant collision occurs at 14 Myr, resulting in a final mass of $0.73M_e$.

One of the most important outstanding questions regarding this late-stage accretion is the amount of water that was delivered to the Earth. The presence of large quantities of water in the early mantle would have profound implications for the oxidation state and composition of the core (see Williams and Hemley, 2001); furthermore, a by-product would be a thick steam atmosphere, which would be sufficiently insulating to ensure a magma ocean (Matsui and Abe, 1986). Although the Earth formed inside the 'snow line,' where water ice becomes unstable, its feeding zone probably expanded over time and some of its constituent planetesimals were likely derived from greater heliocentric distances and thus contained more water. Simulations (Morbidelli et al., 2000; O'Brien et al., 2006; Raymond et al., 2007) suggest that a water-rich Earth is quite likely, but the stochastic nature of the outcomes precludes a firm conclusion. Radial mixing of planetesimals is clearly not completely efficient because of the differing oxygen isotope characteristics of Earth and Mars (e.g., Clayton and Mayeda, 1996).

9.03.2.2 Thermal Evolution

As discussed in the succeeding text in **Section 9.03.2.3**, the actual mechanisms of core formation (metal–silicate

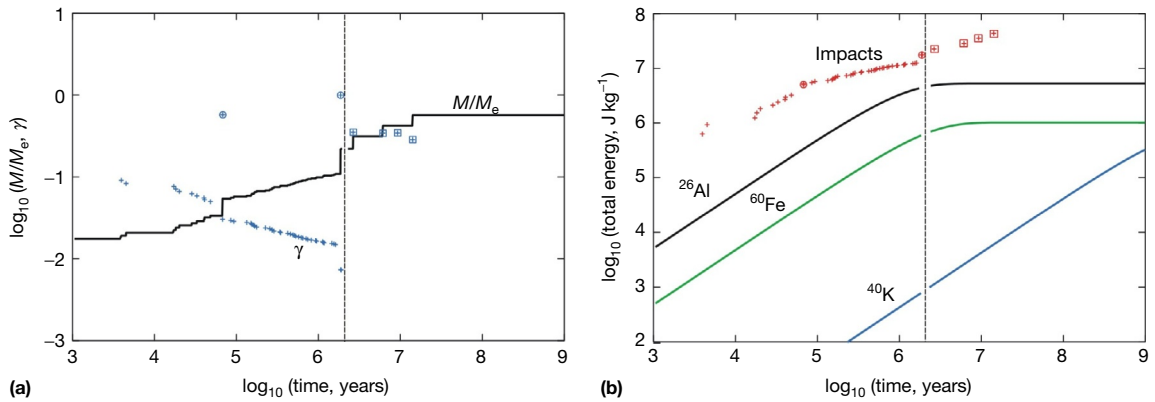

Figure 1 (a) Schematic growth of a proto-Earth, obtained by splicing two accretion simulations together. Early growth is from Agnor (unpublished) where the initial mass distribution consists of 11 embryos ($\approx 0.01 M_e$) and 900 noninteracting planetesimals ($\approx 0.001 M_e$) centered around 1 AU. Late growth is from particle 12 in run 3 of Agnor et al. (1999). The vertical dashed line denotes the splicing time. The solid line shows the mass evolution of the body, and the crosses denote the impactor–target mass ratio γ. Circles denote embryo–embryo collisions; squares denote late-stage giant impacts. The general reduction in γ prior to 2 Myr is a result of the fact that the planetesimals cannot merge with each other, but only with embryos. (b) Corresponding energy production (J kg^{-1}). The cumulative energy due to impacts (crosses) is calculated using eqn [2] for each impact. The solid lines show the cumulative energy associated with the decay of radioactive elements ^{26}Al, ^{60}Fe, and ^{40}K. Half-lives are 0.73 Myr, 1.5 Myr, and 1.25 Gyr, respectively; initial bulk concentrations are 5×10^{-7}, 2×10^{-7}, and 4.5×10^{-7}, respectively (Ghosh and McSween, 1998; Tachibana et al., 2006; Turcotte and Schubert, 2002).

separation) that operate are dependent on the thermal state of a planetary body and at least some degree of partial melting is required. However, in addition to understanding the thermal state of the Earth during core formation, it is also important to understand the thermal histories of small bodies (planetesimals and asteroids) because these determine whether or not the material that accreted to form the Earth had already undergone core–mantle differentiation.

There are three main sources of energy that can produce the melting that is required for core formation. Firstly, the decay of short-lived radioactive nuclides (^{26}Al and ^{60}Fe) is an important source of energy when accretion occurs very soon after the formation of the solar system (**Figure 1(b)**). (These isotopes have half-lives of 0.73×10^6 and 1.5×10^6 years, respectively.) Secondly, the kinetic energy delivered by impacts can be sufficient to generate local or global melting especially during the late stages of Earth accretion (**Figures 1(b)** and **3**). Finally, as discussed in the succeeding text, the process of differentiation itself, by reducing the gravitational potential energy of the body, also releases heat and may lead to runaway differentiation.

9.03.2.2.1 Decay of radioactive nuclides

Thermal models show that the decay of ^{26}Al and ^{60}Fe in a body with a minimum radius of 30 km can result in maximum temperatures that range from below the Fe–FeS eutectic temperature to above silicate melting temperatures, depending on the initial concentrations of these isotopes (**Figure 2**). In contrast, the energy released through collisions between bodies less than a few hundred km radius is insufficient to cause global melting (Keil et al., 1997; see also **Section 9.03.2.2.2**). This means that the melting required for core–mantle differentiation in a small body could only occur at a very early stage during the history of the solar system – for example, within the first 1 Myr (Baker et al., 2005). In support of the thermal models, there is geochemical evidence for large-scale melting

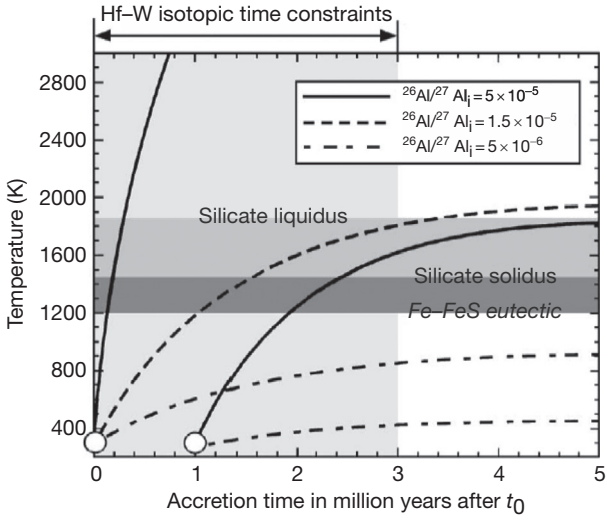

Figure 2 Models of the thermal evolution of a small body (>30 km radius) as a function of the initial concentration of ^{26}Al. Temperature is calculated as a function of time after the start of the solar system (t_0). Depending on the concentrations of ^{26}Al and ^{60}Fe and when accretion starts, maximum temperatures range from below the Fe–FeS eutectic to above the silicate solidus (see also Yoshino et al., 2003, **Figure 2**). Reproduced from Walter MJ and Tronnes RG (2004). Early Earth differentiation. *Earth and Planetary Science Letters* 225: 253–269.

and magma ocean formation on at least some small bodies (Greenwood et al., 2005). In addition, the parent body of the HED meteorites (which is likely asteroid 4 Vesta, 530 km in diameter) underwent early core–mantle differentiation. These considerations support the view that planetesimals that accreted to form the Earth were already differentiated (e.g., Taylor and Norman, 1990). However, if small bodies accreted somewhat later, melting and differentiation may not have occurred because the concentrations of ^{26}Al and ^{60}Fe would

have been too low (Figure 2). The density of the solar nebula must have decreased with increasing distance from the Sun (e.g., Figure 1 in Elser et al., 2012). Because the rate of a body's accretion depends on the density of the solar nebula, bodies in the outer regions would have accreted slower and therefore later than those close to the Sun (Grimm and McSween, 1993). Thus, not all planetesimals would have differentiated. Ceres is an example of an asteroid that may not have differentiated to form a metallic core (Thomas et al., 2005). It is therefore currently not clear whether the Earth accreted from only differentiated bodies or a mixture of differentiated and undifferentiated bodies. The answer depends on the extent of the Earth's feeding zone during accretion.

9.03.2.2.2 Heating due to the energy of impacts

Figure 1(a) shows that the bulk of late-stage Earth accretion involves large impacts well-separated in time. The energetic consequences of such impacts have been discussed elsewhere (Benz and Cameron, 1990; Melosh, 1990; Tonks and Melosh, 1993) and strongly suggest that, even in the absence of a thick primordial (insulating) atmosphere, the final stages of Earth's growth must have involved of one or more deep global magma oceans. This conclusion has important implications for the mode of core formation and may be understood using the following simple analysis.

For an impact between a target of mass M and an impactor of mass γM, the mean change in energy per unit mass of the merged object due to kinetic and gravitational potential energy is

$$\Delta E = \frac{1}{1+\gamma}\left[-\frac{3}{5}\left(\frac{4\pi\rho}{3}\right)^{1/3} GM^{2/3}\left(1+\gamma^{5/3}-(1+\gamma)^{5/3}\right)+\frac{1}{2}\gamma V_\infty^2\right] \quad [2]$$

Here, ρ is the mean density of the merged object, G is the universal gravitational constant, V_∞ is the velocity of the impactor at a large distance from the target, and the factor of 3/5 comes from considering the binding energy of the bodies (assumed uniform) prior to and after the collision. Neglecting V_∞ and taking γ to be small, the global average temperature rise associated with one such impact is given by

$$\Delta T \approx 6000K\left(\frac{\gamma}{0.1}\right)\left(\frac{M}{M_e}\right)^{2/3} \quad [3]$$

where we have assumed that $\rho = 5000\ \mathrm{kg\ m^{-3}}$ and a heat capacity of 1 kJ $\mathrm{kg^{-1}\ K^{-1}}$. Note that this temperature change is a globally averaged value; for small impacts in particular, real temperatures will vary significantly with distance from the impact site.

Equation [2] is based on several simplifying assumptions. It assumes that the energy is deposited uniformly, which is unlikely to be correct. More importantly, it assumes that all the kinetic energy is converted into heat and retained. Such an assumption is unlikely to be correct for small impacts, where most of the energy is deposited at shallow depths where it can be radiated back to space (Stevenson, 1989). For larger impacts, however, the energy will be deposited at greater depths, and thus, the only major energy loss mechanism is the ejection of hot material. The amount and temperature of material ejected depend strongly on the geometry of the impact but are in general rather small compared to the target mass (Canup et al., 2001). Since we are primarily concerned with large impacts ($\gamma > 0.1$), the assumption that the majority of the energy is retained as heat energy is a reasonable one. Thus, impactors with a size similar to the one that is believed to have formed the Moon (Cameron, 2000; Canup and Asphaug, 2001) probably resulted in the bulk of the Earth being melted.

Although a Mars-sized ($0.1M_e$) proto-Earth has a smaller mass, it experiences collisions with bodies comparable in size to itself ($\gamma \approx 1$, see Figure 1) In this case, eqn [2] shows that $\Delta T \approx 4500\ K$. Thus, it seems likely that Mars-sized embryos were also molten and thus differentiated. Although there is currently little direct evidence for an ancient Martian magma ocean (see Elkins-Tanton et al., 2003), Debaille et al. (2007), Blichert-Toft et al. (1999), and Borg and Draper (2003) have used Sm–Nd, Lu–Hf, and incompatible element abundances, respectively, to argue for such an ocean. Dauphas and Pourmand (2011) used Hf–W data to argue for a very early formation time for Mars, in which case global melting due to ^{26}Al would have resulted; however, their results are based on assumptions concerning core–mantle reequilibration which may not be correct (see succeeding text).

In considering the thermal effects of impacts, we can consider the cumulative energy delivered in comparison with other sources of energy. Figure 1(b) shows the cumulative impact energy in joule per kilogram. The bulk of the energy is delivered by the few largest impacts, as expected. For comparison, the radioactive heat production due to one long-lived (^{40}K) and two short-lived isotopes (^{26}Al and ^{60}Fe) is shown. Long-lived isotopes have no effect at all on the thermal evolution of the Earth over its first 100 Myr. The total energy associated with ^{26}Al depends very strongly on the accretion time (Figure 2) and in this case is roughly one order of magnitude smaller than that due to the impacts. Figure 1(b) shows that the thermal evolution of the Earth naturally divides into two stages: the early stage (up to ~100 Myr) when heating due to impacts and short-lived isotopes dominate and the later stage when long-lived isotopes and secular cooling are important.

Figure 3 summarizes the expected mean global temperature change due to impacts and short-lived radionuclides as a function of planetary size. The effect of a single impact (solid lines) is calculated using eqn [2] and demonstrates the strong dependence on both the body mass and the impactor–target mass ratio γ. It should be reemphasized that, particularly for small impacts, the energy will not be distributed evenly and that the calculated temperature rise is only a mean global value. The effect of ^{26}Al decay (dashed lines) does not depend on the body mass, but only on the accretion time relative to CAI formation. For small bodies, only radioactive decay contributes substantially to warming; for large bodies, gravitational energy release will tend to dominate. Figure 3 also emphasizes that the population of impactors a growing planet encounters has a very important effect on its ultimate temperature structure. If all the impactors are small ($\gamma \ll 1$), then the temperature changes are quite modest. Conversely, the later stages of planetary accretion ensure that growing bodies will encounter other bodies of similar size (i.e., $\gamma \sim 1$; Section 9.03.2.1), and thus, melting is expected for bodies of roughly Moon size and larger.

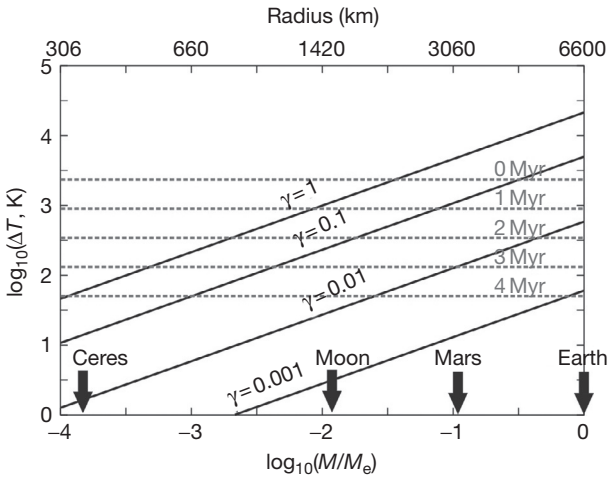

Figure 3 Mean global temperature change ΔT as a function of planetary mass (in units M_e = one Earth mass). Solid lines show gravitational energy due to a single collision where y denotes the impactor–target mass ratio and ΔT is calculated from eqn [2] assuming that $V_\infty = 0$, $C_p = 1000$ J kg^{-1} K^{-1}, and $\rho = 5000$ kg m^{-3}. Dashed lines show temperature change due to ^{26}Al decay as a function of (instantaneous) planet formation time (in Myr) after solar system formation. Total energy release by ^{26}Al is 6.2×10^6 J kg^{-1} (assuming 1 wt% Al and a fractional abundance of ^{26}Al of 5×10^{-5}) and half-life is 0.73 Myr. Planetary melting is expected to be widespread for $\Delta T > 1000$ K.

Although the average temperature jumps in large planets struck by comparably sized objects are impressive, it must be kept in mind that these are averages only. Impacts are not good at homogenizing temperatures. An impact initially deposits a large fraction of its kinetic energy in a region comparable in size to the projectile itself. Shortly after a time measured by D/v_i the projectile diameter D divided by its impact velocity v_i, the shock waves generated by the impact expand away from the impact site, accelerating the target material and depositing heat as they spread out and weaken. The heat is therefore mostly deposited in a region called the 'isobaric core' whose shape is initially approximately that of an immersed sphere tangent to the surface of the target. Outside of this region, the shock pressure, and therefore the amount of heat deposited, falls off rapidly, generally as more than the cube of the distance from the impact (Pierazzo et al., 1997). A velocity field that is established by the spreading shock wave accompanies this heat deposition. The moving material generally opens a crater whose size and form depend on the relative importance of gravity and strength in the crater excavation. In general, about half of the hot, isobaric core is ejected from the impact site, to spread out beyond the crater rim, while the other half remains in the distorted target beneath the crater floor (i.e., for impacts that do not vaporize a large volume of the target, which is the case for all accretional impacts on Earth-sized planets). The major part of the kinetic energy of the impact is thus converted to heat in a roughly hemispheric region centered on the crater. This hot zone extends to a depth of only a few projectile diameters.

For small impacts, generally those of objects less than a kilometer in diameter, the heat is deposited so close to the surface that a major fraction is radiated to space before the next similar-sized impact occurs (Melosh, 1990). Larger impactors deposit more of their energy deeper in the planet, up to the truly gigantic impacts of objects comparable in size to the growing Earth, which may deposit their energy over an entire hemisphere. Nevertheless, detailed computations show that this energy is not homogeneously distributed over the target Earth. Later processes, such as the reimpact of large fractions of the projectile (seen in some of the Moon-forming scenarios: Canup, 2004) or thermal convection of the mantle driven by a suddenly heated core, are needed to homogenize the heat input. Impact heating is thus characterized by large initial temperature variations: The part of the Earth near the impact site becomes intensely hot, while more distant regions remain cold. Averages, therefore, tell only a small part of the overall story: The aftermath of heating by a large impact is characterized by strong temperature gradients, and the evolution of the planet may be dominated by contrasts between very hot and cold, mostly unaffected, portions of the growing Earth.

9.03.2.2.3 Heating through the reduction of gravitational potential energy

Although the energies involved in late-stage impacts imply the formation of at least a regional magma ocean, such an ocean may not reach the CMB, because the solidus temperature of mantle material increases as a function of pressure (see **Figure 9(b)**). The mechanical properties of the magma ocean, which control the rate of iron transport through the ocean, change dramatically when the melt fraction drops below ≈60% (Solomatov, 2000; see also **Chapter 9.04**). The effective base of the magma ocean occurs at this rheological transition. Descending iron droplets will tend to pond at this interface. However, the resulting iron layer is still denser than the underlying (mantle) material and will therefore tend to undergo further transport toward the center of the planet. The transport mechanism might be percolation through a partially molten mantle or the motion of larger iron bodies via brittle fractures (diking) or through a viscously deformable mantle (diapirism). These different mechanisms are discussed in Stevenson (1990) and will be addressed in more detail in the succeeding text (**Section 9.03.2.3**).

The redistribution of mass involved with the descent of iron toward the center of the planet results in a release of gravitational energy. Because the gravitational energy change only depends on the initial and final density distributions, the mechanism by which the iron is transported is of only secondary importance. The extent to which the iron, rather than the surrounding mantle material, is heated depends on the rate of transport and relative viscosities of the iron and silicates (Golabek et al., 2008; Monteux et al., 2009; Samuel et al., 2010), but the total energy released would be the same. The magnitude of the heating can be large and may be calculated as follows.

Consider a uniform, thin layer of iron at the base of the magma ocean, overlying a mantle and core. The top and bottom of the iron layer and the underlying core are at radii R_o, $R_m = (1-\varepsilon) R_o$, and $R_c = \beta R_o$, respectively, where ε is a measure of the thickness of the iron layer ($\varepsilon \ll 1$) and β is a measure of the initial core radius. After the removal of iron to the center, whether by diapirism, diking, or percolation, the core will have grown and the new configuration will have a lower potential

energy. The difference in potential energy may be calculated and used to infer the mean temperature change in the final core, assuming that all the potential energy is converted to core heat (e.g., Solomon, 1979). For the specific case of a constant core density twice that of the mantle density, it may be shown that the mean temperature change of the entire postimpact core is given by

$$\Delta T = \frac{\pi G \rho_c R_o^2}{\beta^2 C_p \left(1 + 3\varepsilon\beta^{-2}\right)} \left[\frac{1}{10}\beta^5 \left(\left(1 + 3\varepsilon\beta^{-3}\right)^{5/3} - 1\right) + \frac{1}{2}\varepsilon - \beta^3\varepsilon\right] \quad [4]$$

Here, C_p is the core-specific heat capacity and ρ_c is the core density, and it is assumed that the core is well mixed (isothermal). As before, the temperature change is a strong function of planetary size, specifically the radial distance to the base of the magma ocean R_o. The temperature change also depends on ε, which controls the mass of iron being delivered to the core, and the initial core radius R_c when $\beta > 0$. The temperature change goes to zero when $\beta = 1$, as expected, while when $\beta = 0$ (i.e., no initial core), the temperature change is essentially independent of the mass of iron delivered. For Earth-sized planets, the addition of iron to the core by individual impacts can lead to core temperature increases of several hundred to a few thousand kelvin. However, this temperature change is generally small compared to that induced by the impact itself, though it may have important effects, for example, regarding the generation of early core dynamos.

For example, consider two cases, appropriate to the Moon-forming impact (Canup and Asphaug, 2001): a $0.9M_e$ planet hit by a $0.1M_e$ impactor and a $0.8M_e$ planet hit by a $0.2M_e$ impactor, all bodies having a core of density 10^4 kg m^{-3} and radius half the body radius. For magma oceans of depths 500 and 1000 km, respectively ($R_o = 5900$ and 5400 km), we obtain $\varepsilon = 0.0054$ and 0.0139 and $\beta = 0.52$ and 0.55. The core adiabat is roughly 1 K km^{-1}, giving temperature increases of 2400 and 1900 K. The further increases from gravitational heating (eqn [4]) are 1250 and 2000 K, respectively. Thus, the postimpact core temperature is likely to have increased by 3500–4000 K from the temperature it attained at the base of the magma ocean. Because the base of the magma ocean is estimated to be in the range 2500–4000 K (**Section 9.03.3.2**), the initial core temperature was probably at least 6000 K, sufficient to cause substantial lower-mantle melting.

This estimate is only approximate, because of the assumptions made (e.g., no transfer of heat to the mantle) and the fact that the Earth probably suffered several comparably sized impacts. However, the result is important because the initial temperature contrast between the core and the lowermost mantle determines the initial CMB heat flux and thus the ability of the core to generate a dynamo (see **Chapter 9.08**).

9.03.2.3 Differentiation Mechanisms

Crucial questions are as follows: at what stage during the accretion history did core–mantle differentiation actually occur and how long did the process take? These questions depend on the thermal history of the accreting body, which, in turn, determines the physical mechanisms by which metal and silicate separate. The physics of differentiation have been reviewed by Stevenson (1990) and Rushmer et al. (2000), and here we provide an updated account. Differentiation occurs because of the large density contrast between silicates and metal, but the rate at which it occurs depends on the length scales and properties of the phases involved. Considering the current size of the Earth, the segregation process involved the transport of metal through the protomantle over length scales of up to almost 3000 km. As reviewed by Stevenson (1990), the process involved the transport of liquid metal through either solid (crystalline) silicates or partially or fully molten silicate (i.e., in a magma ocean). The former mechanism is possible because iron (plus alloying elements) has a lower melting temperature than mantle silicates, so that liquid iron can coexist with solid silicates. In contrast, the separation of solid metal from solid silicate is too sluggish to have been a significant process during core formation (Stevenson, 1990). Identifying whether metal separated from solid or molten silicates during core formation clearly provides information about the early thermal state of the planet. In addition, the separation mechanism may have affected the conditions and extent of chemical equilibration between metal and silicate and therefore affects mantle geochemistry, as discussed further in the succeeding text. Here, we review results pertaining to core formation by (a) grain-scale percolation of liquid metal through crystalline silicates, (b) separation of molten metal from molten silicate in a magma ocean, and (c) descent of large (km-scale) diapirs of molten metal though crystalline silicate.

As discussed in the preceding text, it seems likely that the final stages of Earth's accretion involved large impacts between previously differentiated objects that were at least partly molten. What happens in detail during these impacts is poorly understood. Hydrocode simulations of impacts (Cameron, 2000; Canup and Asphaug, 2001) show that the cores of the target and impactor merge rapidly, within a few free-fall timescales (hours), although a small fraction (typically less than 1%) of core material may be spun out into a disk. Unfortunately, the resolution of these simulations is on the order of 100 km, while the extent to which chemical reequilibration occurs depends on length scales that are probably on the order of centimeters (Stevenson, 1990). Another approach to understanding this important question is presented in the succeeding text in **Section 9.03.2.3.2**.

9.03.2.3.1 Percolation

Liquid metal can percolate through a matrix of polycrystalline silicates by porous flow provided the liquid is interconnected and does not form isolated pockets (Rushmer et al., 2000; Stevenson, 1990). The theory is well developed for the ideal case of a monomineralic system consisting of crystals with isotropic surface energy (i.e., no dependence on crystallographic orientation). Whether the liquid is interconnected depends on the value of the wetting or dihedral angle (θ) between two solid–liquid boundaries that are intersected at a triple junction by a solid–solid boundary (**Figure 4**) (Stevenson, 1990; von Bargen and Waff, 1986). For $\theta < 60°$, the liquid is fully interconnected and can percolate through the solid irrespective of its volume fraction; under such conditions, complete metal–silicate segregation can occur efficiently by porous flow. In the case that $\theta > 60°$, the liquid forms isolated

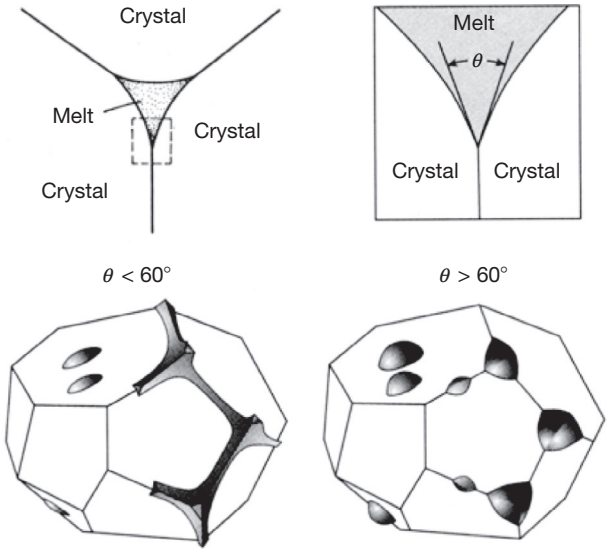

Figure 4 Relation between melt connectivity and dihedral angle in a polycrystalline aggregate containing a small amount of dispersed melt. The dihedral angle is defined in the top diagrams, and the dependence of melt connectivity on the dihedral angle is shown in the lower diagrams. Note that an ideal case is shown here in which the crystals have an isotropic surface energy. Reproduced from Stevenson DJ (1990) Fluid dynamics of core formation. In: Newsom HE and Jones JH (eds.) *Origin of the Earth*. Oxford: Oxford University Press.

pockets when the melt fraction is low and connectivity exists only when the melt fraction exceeds a critical value. This critical melt fraction is known as the connection boundary and ranges from 0% to 6% for dihedral angles in the range 60–85°. If the melt fraction lies above the connection boundary, the melt is interconnected and can percolate. However, as the melt fraction decreases due to percolation, a pinch-off melt fraction is reached below which interconnectivity is broken. At this point, the remaining melt is stranded in the crystalline matrix. The pinch-off melt fraction lies slightly below the connection boundary and ranges from 0% to 4.5% for dihedral angles in the range 60–85°. The dependence of the pinch-off boundary on dihedral angle has been formulated theoretically as 0.009 $(\theta - 60)^{0.5}$ for values of θ in the range 60–100° (von Bargen and Waff, 1986). Yoshino et al. (2003) have shown, through electrical conductivity measurements, that the percolation threshold for Fe–S melt in an olivine matrix is approximately 5 vol.%. This result suggests that core formation could have occurred by percolation under hydrostatic conditions (see succeeding text), but ~5 vol.% metal would have been stranded in the mantle. In fact, 5 vol.% may be a lower bound on the amount of stranded metal because the percolation threshold theory was developed assuming that the liquid is uniformly and finely dispersed throughout the crystalline matrix (von Bargen and Waff, 1986). However, due to the minimization of surface energy, textures might evolve over long time periods (relative to normal experimental timescales of hours to days) such that the liquid becomes concentrated in pools that are widely dispersed and relatively large, in which case the percolation threshold could be much greater than 5 vol.% (Bagdassarov et al., 2009a,b; Stevenson, 1990; Walte et al., 2007).

The effects of crystal anisotropy and crystal faceting are not taken into account by the aforementioned theory (which is based on surface energies being isotropic). It has been argued that the effects of crystal anisotropy and crystal faceting reduce permeability (Faul, 1997; Laporte and Watson, 1995; Yoshino et al., 2006); however, there is no experimental evidence to suggest that such effects are significant for liquid metal–silicate systems relevant to core formation.

The dihedral angle θ depends on the energies of the respective interfaces that intersect at a triple junction that is occupied by a melt pocket (**Figure 4**):

$$\theta = 2\cos^{-1}\left(\frac{\gamma_{ss}}{2\gamma_{sl}}\right) \quad [5]$$

where γ_{sl} is the solid–liquid interfacial energy and γ_{ss} is the solid–solid interfacial energy. Note that, as emphasized previously, this expression is based on the assumption that interfacial energies are independent of crystal orientation and that stress is hydrostatic. When considering metal–silicate systems that are applicable to core formation, the interfacial energies, and therefore the dihedral angle, can be affected by (a) the structure and composition of the crystalline phase, (b) the structure and composition of the liquid metal alloy, and (c) temperature and pressure. Dihedral angles in metal–silicate systems relevant to core formation and the effects of the aforementioned variables have been investigated experimentally (Ballhaus and Ellis, 1996; Gaetani and Grove, 1999; Holzheid et al., 2000a; Minarik et al., 1996; Rose and Brenan, 2001; Shannon and Agee, 1996, 1998; Takafuji et al., 2005; Terasaki et al., 2005, 2007, 2008). These studies, performed on a range of different starting materials at pressure–temperature conditions up to those of the lower mantle, now enable the most important factors that control dihedral angles in metal–silicate systems to be identified.

The effects of pressure, temperature, and the nature of the silicate crystalline phase appear to be relatively unimportant, at least up to ~23 GPa. For example, through experiments on the Homestead meteorite, Shannon and Agee (1996) found that dihedral angles have an average value of 108° and remain essentially constant over the pressure range 2–20 GPa, irrespective of the dominant silicate mineral (e.g., olivine or ringwoodite). However, their subsequent study of the Homestead meteorite under lower-mantle conditions (25 GPa) suggests that dihedral angles decrease to ~71° when silicate perovskite is the dominant silicate phase (Shannon and Agee, 1998). Since this angle is still in excess of 60°, efficient metal segregation from crystalline perovskite under lower-mantle pressures is not possible (see also Terasaki et al., 2007).

The most important parameter controlling dihedral angles is evidently the anion (oxygen and/or sulfur) content of the liquid metal phase. The reason is that dissolved O and S act as 'surface-active' elements in the metallic melt and thus reduce the solid–liquid interfacial energy (e.g., Iida and Guthrie, 1988). Dissolved oxygen, in particular, makes the structure of the metal more compatible with that of the adjacent silicate, thus reducing the interfacial energy and promoting wetting.

Rushmer et al. (2000, their Figure 4) showed that dihedral angles decrease from 100–125° to 50–60° as the anion-to-cation ratio, defined as $(O+S)/(Fe+Ni+Co+Mn+Cr)$, increases from ~0.3 to ~1.2. Based on their data compilation,

only metallic melts with the highest contents of O and S are wetting ($\theta < 60°$). The effects of the anion content of the metallic liquid have been investigated systematically in the stability fields of olivine and ringwoodite by Terasaki et al. (2005) through a study of dihedral angles in the system Fe–S–$(Mg,Fe)_2SiO_4$ in the pressure range 2–20 GPa. By varying the FeO content of the silicate phase (Fe# = FeO/(FeO + MgO) = 0.01–0.44), the oxygen fugacity, which controls the O content of the metal, could be varied over a wide range. They confirmed the importance of the anion content of the liquid phase and showed that the effect of dissolved oxygen is greater than that of dissolved S (**Figure 5**). Because the oxygen content of the metallic liquid decreases with pressure up to 10–15 GPa (Asahara et al., 2007; Frost et al., 2010; Rubie et al., 2004), dihedral angles increase with increasing pressure in this range. Terasaki et al. (2008) showed that for metallic liquids with a high O + S content, dihedral angles lie below 60° at pressures below 2–3 GPa, depending on the FeO content of the silicate phase. Percolation could therefore contribute significantly to core formation in planetesimals during the early stages of heating before the temperatures reach the silicate solidus.

Based on a study of liquid Fe + silicate perovskite at 24–47 GPa and 2400–3000 K, Takafuji et al. (2004) have suggested that dihedral angles decrease to ~51° under deep mantle conditions. This result may be consistent with results that show that the solubility of oxygen in liquid Fe increases strongly with temperature and weakly with pressure above 10–15 GPa (Asahara et al., 2007; Frost et al., 2010). However, the study of Takafuji et al. (2004) was performed using a laser-heated diamond anvil cell (LH-DAC), in which samples are exceedingly small and temperature gradients are very high. Furthermore, dihedral angles had to be measured using transmission electron microscopy – a technique that is far from ideal for obtaining good statistics. This preliminary result therefore awaits confirmation from further studies. In addition, in a study of wetting in a similar system at the lower pressures of 25 GPa, Terasaki et al. (2007) found that the dihedral angle increases with the $FeSiO_3$ component of silicate perovskite but failed to find any obvious correlation with the oxygen content of the metal liquid.

In summary, experimental results for systems under hydrostatic stress show that dihedral angles significantly exceed the critical angle of 60° at pressures of 3–25 GPa in chemical systems that are relevant for core formation in terrestrial planets. This means that, for percolation under static conditions, at least several vol% metal would have been stranded in the mantle – which is inconsistent with the current concentration of siderophile elements in the mantle (see **Section 9.03.3.2**). Efficient percolation can occur at low pressures (<3 GPa) when the S and O contents of the metal are very high (i.e., close to the Fe–S eutectic), but such conditions are not applicable to core formation in a large planet such as the Earth. There is a preliminary indication that efficient percolation ($\theta < 60°$) may be a feasible mechanism under deep lower-mantle conditions, but this result awaits confirmation.

When dihedral angles significantly exceed 60°, experimental evidence suggests that liquid metal can separate from crystalline silicates when the material is undergoing shear deformation due to nonhydrostatic stress (Bruhn et al., 2000; Groebner and Kohlstedt, 2006; Hustoft and Kohlstedt, 2006; Rushmer et al., 2000). The most recent results indicate that ~1 vol.% liquid metal remains stranded in the silicate matrix so that reasonably efficient percolation of liquid metal, with percolation velocities on the order of 150 km year^{-1}, might occur in crystalline mantle that is undergoing solid-state convection (Hustoft and Kohlstedt, 2006). There

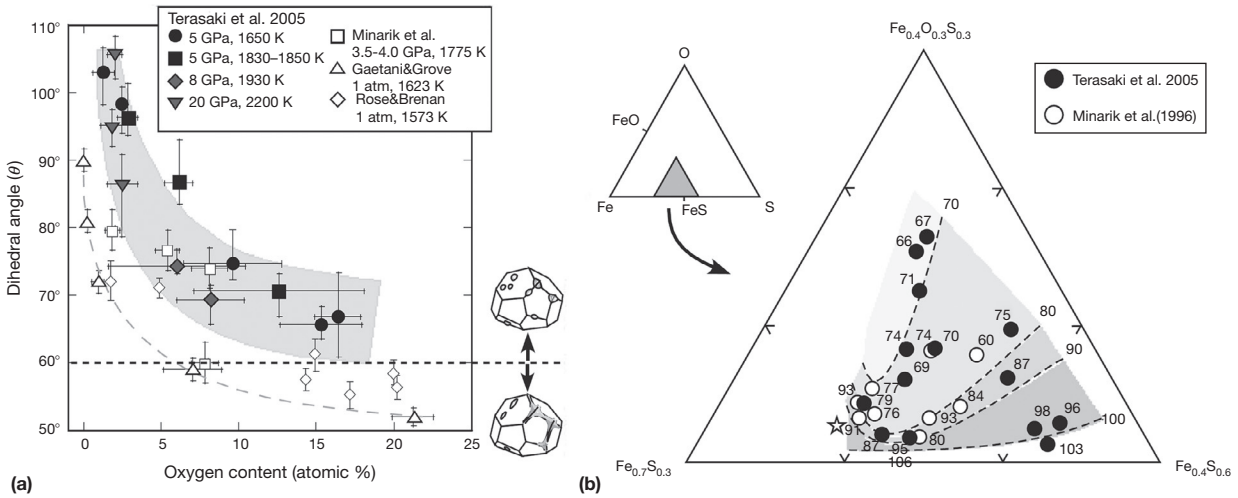

Figure 5 Dihedral angles in aggregates of olivine (≤8 GPa) and ringwoodite (20 GPa) containing several vol.% Fe–FeS melt as a function of the melt composition. (a) Dihedral angle as a function of the oxygen content of the Fe-alloy liquid. As the oxygen content increases, the structures of the silicate and liquid Fe alloy become more similar with the result that both the interfacial energy and the dihedral angle decrease. (b) Effects of O and S contents of the Fe-alloy liquid on dihedral angles. The data points are plotted on a triangular section of the Fe–O–S system, and each data point is labeled with the dihedral angle. The dashed lines are contours of constant dihedral angle. These results suggest that the effect of dissolved O on the dihedral angle is greater than that of dissolved S. Reproduced from Terasaki H, Frost DJ, Rubie DC, and Langenhorst F (2005) The effect of oxygen and sulphur on the dihedral angle between Fe–O–S melt and silicate minerals at high pressure: Implications for Martian core formation. *Earth and Planetary Science Letters* 232: 379–392, http://dx.doi.org/10.1016/j.epsl.2005.01.030.

are, however, two potential problems with this shear-induced percolation mechanism. First, experiments have been performed at high strain rates (10^{-2} to $10^{-5}\,s^{-1}$), and it is unlikely that the mechanism would also be effective at much lower strain rates. This is a consequence of deformation being strongly localized by the liquid phase at high strain rates, so that liquid interconnection and segregation occur, whereas at low strain rates, the geometry of liquid pockets is controlled predominantly by surface tension that results in little or no interconnection (Walte et al., 2011). Secondly, the conversion of potential energy to heat during percolation of iron liquid in a planet the size of Earth might be sufficient to melt the silicates and thus change the mechanism to the one discussed in the next section (see **Section 9.03.2.2.3**).

9.03.2.3.2 Metal-silicate separation in a magma ocean

According to the results of calculations of the energy released by giant impacts, it is clear that the collision of a Mars-sized body with the proto-Earth would have resulted in the melting of a large part of or even the entire planet (**Section 9.03.2.2.2**). In the case of partial melting, although the distribution of melt may initially have been concentrated on the side affected by the impact, isostatic readjustment would have led rapidly to the formation of a global magma ocean of approximately uniform depth (Tonks and Melosh, 1993). An important, and presently unresolved, question is whether this isostatic adjustment takes place on a timescale longer or shorter than that of iron separation. The mechanics of separation and chemical equilibration is quite different if the isostatic adjustment is much slower than iron separation, because then the melt region is not a global ocean of approximately uniform depth, but a restricted 'sea' that is both hotter and deeper than the ocean that eventually develops. This question is further raised in the succeeding text in **Section 9.03.3.2.3**.

Because of the large density difference between liquid iron and liquid silicate, magma ocean formation provides a rapid and efficient mechanism for the separation of these two phases. Here, we examine the physics of metal–silicate separation in some detail because of the consequences for interpreting mantle geochemistry, as discussed in the succeeding text in **Section 9.03.3.2**.

A fundamental property that controls the dynamic behavior of a deep magma ocean is the viscosity of ultramafic silicate liquid. The viscosity of peridotite liquid has been determined experimentally at 2043–2523 K and 2.8–13.0 GPa by Liebske et al. (2005). Their results (**Figure 6**) show that viscosity increases with pressure up to 9–10 GPa and then decreases to at least 13 GPa (Reid et al., 2003 found a similar trend for $CaMgSi_2O_6$ liquid). Based on a study of the self-diffusion of O and Si in silicate liquid, viscosity is expected to increase again at pressures above 18 GPa (Schmickler et al., 2005). The transient decrease in viscosity in the pressure range 9–18 GPa may be caused by pressure-induced coordination changes (e.g., formation of five- and sixfold coordinated Si) in the melt structure (Liebske et al., 2005). Unfortunately, it is currently not possible to extrapolate these experimental results reliably in order to make predictions of melt viscosities at pressures significantly higher than 18 GPa; the large uncertainties involved in doing this are illustrated by Liebske et al. (2005, their Figure 7). An alternative approach is to use first-principles

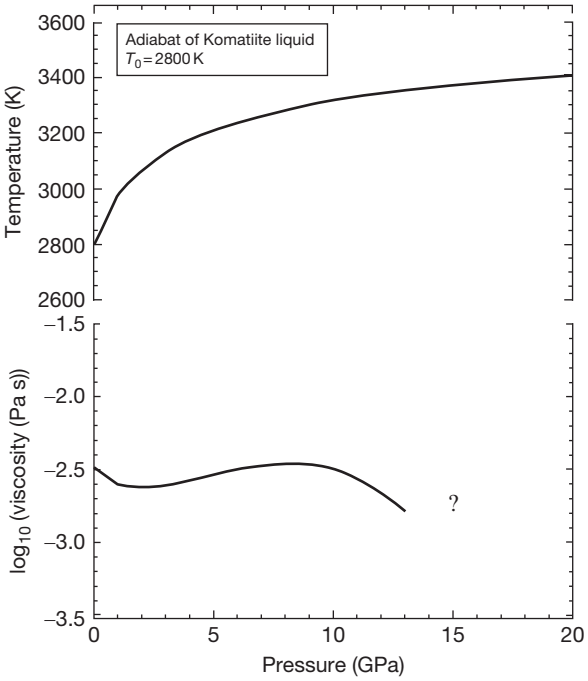

Figure 6 The viscosity of the upper part of a peridotitic magma ocean that has a total depth of ~1800 km (bottom). The viscosity is shown only to a depth of ~400 km because the existing experimental data cannot be extrapolated reliably to higher pressures. Based on the results of Schmickler et al. (2005), the viscosity likely increases again above ~18 GPa, as suggested also by molecular dynamics simulations (Karki and Stixrude, 2010). The viscosity profile is based on the adiabat shown in the top part of the figure. '?' means that the continuation of the lower curve to higher pressures is unknown. Reproduced from Liebske C, Schmickler B, Terasai H, et al. (2005) Viscosity of peridotite liquid up to 13 GPa: Implications for magma ocean viscosities. *Earth and Planetary Science Letters* 240: 589–604.

molecular dynamics simulations to estimate melt viscosity at conditions beyond those achievable experimentally. The viscosity of $MgSiO_3$ liquid has thus been determined by Karki and Stixrude (2010) to 150 GPa and was found to vary by two orders of magnitude over the pressure range of the Earth's mantle.

On the basis of the experimental data of Liebske et al. (2005), the viscosity of a magma ocean, at least to a depth of ~500 km, is estimated to lie in the range 0.01–0.003 Pa s, which is extremely low (for comparison, the viscosity of water at ambient conditions is 0.001 Pa s). Consequently, the Rayleigh number (which provides a measure of the vigor of convection) is extraordinarily high, on the order of 10^{27}–10^{32} (e.g., Rubie et al., 2003; Solomatov, 2000; **Chapter 9.04**). This means that a deep magma ocean undergoes vigorous turbulent convection, with convection velocities on the order of at least a few meters per second. Using a simple parameterized convection model, the rate of heat loss can also be estimated, which leads to the conclusion that, in the absence of other effects (see succeeding text), the lifetime of a deep magma ocean on Earth is only a few thousand years (Solomatov, 2000).

What is the physical state of molten iron in a vigorously convecting magma ocean? Initially, iron metal may be present in states that range from finely dispersed submillimeter

particles (as in undifferentiated chondritic material) to large molten masses that originated as cores of previously differentiated bodies (ranging in size from planetesimals to Mars-sized planets) that impacted the accreting Earth. In a molten system, very small particles tend to grow in size by coalescing with each other in order to reduce surface energy. Large molten bodies, on the other hand, are unstable as they settle and tend to break up into smaller bodies. A crucial question concerns the extent to which an impactor's core breaks up and becomes emulsified as it travels through the target's molten mantle (see Karato and Murthy, 1997; Rubie et al., 2003; Stevenson, 1990, for discussions of this issue). Hallworth et al. (1993) noted that laboratory-scale turbidity currents travel only a few times their initial dimension before being dispersed by turbulent instabilities. Such a core will experience both shear (Kelvin–Helmholtz) and buoyancy (Rayleigh–Taylor) instabilities. These processes operate at different length scales (R–T instabilities are small-scale features; see Dalziel et al., 1999), but both processes will tend to break the body up until a stable droplet size is reached at which surface tension inhibits further breakup. The stable droplet size can be predicted using the dimensionless Weber number, which is defined as

$$W_e = \frac{(\rho_m - \rho_s) d v_s^2}{\sigma} \quad [6]$$

where ρ_m and ρ_s are the densities of metal and silicate, respectively, d is the diameter of metal bodies, v_s is the settling velocity, and σ is the surface energy of the metal–silicate interface (Young, 1965). A balance between coalescence and breakup is reached when the value of W_e is approximately 10: When the value is larger than 10, instabilities cause further breakup to occur, and when it is less than 10, coalescence occurs. The settling velocity v_s is determined using Stokes' law when the flow regime is lamellar or an equation that incorporates a drag coefficient when the flow around the falling droplet is turbulent (Rubie et al., 2003). Both the settling velocity and the droplet size depend on silicate melt viscosity. For likely magma ocean viscosities and assuming a metal–silicate surface energy of 1 $N\,m^{-1}$, the droplet diameter is estimated to be ~1 cm and the settling velocity ~0.5 $m\,s^{-1}$ (**Figure 7**; Rubie et al., 2003, see also Karato and Murthy, 1997; Stevenson, 1990). However, exact value of the surface energy in eqn [6] is dependent on the concentrations of elements such as S, Si, and O in the liquid metal, as shown experimentally up to 1.5 GPa (Terasaki et al., 2009, 2012). Thus, settling velocities and droplet sizes could deviate from the aforementioned values by a factor of 2, depending on the liquid metal composition (Terasaki et al., 2012).

Having estimated the stable size of metal droplets, the next question is as follows: how quickly does a large mass of metal (e.g., 50–500 km in diameter) become emulsified and break up into a 'rain' of small droplets of stable diameter? Although the process is currently not well understood, Rubie et al. (2003) argued that emulsification should occur within a falling distance equal to a few times the original diameter of the body. Thus, the cores of all, except perhaps the largest, impacting bodies should have experienced a very large degree of emulsification.

Several authors have recently approached the question of emulsification of large bodies of iron sinking in a silicate magma ocean. Dahl and Stevenson (2010) argued that emulsification during accretion is incomplete, with only 1–20% of the Earth's core having equilibrated with the mantle. They applied analytic fluid dynamic models to investigate the dispersion of masses of iron originating from the cores of large accreting planetesimals. They analyzed both the Rayleigh–Taylor and the Kelvin–Helmholtz instabilities to estimate the mixing of an initially compact spherical blob of iron in a

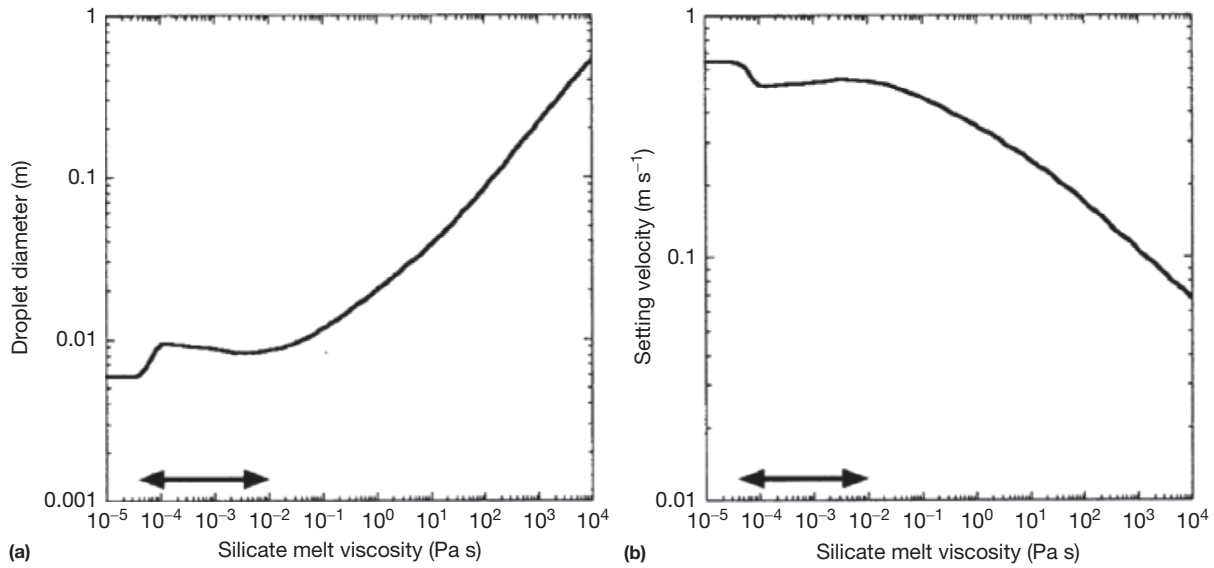

Figure 7 (a) Stable diameter of liquid iron droplets dispersed in a magma ocean as a function of silicate melt viscosity. The droplet diameter is calculated using the Weber number, as explained in the text. (b) Terminal settling velocity of liquid Fe droplets (of stable droplet diameter) as a function of silicate melt viscosity. The nonlinear trend arises from a transition from Stokes to turbulent flow at low viscosities. In both (a) and (b), the arrowed lines indicate the range of likely magma ocean viscosities. Reproduced from Rubie DC, Melosh HJ, Reid JE, Liebske C, and Righter K (2003). Mechanisms of metal–silicate equilibration in the terrestrial magma ocean. *Earth and Planetary Science Letters* 205: 239–255.

silicate liquid magma ocean and concluded that the blob must sink many times its own diameter before it is reduced to droplets small enough for chemical equilibration. On this basis, they argued that planetesimal cores larger than about 10 km diameter are unable to chemically equilibrate with the surrounding silicate. Their analytic models were qualitatively confirmed in a suite of experiments by Deguen et al. (2011) who created laboratory-scale models of the turbulent descent of an initially concentrated mass of dense, immiscible liquid into a tank of less dense fluid. In contrast, Samuel (2012) numerically modeled the breakup of iron diapirs and argued instead that initially concentrated iron masses smaller than the depth of the magma ocean may rapidly break up and emulsify during sinking under plausible conditions. None of these models, however, properly address the initial conditions following the high-speed impact of a planetesimal with a pre-differentiated core upon the accreting Earth. Preliminary work by Kendall and Melosh (2012a,b) examined the dispersion of planetesimal cores of various sizes during accretion using both vertical 2D and oblique 3D numerical impact models. They concluded that the cores are stretched by factors of about 1000 during such impacts and that the proper initial condition is that of an already-mixed cloud of liquid metal blobs dispersed in the silicate magma ocean. In this case, the impact itself produces a large reduction of the initial size of the planetesimal cores near the top of the magma ocean. Subsequent dispersion during sinking may then reduce the size of the iron masses to the point where chemical equilibration will readily occur. It is clear that understanding this crucial question is still in a state of flux and further progress will be needed to settle the issue of emulsification of the cores of impacting objects.

The primary importance of emulsification is that it determines the degree to which chemical and thermal reequilibration occurs (Karato and Murthy, 1997; Rubie et al., 2003). Because thermal diffusivities are higher than chemical diffusivities, thermal equilibrium is always reached first. For typical settling velocities, iron blobs on the order of ~0.01 m in diameter will remain in chemical equilibration with the surrounding silicate liquid as they fall (Rubie et al., 2003). Droplets that are much larger (e.g., on the order of meters or more in diameter) will fall rapidly and will not remain in equilibrium with the adjacent silicate because diffusion distances are too large. The physical arguments for emulsification summarized here are supported by evidence for chemical equilibration from both Hf–W observations (**Section 9.03.3.1**) and siderophile element abundances in the mantle (**Section 9.03.3.2**). Since chemical equilibration of macroscale iron bodies is very slow, this apparent equilibration strongly suggests that the iron was present, at least to a large extent, as small dispersed droplets (Righter and Drake, 2003).

Because likely settling velocities (~0.5 $m\,s^{-1}$) of small iron droplets are much lower than typical convection velocities (~10 $m\,s^{-1}$), iron droplets may remained entrained for a significant time in the magma ocean, and accumulation through sedimentation at the base of the ocean will be a slow and gradual process. The dynamics of the settling and accumulation processes are important because they determine the chemical consequences of core formation (e.g., siderophile element geochemistry), as discussed in the succeeding text in **Section 9.03.3.2.3**.

The time taken for a magma ocean to start to crystallize is an important parameter when evaluating metal–silicate equilibrium models, as discussed in the succeeding text (**Section 9.03.3.2.3**). The existence of an early, thick atmosphere has little effect on large incoming impactors but may be sufficiently insulating that, by itself, it ensures a magma ocean (e.g., Matsui and Abe, 1986). The depth to the (rheologically determined) base of the magma ocean is determined by the point at which the adiabat crosses the geotherm defining a melt fraction of roughly 60% (Solomatov, 2000). The survival time of the magma ocean depends on both the atmosphere and whether or not an insulating lid can develop. In the absence of these two effects, the lifetimes are very short, on the order of 10^3 years (e.g., Pritchard and Stevenson, 2000; Solomatov, 2000). However, if a conductive lid develops, the lifetime may be much longer, on the order of 10^8 years (Spohn and Schubert, 1991), and similar lifetimes can arise due to a thick atmosphere (Abe, 1997). Thus, the lifetime of magma oceans is currently very unclear. The Moon evidently developed a chemically buoyant, insulating crust on top of its magma ocean (Warren, 1985). However, it did so because at low pressures aluminum partitions into low-density phases, especially plagioclase. At higher pressures, Al instead partitions into dense garnet, in which case a chemically buoyant crust will not develop (e.g., Elkins-Tanton et al., 2003, 2011). In the absence of chemical buoyancy, a solid crust will still develop but will be vulnerable to disruption by impacts or foundering (Stevenson, 1989). The latter process in particular is currently very poorly understood, and thus, the lifetime of magma oceans remains an open question. Fortunately, even the short-lived magma oceans persist for timescales long compared to most other processes of interest.

The conventional view has been that a deep magma ocean would crystallize from the bottom up, as suggested by the relationship between the adiabat and melting curves shown in **Figure 8(b)**. However, recent investigations of the thermodynamic properties of Mg_2SiO_4 and $MgSiO_3$ liquids at high pressure, through shock experiments (Mosenfelder et al., 2007, 2009) and molecular dynamics simulations (Stixrude and Karki, 2005), suggest that temperatures along a magma ocean adiabat increase much more rapidly than shown in **Figure 8(b)**. These results lead to the possibility that a magma ocean starts to crystallize at mid-depths. This proposal has led to the idea that a basal magma ocean existed above the CMB early in Earth's history (Labrosse et al., 2007).

9.03.2.3.3 Diapirs and diking

If percolation is not an effective mechanism, then differentiation may occur either by downward migration of large iron blobs (diapirism) or by propagation of iron-filled fractures (diking). The mode of descent of a dense, low-viscosity fluid through a less dense high-viscosity fluid has been the subject of much debate. Many authors have assumed that the dense fluid (liquid iron in our case) penetrates the underlying less dense material (unmelted mantle) as diapirs, somewhat analogous to the (inverted) penetration of high-viscosity sediments by low-density salt diapirs or the penetration of the lower crust by granitic magma above subduction zones. Rubin (1993), however, argued that the mode of penetration, dikes vs. diapirs, depends mainly upon the ratio of viscosity between the intruding fluid and the host material.

The transport of iron though crystalline mantle as large diapirs, 1–10 km in diameter or larger, has been discussed in

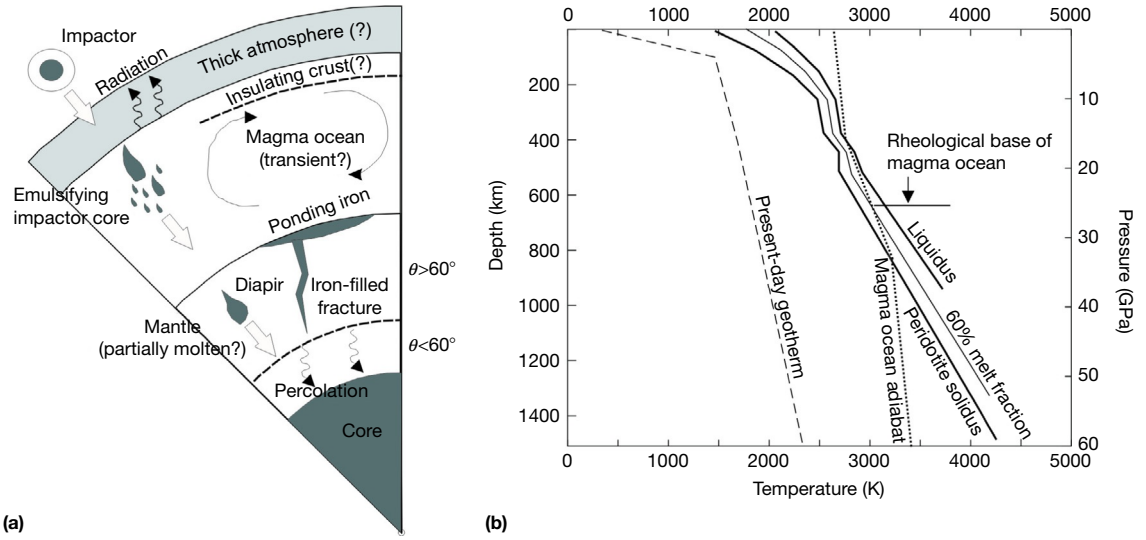

Figure 8 (a) Schematic diagram showing the various processes of metal–silicate segregation that could have operated during Earth accretion and core formation. The rheological base of the magma ocean is defined as the point at which the melt fraction drops below ~60% (Solomatov, 2000). (b) Schematic illustration of the temperature structure in the early Earth, adapted from Walter MJ and Tronnes RG (2004) Early Earth differentiation. *Earth and Planetary Science Letters* 225: 253–269. The solidus curve in the lower mantle is based on Boehler (2000), but according to more recent determinations (Fiquet et al., 2010; Andrault et al., 2011; Liebske and Frost, 2012), solidus temperatures are considerably lower (e.g., ~3200 K at 60 GPa). The 60% melt fraction line is schematic.

detail by Karato and Murthy (1997). When liquid iron ponds as a layer at the base of a magma ocean (Figure 8), gravitational instabilities develop due to the density contrast with the underlying silicate-rich material and cause diapir formation. Their size and rate of descent through the mantle depend on the initial thickness of the metal layer and the viscosity of the silicate mantle. Clearly, gravitational heating will be important and will facilitate diapir descent by reducing the viscosity of the adjacent mantle. In contrast to magma ocean segregation, there will be no significant chemical exchange between metal and silicate, chemical disequilibrium will result, and siderophile element abundances in the mantle cannot be a consequence of this mechanism (Karato and Murthy, 1997; see also Chapter 9.02).

Liquid iron ponded at the base of the magma ocean may also, under the right conditions, sink rapidly toward the Earth's core by diking. Although it may be supposed that the hot, but nevertheless crystalline, mantle underlying the magma ocean cannot support brittle cracks, numerical studies summarized in Rubin (1995) indicate that dikes can still form, so long as the contrast in viscosity between the fluid in the dike and the surrounding host rocks is greater than 10^{11}–10^{14}. With a viscosity around 10^{-2} Pa s, liquid iron is thus expected to form dikes if the viscosity of the host rock exceeds 10^{9}–10^{12} Pa s. Given that the viscosity of the asthenosphere today is around 10^{19} Pa s, it is not unreasonable to expect the iron to reach the core via narrow dikes rather than as diapirs. In this case, even less time is required for the rapidly descending iron to reach the core and thus less time for the iron to chemically equilibrate with the surrounding mantle. Indeed, even in the present Earth, Stevenson (2003) has proposed that masses of molten iron as small as 10^{8} kg (which would fill a cube about 25 m on a side) could travel from the Earth's surface to the core in about 1 week.

9.03.2.3.4 Summary and implications for chemical equilibration

A schematic illustration of how the various differentiation mechanisms might operate together is shown in Figure 8. Liquid metal separates rapidly from liquid silicate in a deep magma ocean and accumulates as ponded layers at the rheological base of the magma ocean. The ponded iron then migrates through the largely crystalline underlying mantle toward the protocore by either percolation, diapirism, or diking. According to experimental results summarized earlier, percolation is unlikely to be a completely efficient mechanism, even when catalyzed by shear deformation, but the mechanism may at least contribute to core formation. Whether the diking mechanism shown in Figure 8 is dominant or the iron descends in diapirs initiated by Rayleigh–Taylor instabilities depends upon poorly known material properties, such as viscosity, that make it difficult to make definite inferences about the mechanism. What seems to be clear is that, once liquid iron accumulates in large masses on the floor of the magma ocean, it then descends rapidly to the Earth's core without further chemical interaction with the underlying silicate.

Despite the rapid transit times associated with falling iron drops and the somewhat longer timescales of percolative flow, the inferred length scales are small enough that complete chemical equilibration is expected. Conversely, descending iron diapirs are sufficiently large that chemical equilibrium is expected to be negligible (Karato and Murthy, 1997). Thus, the different differentiation mechanisms have very different chemical consequences. However, the magnitude of these chemical effects also depends on the relative abundances: a late passage of 1% core material through the mantle may well have a strong effect on mantle siderophile element abundances (e.g., W or Pt) but will have little effect on major element concentrations (e.g., oxygen) simply because the core material will become

saturated and thus transport insignificant amounts of these more abundant elements.

9.03.3 Observational and Experimental Constraints

Having discussed our theoretical expectations of accretion and core formation processes, we will now go on to discuss the extent to which observations and experimental data may be used to differentiate between the various theoretical possibilities. Excellent summaries of many of these observations and experimental results may be found in Halliday (2003) and in the volume edited by Canup and Righter (2000).

9.03.3.1 Core Formation Timescales

An extremely important development has been the recognition that some isotopic systems provide an observational constraint on core formation timescales and thus planetary accretion rates. The most useful isotopic system is Hf–W (Jacobsen, 2005; Kleine et al., 2009). The Pd–Ag system is similar (Schönbächler et al., 2010) but is more complicated to interpret because silver is a volatile element. The U–Pb system has similar volatility problems but generates results that can be reconciled with the more robust Hf–W technique (Rudge et al., 2010; Wood and Halliday, 2005, 2010).

The Hf–W chronometer works as follows. W is siderophile (i.e., 'metal-loving'), while Hf is lithophile (it remains in silicates). Furthermore, ^{182}Hf decays to stable ^{182}W with a half-life of 9 Myr. If an initially undifferentiated object suddenly forms a core after all the ^{182}Hf has decayed, the W will be extracted into the core and the mantle will be strongly depleted in all tungsten isotopes. However, if core formation occurs early, while ^{182}Hf is live, then the subsequent decay of ^{182}Hf to ^{182}W will enrich the mantle in radiogenic tungsten compared with nonradiogenic tungsten. Thus, a radiogenic tungsten excess, or tungsten anomaly, in the mantle is a sign of early core formation. Furthermore, if the silicate–iron mass ratio and the mantle concentrations of Hf and W compared with undifferentiated materials (chondrites) are known, then the observed tungsten anomaly can be used to infer a single-stage core formation age. In the case of the Earth, this single-stage age is roughly 30 Myr (Jacobsen, 2005). The lunar Hf–W record is difficult to interpret but may imply a formation time for the Moon of 50–150 Myr after solar system formation (Touboul et al., 2007).

There are three characteristics of the Hf–W system that makes it especially suitable for examining core formation. Firstly, the half-life is comparable to the timescale over which planets are expected to form. Secondly, there are few other processes likely to lead to tungsten fractionation and perturbation of the isotopic system, though very early crustal formation or neutron capture (Kleine et al., 2005) can have effects. Finally, both Hf and W are refractory; certain other isotopic systems suffer from the fact that one or more elements (e.g., lead and silver) are volatile and can be easily lost during accretion.

The fact that tungsten isotope anomalies exist in the terrestrial mantle implies that core formation was essentially complete before about five half-lives (50 Myr) had elapsed. Mars and Vesta have larger tungsten anomalies, indicating that core formation ended earlier on these smaller bodies (Dauphas and Pourmand, 2011; Kleine et al., 2009). The timescales implied are compatible with the theoretical picture of planetary accretion described in **Section 9.03.2.1**. The simple model of a single core formation event is of course a simplification of the real picture, in which the bulk of the core mass is added during stochastic giant impacts. However, more complicated models, in which the mass is added in a series of discrete events, do not substantially alter the overall timescale derived.

The observed tungsten anomaly depends mainly on the timescale over which the core forms, the relative affinities of Hf and W for silicates, and the extent to which the cores of the impactors reequilibrate with the target mantle. The relative affinities of Hf and W can be determined, in a time-averaged sense, by measuring the present-day concentrations of these elements in the mantle. These affinities (i.e., the partition coefficients) may have varied with time, due to changing conditions (P, T, and oxygen fugacity f_{O_2}) in the Earth. Although the dependence of the partition coefficients on these variables is known (e.g., Cottrell et al., 2009; Wade et al., 2012), how the variables actually evolved as the Earth grew is very poorly understood (e.g., Halliday, 2004). This caveat aside, if one accepts that the accretion timescales determined by numerical accretion models are reasonable, these models can then be used to investigate the extent to which reequilibration must have occurred.

Figure 9 shows examples of the tungsten anomalies generated from numerical models of late-stage accretion (Nimmo et al., 2010). In **Figure 9(a)**, it is assumed that 50% of incoming core material reequilibrates with the silicate mantle. Because of the stochastic nature of the accretion process, there is considerable scatter; nonetheless, bodies that resemble Mars and Earth in both their tungsten anomalies and the Hf/W ratios can be produced. **Figure 9(b)** shows how the average tungsten anomaly for Earth-mass bodies varies as the equilibration factor k is varied. If little equilibration occurs, the resulting tungsten anomalies are large. This is because the larger bodies then inherit their anomalies from smaller bodies that (by assumption) differentiated early and thus developed large tungsten anomalies. By contrast, if equilibration is efficient, then the isotopic memory of earlier events is erased and each impact tends to drive down the overall tungsten anomaly. Assuming that the accretion timescales generated by the simulations are correct, **Figure 9(b)** suggests that an intermediate reequilibration amount ($k \approx 50\%$) is required to reproduce the observations; similar results have been obtained by other authors (e.g., Rudge et al., 2010). This conclusion in turn places constraints on the physics of these very large impacts and, in particular, suggests that some emulsification of the impacting core occurs as it travels through the magma ocean (see also Rubie et al., 2011; **Section 9.03.2.3.2**).

One example of the importance of the equilibration factor k is in the accretion of Mars. Mars has an Earthlike tungsten anomaly but a lower Hf/W ratio, implying rapid accretion. If equilibration is efficient ($k \approx 1$), then accretion must have been so rapid that Mars would have melted via ^{26}Al decay – this is the hypothesis advanced by Dauphas and Pourmand (2011). However, less extreme reequilibration would permit more prolonged accretion and thus reduce the likelihood of melting. A better understanding of k is thus crucial to understanding Mars' early evolution.

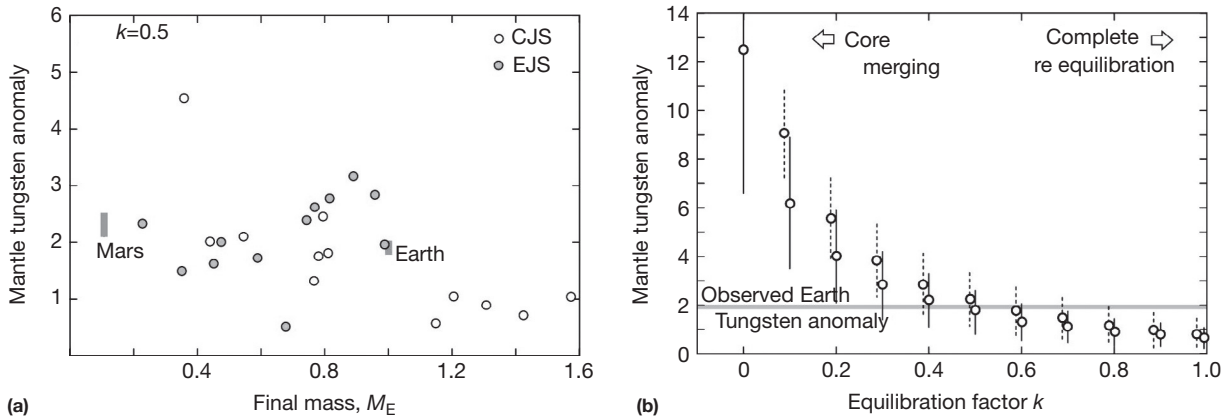

Figure 9 Isotopic outcomes of core formation based on N-body accretion codes (from Nimmo et al., 2010). M_E is the mass of the final bodies in Earth masses; k is the equilibration factor between core and mantle (see text). Shaded regions are observed values; circles are model results. (a) Individual outcomes with $k = 0.5$. Open and filled circles are based on N-body simulations with Jupiter and Saturn on their current orbits and on smaller, eccentric orbits, respectively (see O'Brien et al., 2006). (b) Mean and standard deviations of tungsten anomalies for bodies with masses $>0.7\ M_E$ as a function of equilibration factor. Solid and dashed lines are for models with a variable and fixed tungsten partition coefficient, respectively (see Nimmo et al., 2010).

The palladium–silver (^{107}Pd–^{107}Ag) system is in some ways very similar to the Hf–W system. Pd is strongly siderophile and ^{107}Pd has a half-life of 6.5 Myr, making it suitable for investigating core formation processes. However, there are fewer isotopes of Ag than of W, making precise isotopic measurements more difficult; more importantly, Ag is volatile which complicates interpretation of the isotopic data. Nonetheless, precise ^{107}Ag/^{109}Ag measurements have been used to argue for an Earth accretion timescale compatible with that derived from Hf–W systematics and also involving a change from volatile-depleted to volatile-enriched material as accretion proceeded (Schönbächler et al., 2010). This latter conclusion is entirely consistent with dynamical simulations in which the Earth's feeding zone expanded outward beyond the 'snow line' with time (O'Brien et al., 2006).

Finally, because the early history of the core and the mantle is intimately coupled, there are some isotopic systems governed by mantle processes that are also relevant to core formation timescales. In particular, the nonchondritic ^{142}Nd isotope signature of the Earth's upper mantle has been used to argue for global melting of the mantle within 30 Myr of solar system formation (Boyet and Carlson, 2005). Sm–Nd and Lu–Hf chronometers are also consistent with the solidification of a magma ocean within the first ~100 Myr of Earth history (Caro et al., 2005), and U–Pb dates have been interpreted as resulting from the final stage of magma ocean crystallization at about 80 Myr after solar system formation (Wood and Halliday, 2005, 2010). Xe isotope data give a comparable time for loss of xenon from the mantle (e.g., Halliday, 2003; Porcelli et al., 2001) and also support early differentiation scenarios (Mukhopadhyay, 2012) and multiple magma ocean generations (Tucker and Mukhopadhyay, 2014).

In summary, the Hf–W (and, to a lesser extent, Pd–Ag and U–Pb) systems are important for two reasons: they constrain the timescale over which core formation occurred and also constrain the extent of reequilibration between core material and mantle material. To obtain the pressure–temperature conditions under which this reequilibration took place, it is necessary to look at other siderophile elements as well. Inferring the equilibration conditions is important both because constraints are then placed on the early thermal state of both core and mantle and because these conditions strongly influence the ultimate composition of the core.

9.03.3.2 Constraints from Siderophile Element Geochemistry

9.03.3.2.1 Introduction to siderophile element geochemistry

The primary geochemical evidence for core formation in the Earth is provided by a comparison of the composition of the Earth's silicate mantle with its bulk composition. Estimates of the composition of the mantle are based on numerous geochemical studies of mantle peridotites and are well established (e.g., McDonough and Sun, 1995; Palme and O'Neill, 2003), assuming of course that the mantle is homogeneous. Although the bulk composition of the Earth is not known precisely (Drake and Righter, 2002; O'Neill and Palme, 1998), it is often approximated by the refractory-element composition of C1 carbonaceous chondrites, which are the most pristine (undifferentiated) relicts known from the early solar system. As seen in **Figure 10**, refractory lithophile elements (e.g., Al, Ca, Ti, Ta, Zr, and the rare earth elements, REEs) are present in the mantle in CI chondritic concentrations, and their concentrations have therefore been unaffected by accretion or differentiation processes. Compared with the bulk composition of the Earth, the mantle is strongly depleted in (a) siderophile (metal-loving) elements that have partitioned into iron-rich metal during formation of the Earth's core (Walter et al., 2000) and (b) volatile elements that are considered to have been partly lost during accretion. Note that some of the volatile elements are also siderophile (e.g., sulfur) so that current mantle concentrations can be the result of both core formation and volatility (for a full classification of depleted elements, see Table 1 in Walter et al. (2000)). Siderophile elements that are unaffected by volatility are most valuable for understanding core formation, and these include the moderately siderophile elements (MSEs; e.g., Fe, Ni, Co, W, and Mo) and the HSEs, which include the platinum group elements (e.g., Re, Ru, Rh, Os, Ir, Pd, Pt, and Au).

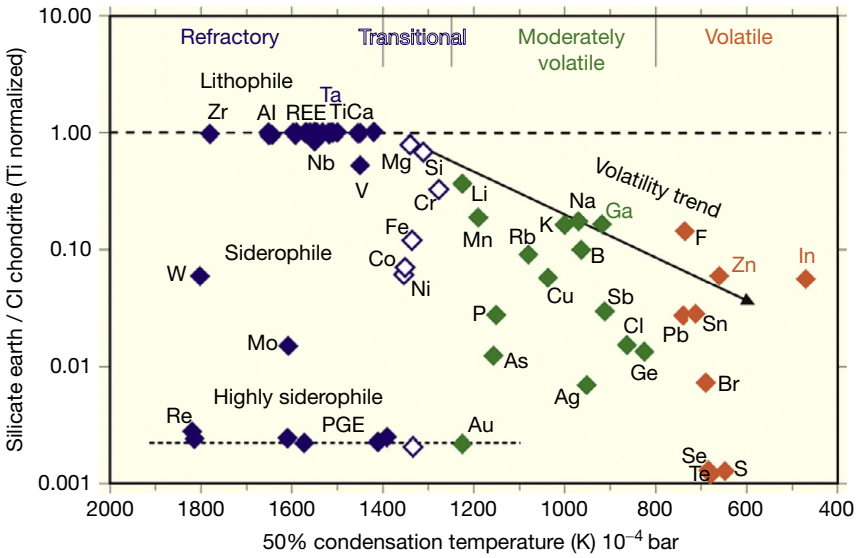

Figure 10 Element abundances of the Earth's mantle normalized to CI chondrite and the refractory element Ti (data after Palme and O'Neill, 2003) plotted against their 50% condensation temperatures as given by Wasson (1985) and, in the case of Pb, by Lodders (2003). Note that the errors on these data points may be large (e.g., at least an order of magnitude for some volatile elements). Courtesy of Ute Mann.

The degree of siderophile behavior is described for element M by the metal–silicate partition coefficient $D_M^{met-sil}$, which is defined as

$$D_M^{met-sil} = \frac{C_M^{met}}{C_M^{sil}} \quad [7]$$

where C_M^{met} and C_M^{sil} are the wt% or molar concentrations of M in metal and silicate, respectively. MSEs are defined as having values (determined experimentally at 1 bar) of $D_M^{met-sil} < 10^4$, whereas HSEs have 1 bar values that are greater than 10^4 and can be, in the case of Ir, for example, as high as 10^{10}. The boundary between siderophile behavior and lithophile behavior is defined as $D_M^{met-sil} = 1$.

As discussed in the succeeding text, partition coefficients are a function of pressure, temperature, and the compositions of the metal and silicate phases. An additional controlling parameter, which is critical in the context of core formation, is oxygen fugacity, f_{O_2}. The effect of f_{O_2} on the partitioning of a siderophile element depends on its valence state when it is dissolved in the silicate phase, as shown by the following metal–silicate equilibrium:

$$\underset{\text{metal}}{M} + (n/4)O_2 = \underset{\text{silicate liquid}}{MO_{n/2}}$$

(e.g., Righter and Drake, 2003). Here, M is the element of interest and n is its valence when it is dissolved in silicate liquid. Increasing the oxygen fugacity drives the equilibrium toward the right-hand side, thus increasing the concentration of M in the silicate liquid and reducing the value of $D_M^{met-sil}$. Typically, the dependence of $D_M^{met-sil}$ on f_{O_2}, pressure (P), and temperature (T) is expressed by a relationship of the form

$$\ln D_M^{met-sil} = a \ln fO_2 + b/T + cP/T + g \quad [8]$$

where a is related to the valence state of M in the silicate liquid and b, c, and g are related to thermodynamic free energy terms that have generally assumed to be constants even when the P–T range of extrapolation is large (see Righter and Drake, 2003). In reality, these parameters are not likely to be constant over large ranges of pressure, temperature, and f_{O_2}. For example, the valence state of an element can change as a function of f_{O_2}. Pressure-induced changes in the structure of the silicate melt and/or the metal liquid may also cause a strong nonlinear pressure dependence at certain conditions (Kegler et al., 2008; Keppler and Rubie, 1993; Sanloup et al., 2011). In addition to P, T, and f_{O_2}, the effects of additional factors, such as the composition/structure of the silicate melt and the sulfur, silicon, and carbon contents of the metal, may also need to be included (Cottrell et al., 2009; Tuff et al., 2011; Wade et al., 2012; Walter et al., 2000).

For core formation, the value of f_{O_2} is constrained by the partitioning of Fe between the mantle and the core (see Mann et al., 2009) and has been estimated to have been 1–2 log units below the oxygen fugacity defined by the iron–wüstite (Fe–FeO or 'IW') buffer (which is abbreviated as IW-1 to IW-2). However, in recent models, f_{O_2} is considered to have been initially very low and to have increased during core formation to a final value of around IW-2 (see succeeding text).

The oxygen fugacity term in eqn [8] can be eliminated by considering the exchange reaction

$$\underset{\text{silicate}}{MO_{n/2}} + \frac{n}{2}\underset{\text{metal}}{Fe} = \underset{\text{metal}}{M} + \frac{n}{2}\underset{\text{silicate}}{FeO} \quad [9]$$

and by describing the partitioning of element M in terms of a distribution coefficient K_D, instead of $D_M^{met-sil}$, where

$$K_D = \frac{X_M^{met}\left(X_{FeO}^{sil}\right)^{n/2}}{X_{MO_{n/2}}^{sil}\left(X_{Fe}^{met}\right)^{n/2}} \quad [10]$$

(e.g., Mann et al., 2009). Here, X represents the mole fractions of M, $MO_{n/2}$, Fe, and FeO in metal (met) and silicate (sil). In a system in which mixing is ideal or the ratios of activity coefficients are constant, K_D is independent of composition and

oxygen fugacity and its pressure and temperature dependences can be described by an expression similar to eqn [8] but without the oxygen fugacity term (e.g., Mann et al., 2009). However, when the activities of components in the silicate and metal are dependent on composition, an equilibrium constant K must be used and is defined as

$$K = \frac{X_{\mathrm{M}}^{\mathrm{met}} \gamma_{\mathrm{M}}^{\mathrm{met}} \left(X_{\mathrm{FeO}}^{\mathrm{sil}} \gamma_{\mathrm{FeO}}^{\mathrm{sil}}\right)^{n/2}}{X_{\mathrm{MO}_{n/2}}^{\mathrm{sil}} \gamma_{\mathrm{MO}_{n/2}}^{\mathrm{sil}} \left(X_{\mathrm{Fe}}^{\mathrm{met}} \gamma_{\mathrm{Fe}}^{\mathrm{met}}\right)^{n/2}} \quad [11]$$

where γ represents the activities of the components in silicate and metal. Activity coefficients for the metal phase are formulated using the epsilon model (Wagner, 1962) as modified by Ma (2001) (e.g., Siebert et al., 2011; Tuff et al., 2011; Wade et al., 2012). For Mo and W, the silicate melt composition has a strong influence on partitioning and activity models have been discussed by Wade et al. (2012).

Note that carbon dissolved in liquid metal has a very large effect on the metal–silicate partitioning of Si and many siderophile elements. Consequently, experimental studies that have utilized graphite capsules can produce erroneous results (see Cottrell et al., 2009; Mann et al., 2009).

Values of $D_{\mathrm{M}}^{\mathrm{met-sil}}$ for the core–mantle system lie in the range 13–30 for MSEs and 600–1000 for HSEs (for compilations of values, see Wade and Wood, 2005; Wood et al., 2006). These values are much lower than experimentally determined 1 bar metal–silicate partition coefficients, in some cases by a few orders of magnitude, and show that the mantle contains an apparent *overabundance* of siderophile elements. Possible explanations of this anomaly, the so-called excess siderophile element problem, form the basis of theories of how and under which conditions the Earth's core formed (e.g., Newsom, 1990; Righter, 2003), as described further in **Section 9.03.3.2.2**. An important additional constraint is provided by the observation that the HSEs are present in the mantle in approximately chondritic relative abundances (**Figures 10** and **11**), even though the experimentally determined 1 bar $D_{\mathrm{M}}^{\mathrm{met-sil}}$ values vary by orders of magnitude.

Important constraints on how the Earth's core formed are potentially provided by also considering the geochemical consequences of core formation in other planetary bodies. If the sizes of such bodies differ significantly from that of the Earth, pressure–temperature conditions of metal–silicate equilibration will also be different, thus enabling some of the theories detailed in the succeeding text (**Section 9.03.3.2.2**) to be tested. Estimates of the geochemical effects of core formation in Mars, Vesta, and the Moon are also based on comparisons of siderophile element concentrations in the mantles of these bodies with their likely bulk compositions (e.g., Drake, 2001; Righter and Drake, 1996; Treiman et al., 1987; Walter et al., 2000). Both bulk and mantle compositions are poorly constrained compared with the Earth. Mantle compositions are inferred from studies of SNC meteorites for Mars, the eucritic meteorites for Vesta, and samples collected from the Moon's surface (McSween, 1999; Warren, 1993). In all cases, the samples (e.g., lavas and cumulates) are the products of crustal differentiation processes, and therefore, mantle compositions have to be inferred by taking the effects of differentiation into account. In the case of the Moon, there is an additional problem because the petrogenesis of samples is poorly constrained because of their extremely small size (Warren, 1993).

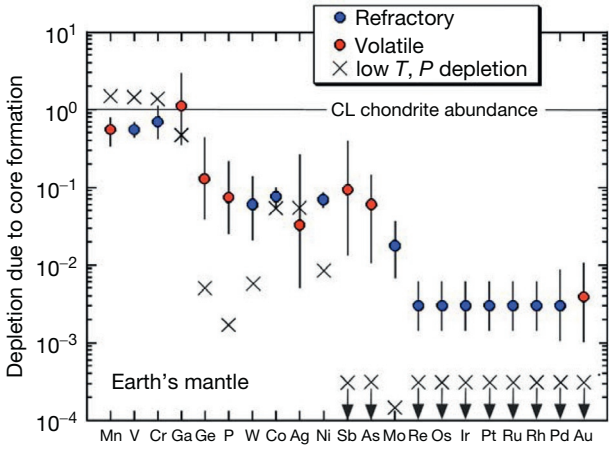

Figure 11 Depletion of siderophile elements in the Earth's mantle as the result of core formation. The siderophile elements are distinguished as being either refractory or volatile. The crosses show depletion values that would be expected on the basis of partitioning experiments performed at one bar and moderate temperatures (e.g., 1300 °C); in the case of the highly siderophile elements, the predicted values plot far below the bottom of the graph and are highly variable. The large discrepancies between the observed and the calculated values shown here form the basis for the 'siderophile element anomaly.' For further details, see Walter et al. (2000). Reproduced from Walter MJ, Newsom HE, Ertel W, and Holzheid A (2000). Siderophile elements in the Earth and Moon: Metal/silicate partitioning and implications for core formation. In: Canup RM and Righter K (eds.) *Origin of the Earth and Moon*, pp. 265–290. Tucson: University of Arizona Press; courtesy of Michael Walter.

Compared to the Earth's mantle, current assessments indicate that the Martian mantle is relatively depleted in Ni and Co, whereas concentrations of HSEs are similar. As in the Earth's mantle, the HSEs appear to be present in chondritic relative abundances (Jones et al., 2003; Kong et al., 1999; McSween, 1999; Warren et al., 1999). The mantles of both the Moon and Vesta show relatively large depletions in most siderophile elements (Righter and Drake, 1996; Walter et al., 2000). It is not possible in any of these cases to explain mantle siderophile element abundances by simple metal–silicate equilibrium at moderate pressures and temperatures, that is, based on 1 bar experimental data.

9.03.3.2.2 Core formation/accretion models

As described in the previous section, siderophile element concentrations are depleted in the Earth's mantle relative to chondritic compositions as a consequence of core formation (**Figures 10** and **11**). However, compared with predicted depletions based on element partitioning studies at 1 bar and moderate temperatures (e.g., 1300–1400 °C), the concentrations of siderophile elements are too high (**Figure 12**; Table 1 in Wood et al., 2006). In the case of MSEs, the discrepancies are around 1–2 orders of magnitude. In the case of the HSEs, the discrepancies are on the order of 5–10 orders of magnitude.

The apparent overabundance of siderophile elements in the mantle has led to a number of core formation hypotheses, most notably the following:

- Heterogeneous two-stage accretion models
- Metal–silicate equilibration at high pressures and temperatures

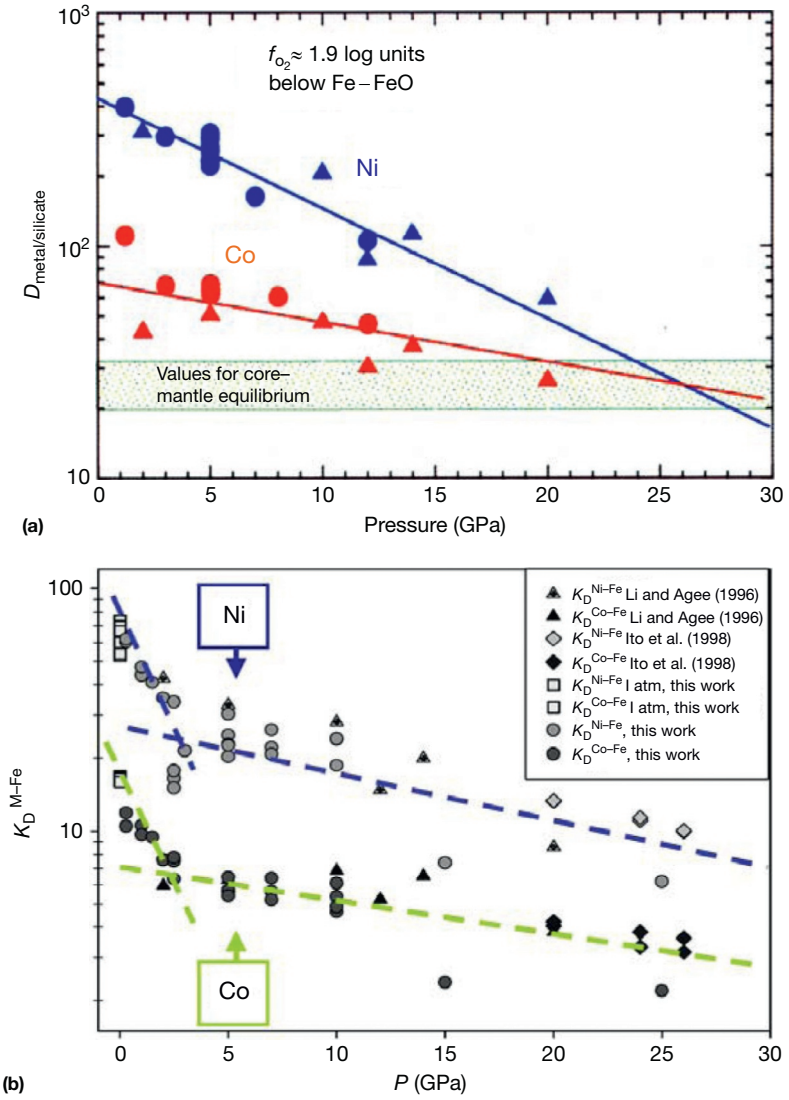

Figure 12 (a) Early experimental results on the effects of pressure on the partitioning of Ni (blue symbols) and Co (red symbols) between liquid Fe alloy and liquid silicate melt, at 2123–2750 K and f_{O_2} = IW-1.9, that led to the hypothesis of metal and silicate equilibrating during core formation at the bottom of a deep magma ocean. Triangles show data from Li and Agee (1996) and filled circles show data from Thibault and Walter (1995) (from Wood et al., 2006). (b) More recent results on the partitioning of Ni and Co (Kegler et al., 2008) show that the pressure dependence undergoes a pronounced change at 3–5 GPa, probably because of pressure-induced structural changes in the silicate liquid (Keppler and Rubie, 1993) and/or the metallic liquid (Sanloup et al., 2011); above 5 GPa, the pressure dependences for both Ni and Co are considerably weaker than the trends shown in (a). Here, $K_D^{M\text{-}Fe}$ is a distribution coefficient in which the partition coefficient has been normalized to Fe partitioning and is thus independent of f_{O_2} (see eqn [10]); in addition, the data have all been normalized to 2273 K by extrapolation. Reproduced from Kegler P, Holzheid A, Rubie DC, Frost DJ, and Palme H (2005) New results of metal/silicate partitioning of Ni and Co at elevated pressures and temperatures. *XXXVI Lunar and Planetary Science Conference*, Abstr. #2030.

- Models of continuous and multistage core formation
- The late-veneer hypothesis
- Addition of core material to the lower mantle

We briefly review each of these hypotheses in turn.

9.03.3.2.2.1 Heterogeneous two-stage accretion models

An early solution to the apparent 'excess siderophile element problem' was proposed by Wänke (1981). His model involved the Earth initially accreting from small bodies that had differentiated under highly reducing conditions at low pressure such that all elements more siderophile than Fe were effectively removed from the silicate mantles into the metallic cores. When these bodies accreted to the Earth, their cores merged with the Earth's protocore without any further chemical equilibration between metal and silicate, thus resulting in the mantle being highly depleted in siderophile elements. During a later second stage, oxidized CI-like material accreted to the Earth and, through the mixing of this material into the Earth's mantle, the current mantle abundances of the siderophile

elements were established. This low-pressure heterogeneous core formation model was further developed by O'Neill (1991) to also explain the concentrations of the HSEs in the mantle.

The evolution from initially highly reducing conditions to later oxidizing conditions during Earth's accretion, proposed by Wänke (1981) and O'Neill (1991), is also an essential feature of more recent core formation models discussed in the succeeding text (Rubie et al., 2011; Wade and Wood, 2005).

However, metal–silicate equilibration only under low-pressure conditions can be excluded on the basis of experimental partitioning data of Mann et al. (2009). This study shows that the chondritic Ga/Mn and ln/Zn ratios of the Earth's mantle require metal–silicate equilibration at an average pressure on the order of 30–60 GPa (see also Figure 1 in Rubie et al. (2011)).

9.03.3.2.2.2 Metal–silicate equilibration at high pressure and temperature

Murthy (1991) proposed that mantle siderophile element abundances could be explained if temperatures during core formation were extremely high. Although there were significant problems with the thermodynamic arguments on which this suggestion was based (Jones et al., 1992; O'Neill, 1992), metal–silicate equilibration at combined high temperatures and pressures may provide the explanation for at least the MSE abundances. This topic has been reviewed in detail by Walter et al. (2000), Righter and Drake (2003), and Wood et al. (2006).

Preliminary high-pressure studies produced results that were inconclusive in determining whether metal–silicate equilibration can explain the siderophile element anomaly (Hillgren et al., 1994; Thibault and Walter, 1995; Walter and Thibault, 1995; Walker et al., 1993). However, an early study of the partitioning of Ni and Co between liquid Fe alloy and silicate melt suggested that the metal–silicate partition coefficients for these elements reach values that are consistent with mantle abundances at a pressure of 25–30 GPa (**Figure 12(a)**; Li and Agee, 1996). This important result led to the idea that metal–silicate equilibration at the base of a magma ocean ~800 km deep can explain the mantle abundances of at least the MSEs (Li and Agee, 1996; Righter et al., 1997). Since the late 1990s, there have been numerous subsequent studies of the partitioning of the MSEs (e.g., Bouhifd and Jephcoat, 2003, 2011; Chabot and Agee, 2003; Chabot et al., 2005; Gessmann and Rubie, 1998, 2000; Kegler et al., 2008; Li and Agee, 2001; Mann et al., 2009; O'Neill et al., 1998; Righter, 2011; Righter and Drake, 1999, 2000, 2001; Siebert et al., 2011, 2012, 2013; Tschauner et al., 1999; Tuff et al., 2011; Wade and Wood, 2005; Wade et al., 2012). A growing consensus emerging from such studies is that the pressures and temperatures required for metal–silicate equilibration were considerably higher than originally suggested. Estimated conditions are quite variable and range up to >4000 K and 60 GPa (**Table 3**; **Figure 13**). One of the reasons for the large scatter of P–T estimates is that, based on the current experimental data set and the associated uncertainties, a wide range of P–T–f_{O_2} conditions can satisfy mantle abundances of the MSEs (**Figure 13**). In addition, the difficulty of identifying a unique set of conditions is hardly surprising considering that core formation occurred over a protracted time period during accretion as the likely consequence of multiple melting events under a range of conditions.

The solubilities of HSEs in silicate liquid have been investigated extensively at 1 bar and moderate temperatures of 1300–1400 °C (e.g., Ertel et al., 1999, 2001; Fortenfant et al., 2003a, 2006), whereas there have been relatively few studies of the solubility or partitioning of HSEs at high pressure. All such studies are beset by a serious technical problem. The quenched samples of silicate liquid inevitably contain numerous metal micronuggets consisting of, or rich in, the element of interest, especially at low f_{O_2}, which make it very difficult to obtain reliable chemical analyses. Although it is normally considered that such nuggets were present in the melt at high temperature (e.g., Holzheid et al., 2000b; Lindstrom and Jones, 1996), it has also been suggested that they form by exsolution from the silicate liquid during quenching (Cottrell and Walker, 2006). However, this latter interpretation can be excluded because Médard et al. (2010) have shown unequivocally, through a high-pressure centrifuge study, that Pt nuggets are present at high temperature and are not the product of quenching. In early studies, the solubilities of Pt and Pd in silicate liquid (Cottrell and Walker, 2006; Ertel et al., 2006; Holzheid et al.,

Table 3 Metal–silicate equilibration conditions during core formation inferred from a selection of studies of siderophile element partitioning

P *(GPa)*	T *(K)*	*References*	*Notes*
28	2400–2700	Li and Agee (1996)	Ni, Co; **T* fixed by peridotite liquidus; $f_{O_2} \approx$ IW-0.5 (expt.)
27	2200	Righter et al. (1997)	Ni, Co, P, Mo, W; f_{O_2} = IW-0.15 (inf.)
37	2300	O'Neill et al. (1998)	Ni, Co, Fe, Cr require 3400 K
>35	>3600	Gessmann and Rubie (2000)	V, Cr, Mn; f_{O_2} = IW-2.3 (inf.)
43–59	2400–4200	Li and Agee (2001)	Ni, Co; f_{O_2} = IW to IW-2 (expt.)
25	3350	Gessmann et al. (2001)	Si; **P* fixed by Ni/Co data; temp exceeds peridotite liquidus
27	2250	Righter and Drake (2003)	P, W, Co, Ni, Mo, Re, Ga, Sn, Cu; f_{O_2} = IW-0.4 (inf.)
40	2800	Walter and Tronnes (2004)	Ni, Co
40	3750	Wade and Wood (2005)	V, Ni, Co, Mn, Si; **T* fixed by peridotite liquidus; evolving f_{O_2}
30–60	>2000	Chabot et al. (2005)	Ni, Co; f_{O_2} = IW-2.2 (inf.); demonstrates solution tradeoffs
22.5	2700	Righter et al. (2010)	11 MSEs; f_{O_2} = IW-2
27–45	3300–3600	Righter (2011)	Compilation of data for 11 MSEs; f_{O_2} = IW-1 to IW-1.5

f_{O_2} is the oxygen fugacity, IW indicates the iron–wüstite buffer, 'inf.' means inferred f_{O_2} for the magma ocean, and 'expt.' indicates the experimental value.

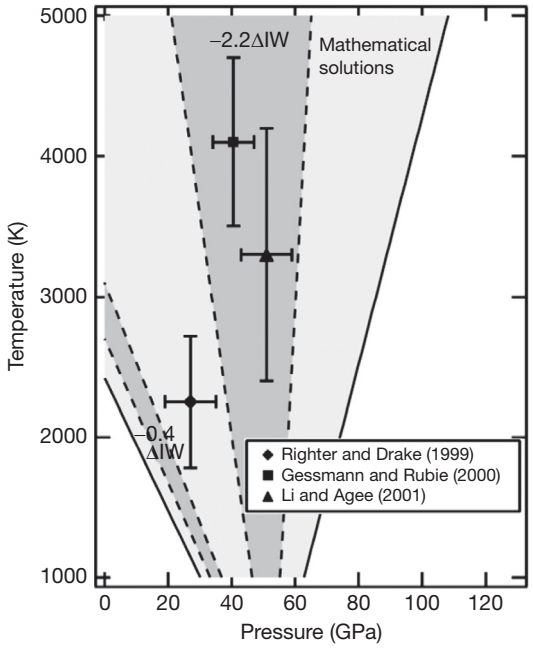

Figure 13 Pressure–temperature conditions of metal–silicate equilibration during core formation that are consistent with the concentrations of Ni and Co in the Earth's mantle, based on experimental studies of the metal–silicate partitioning of these elements. The two dark gray-shaded regions show results calculated for oxygen fugacities of IW-0.4 and IW-2.2, respectively, whereas the light-shaded region shows solutions for all oxygen fugacities. *P–T* estimates from three previous studies are shown by the symbols with error bars. Temperature is poorly constrained because the partition coefficients for Ni and Co depend only weakly on this variable. In order to better constrain the *P–T* conditions of equilibration, it is necessary to consider additional siderophile elements for which partitioning is more strongly temperature-dependent (e.g., Wade and Wood, 2005). Reproduced from Chabot NL, Draper DS, and Agee CB (2005) Conditions of core formation in the Earth: Constraints from nickel and cobalt partitioning. *Geochimica et Cosmochimica Acta* 69: 2141–2151.

2000b), the metal–silicate partitioning of Re (Ohtani and Yurimoto, 1996), the partitioning of Re and Os between magnesiowüstite and liquid Fe (Fortenfant et al., 2003b), and the partitioning of Pd (Righter et al., 2008) were investigated at high pressure. It has been argued that the concentrations of Re, Pt, and Pd in the mantle can be explained by metal–silicate equilibration at high pressure (Cottrell and Walker, 2006; Righter and Drake, 1997; Righter et al., 2008). However, the study of Mann et al. (2012), of the partitioning of Ru, Rh, Pd, Re, Ir, and P between metal and silicate liquids at pressures up to 18 GPa, shows that the concentrations of all HSEs in the mantle and, in particular, their chondritic ratios cannot be explained by high-pressure equilibration, as concluded also by the majority of the studies cited earlier (see also Brenan and McDonough, 2009). In addition, based on studies of Martian meteorites, HSE abundances are similar in the mantles of both Earth and Mars (Walker, 2009; Warren et al., 1999). This cannot be explained by metal–silicate equilibration because, in planets of dissimilar sizes, *P–T* conditions of core formation must be quite different. Therefore, metal–silicate HSE partitioning results are generally interpreted to support the late-veneer hypothesis (see next section) for both Earth and Mars (e.g., Day et al., 2012; Righter, 2005).

There are serious problems with the simple concept of metal–silicate equilibration at the base of a magma ocean (Rubie et al., 2003) and, in particular, with the so-called 'single-stage' core formation models as proposed, for example, by Corgne et al. (2009) and Righter (2011). The complete process of core formation in the Earth cannot have been accomplished physically through a single event involving a magma ocean of limited depth (e.g., 800–1500 km). Several large impacts are likely to have occurred during accretion, each generating a magma ocean with different characteristics, while there may also have been a steady background flux of smaller impactors.

Each impact would have caused an episode of core formation, with conditions varying from one impact to the next. The claim of Righter (2011) that "The single PT point of this study is likely the last record of major equilibration in this series of large magnitude impacts and subsequent melting leading to the Earth's final size. The energy associated with a large impact and subsequent heating due to metal–silicate segregation, will cause extensive reequilibration" requires that the entire core and mantle of the Earth reequilibrated chemically at a depth of 700–1200 km after accretion was almost complete. Because of the large density difference between core and mantle and the need for the core to fully emulsify, such reequilibration is physically impossible, especially at a relatively shallow depth. Thus, the conditions listed in **Table 3** must be considered, at best, to be average values of a broad range of conditions.

9.03.3.2.2.3 Models of continuous and multistage core formation

In order to study core formation more realistically, two approaches have been adopted, involving (a) continuous core formation (e.g., Wade and Wood, 2005) and (b) multistage core formation (Rubie et al., 2011, 2015). Both models have an important feature in common with the heterogeneous two-stage accretion models described earlier – a transition from initially very reducing to more oxidizing conditions during accretion. However, they differ from the earlier models by requiring metal–silicate equilibration at high pressures.

Wade and Wood (2005) presented a model in which core formation occurs continuously during accretion (see also, e.g., Tuff et al., 2011; Wade et al., 2012; Wood et al., 2006). This model utilizes the metal–silicate partitioning of a range of elements, including Fe, Ni, Co, V, W, Nb, and Cr, and is based on the assumption of metal–silicate equilibration at or near the base of a magma ocean that deepens as the Earth grows in size. The temperature at the base of the magma ocean is constrained to lie on the peridotite liquidus. Wade and Wood (2005) discovered that, in order to satisfy the observed mantle abundances of all elements considered (and especially V), it is necessary that the oxygen fugacity is initially very low but increases during accretion to satisfy the current FeO content of the mantle (**Figure 14**). Typically in such models, equilibration pressures increase up to a maximum of 40–50 GPa during accretion (e.g., **Figure 14(b)**).

The exact oxygen fugacity path followed during accretion cannot be defined uniquely in these models (e.g., see **Figure 14(a)**). The original explanation for the increase in f_{O_2}

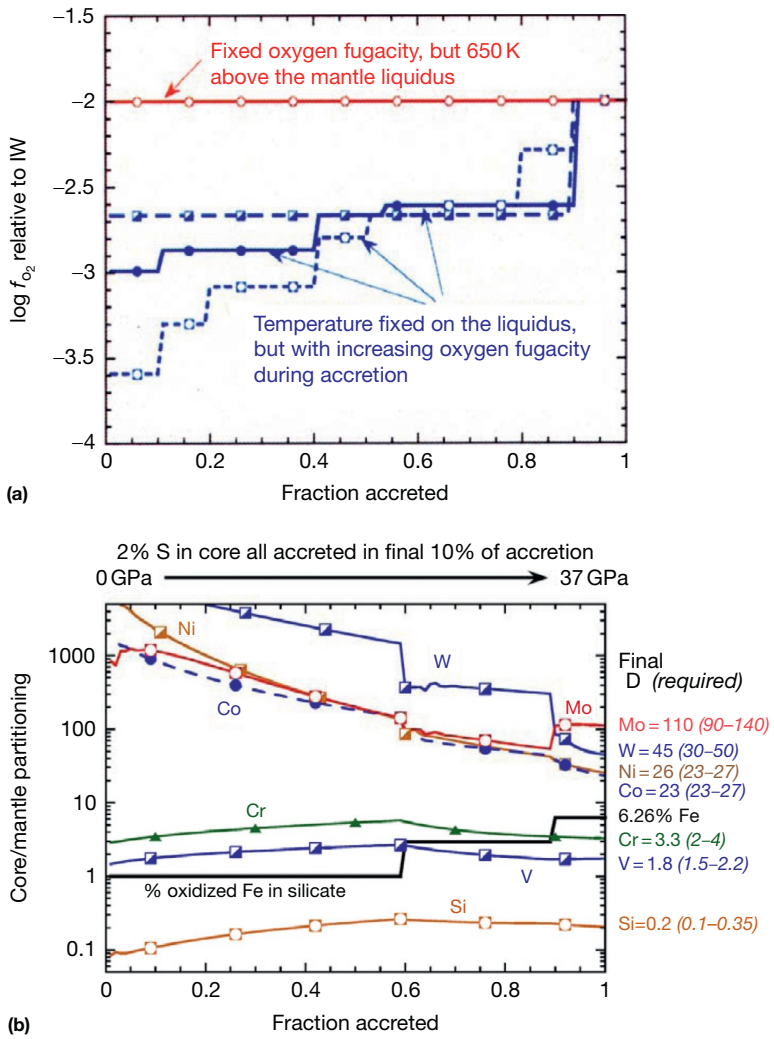

Figure 14 Models involving continuous core formation during accretion of the Earth based on metal–silicate equilibration at the base of a deepening magma ocean. (a) Oxygen fugacity is plotted as a function of fraction accreted. The temperature at the base of the magma ocean is constrained to lie on the peridotite liquidus for the variable oxygen fugacity models. In order to satisfy concentrations of a range of siderophile elements in the mantle, the oxygen fugacity has to be low initially and then increase during accretion for reasons described in the text. Several possible oxygen fugacity evolution paths are shown (Reproduced from Wood BJ, Walter MJ, and Wade J (2006) Accretion of the Earth and segregation of its core. *Nature* 441: 825–833. http://dx.doi.org/10.1038/nature04763.). (b) The evolution of core–mantle partition coefficients for Si, Fe, V, Cr, Ni, Co, W, and Mo as a function of the fraction of the Earth accreted. The addition of S to the core during the final stages of accretion enables the final values for W and Mo to be achieved (Reproduced from Wade J, Wood BJ, and Tuff J (2012) Metal–silicate partitioning of Mo and W at high pressures and temperatures: Evidence for late accretion of sulphur to the Earth. *Geochimica et Cosmochimica Acta* 85: 58–74.).

is based on the so-called 'oxygen pump' mechanism. This involves the crystallization of silicate perovskite from the magma ocean, which can only occur once the Earth has reached a critical size such that the pressure at the base of the magma ocean reaches ~24 GPa. Because of its crystal chemistry, the crystallization of silicate perovskite causes ferrous iron to dissociate to ferric iron + metallic iron by the reaction

$$\underset{\text{silicate liquid}}{Fe^{2+}} \rightarrow \underset{\text{perovskite}}{Fe^{3+}} + \underset{\text{metal}}{Fe}$$

(Frost et al., 2004). If some or all of the metal produced by this reaction is transferred from the mantle to the core, the Fe^{3+} content and the f_{O_2} of the mantle both increase. Wade and Wood (2005), however, incorrectly argued that this 'oxygen pump' mechanism could have increased the f_{O_2} of the mantle during core–mantle equilibration from the reduced levels (<ΔIW-3) required in the early stages of their model, where Si and V would have entered the core, to the more oxidized levels (~ΔIW-2) that allowed elements such as Fe, Ni, and Co to partially remain in the mantle. This is not possible because raising the f_{O_2} from this level requires the FeO content of the silicate mantle to increase, whereas the 'oxygen pump' mechanism can only raise the Fe^{3+} content (i.e., the Fe^{3+}/Fe^{2+} ratio) of the mantle. Although the oxygen content of the mantle is increased through disproportionation, the total Fe content of the mantle is actually lowered as Fe must be lost to the core. Although disproportionation raises the O/Fe ratio of the silicate mantle, further reaction of the newly liberated oxygen with

more accreting Fe metal only leaves the FeO content of the mantle at the same level as it was before disproportionation occurred. While the 'oxygen pump' mechanism is effective at raising the Fe^{3+} content of the mantle and the f_{O_2} of the upper mantle to levels above those of iron saturation, it cannot influence the f_{O_2}, while the mantle remains at iron saturation, that is, while core formation was still occurring (see also Frost et al., 2008).

Other possible causes of an increase in f_{O_2} are (a) the partitioning of Si into core-forming metal, which increases the FeO content of the mantle (see succeeding text); (b) the addition of bodies to the Earth that are increasingly oxidized as accretion progresses (see also succeeding text); and (c) the dissociation of accreted water due to hydrogen loss.

A model of multistage core formation has been formulated by Rubie et al. (2011). This involves the Earth accreting through a series of violent collisions with smaller differentiated bodies, with each collision resulting in a magma ocean and an episode of metal–silicate segregation. The model is based on a simple and idealized accretion scenario whereby each impacting body has a mass around 10% of the Earth's mass at the time of impact. Thus, as the Earth grows in size, the impacting bodies also become larger. The metallic cores of the impactors fully or partially equilibrate in the magma ocean before merging with the Earth's protocore. It is further assumed that the metal–silicate equilibration pressure is a constant fraction of the CMB pressure at the time of impact and that the corresponding equilibration temperature lies on the peridotite liquidus. In contrast to previous core formation models, no assumptions are made about oxygen fugacity. Instead, the bulk composition of accreting material is defined in terms of the nonvolatile elements Si, Al, Mg, Fe, Al, Ni, Co, Cr, V, Nb, W, and Ta. These elements are considered to have solar system (CI chondritic) relative abundances but with enhanced concentrations of the refractory elements Ca, Al, V, Nb, W, and Ta (Palme and O'Neill, 2003). Different bulk oxygen contents result in different oxidation states. For example, an oxygen-poor (reduced) composition would result in a high proportion of total Fe being present as metal and a significant amount of Si being dissolved in the metal. A more oxidized composition would have a significant proportion of total Fe as FeO and zero Si in the metal. In order to determine the compositions of coexisting silicate and metal liquids after equilibration at high pressure and temperature, the compositions are expressed in terms of the molar concentrations of major elements, as follows:

$$\underset{\text{silicate liquid}}{\left[(\mathrm{FeO})_x(\mathrm{NiO})_y(\mathrm{SiO_2})_z(\mathrm{Mg}_u\mathrm{Al}_m\mathrm{Ca}_n)\mathrm{O}\right]} + \underset{\text{metal liquid}}{[\mathrm{Fe}_a\mathrm{Ni}_b\mathrm{O}_c\mathrm{Si}_d]}$$

Here, the indexes u, m, and n, which describe the concentrations of lithophile elements, are determined from the bulk composition. The other seven indexes, x, y, z, a, b, c, and d, are determined using four mass balance equations (for Fe, Ni, Si, and O), based on the bulk composition, and three models that describe the metal–silicate partitioning of Ni, Si, and O. The concentrations of the trace elements Co, Cr, V, Nb, W, and Ta have a negligible effect on the mass balance and are determined from partitioning alone. As mentioned earlier, this approach avoids making any assumptions about oxygen fugacity, although this parameter can be determined from the partitioning of Fe (e.g., **Figure 2** in Rubie et al., 2011).

Using this approach to model core formation, the evolving compositions of the mantle and core were determined as a function of mass accreted (**Figure 15**). The main constraint is the composition of the Earth's primitive mantle (e.g., Palme and O'Neill, 2003), and this composition was achieved in the model through a least squares optimization of several fitting parameters. The latter include the oxygen content(s) of accreting material, the metal–silicate equilibration pressure, and the fraction of metal that equilibrates in the magma ocean. Poor results were obtained for homogeneous accretion – that is, when the oxygen content of the accreting material is constant. Best results were obtained with heterogeneous accretion with the initial 60–70% of the Earth accreting from highly reduced material and the final 30–40% accreting from more oxidized material. This scenario is consistent with accretion models because material originating relatively close to the Sun (e.g., ~1 AU) is expected to be volatile-poor and reduced, while material originating far from the Sun would be richer in volatiles (including water) and therefore more oxidized. The evolution from reduced to oxidized compositions results in an oxygen fugacity evolution (**Figure 15(c)**) that is qualitatively similar to those of the models of Wänke (1981), O'Neill (1991), and Wade and Wood (2005) (see preceding text). It is also consistent with conclusions regarding heterogeneous accretion based on Pd–Ag isotopes (Schönbächler et al., 2010). The initially reduced composition is required in order to partition sufficient V, Cr, and Si into the core, whereas the later addition of oxidized material enables the FeO content of the mantle to be achieved. In addition to requiring heterogeneous accretion, some degree of disequilibrium (incomplete equilibration of the impactors' metallic cores) was found to be necessary in this model.

In addition to the effects of the late accretion of oxidized material, a progressive increase in oxygen fugacity results from the following reaction (originally proposed by Javoy, 1995):

$$\underset{\text{metal}}{2\mathrm{Fe}} + \underset{\text{silicate}}{\mathrm{SiO_2}} = \underset{\text{metal}}{\mathrm{Si}} + \underset{\text{silicate}}{2\mathrm{FeO}}$$

As temperature increases, Si partitions increasingly into the metal (e.g., Mann et al., 2009; see also **Section 9.03.3.3**) with the result that the FeO content of the silicate and f_{O_2} both increase.

9.03.3.2.2.4 The 'late-veneer' hypothesis

According to this hypothesis, the main stage of core formation resulted in the almost complete extraction of HSEs from the mantle into the metallic core, under reducing oxygen fugacity conditions (e.g., Kimura et al., 1974; Morgan, 1986; O'Neill, 1991; O'Neill and Palme, 1998; Righter, 2005; Walker, 2009). At a very late stage of accretion, a thin veneer of chondritic material was added to the Earth under relatively oxidizing conditions, such that the HSEs were retained in the mantle in approximately chondritic ratios. The mass of material added at this late stage is considered to be <1% of the entire mantle. This is currently the most widely accepted 'heterogeneous' core formation model (e.g., Mann et al., 2012; Walker, 2009). An

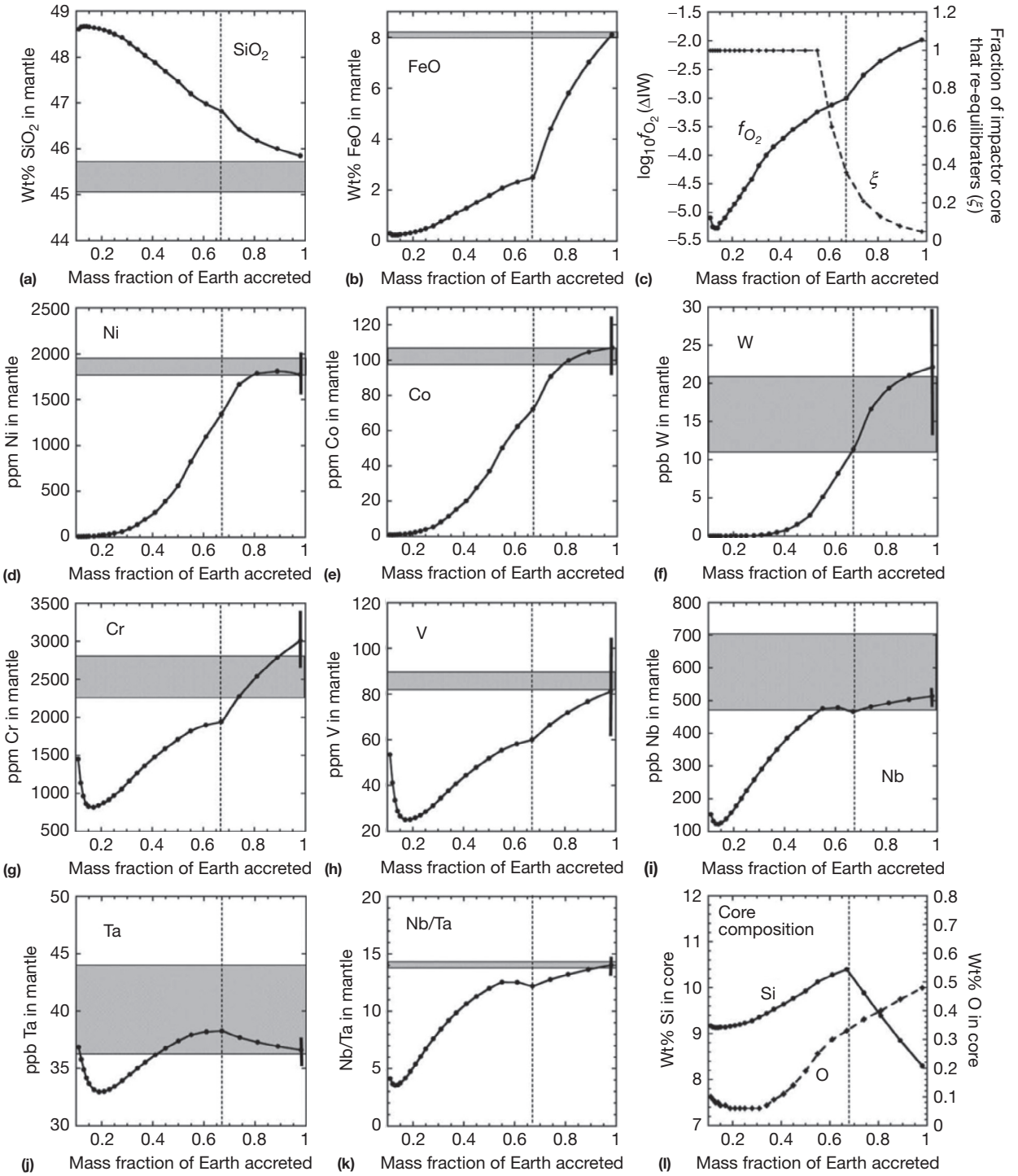

Figure 15 The evolution of mantle (a and b, d–k) and core (l) compositions as a function of mass accreted in the multistage core formation model of Rubie et al. (2011). The evolution of f_{O_2} and the extent of metal–silicate disequilibrium are shown in (c). Reproduced from Rubie DC, Frost DJ, Mann U, et al. (2011) Heterogeneous accretion, composition and core–mantle differentiation of the Earth. *Earth and Planetary Science Letters* 301: 31–42, http://dx.doi.org/10.1016/j.epsl.2010.11.030.

important constraint on this process is that, while the Earth's abundance of HSEs requires a late addition of undifferentiated material, the lack of HSEs intrinsic to the Moon indicates that it did not receive the same addition. Different arguments have been put forth to explain this puzzle, one of the most recent being that the late veneer was added in a collision with a single, large body that struck the Earth but, by the statistics of small numbers, happened to miss the Moon. The dynamics of this late accretion process have been discussed by Bottke et al. (2010).

9.03.3.2.2.5 Addition of outer core material to the lower mantle

It has been suggested that HSE abundances in the Earth's mantle have resulted from core–mantle interaction (Brandon and Walker, 2005), for example, by the addition of a small amount of core metal to the mantle (Snow and Schmidt, 1998). This could potentially occur by capillary action (considered highly unlikely by Poirier et al., 1998) or by dilatancy caused by volume strain (Kanda and Stevenson, 2006; Rushmer et al., 2005). Alternatively, siderophile elements could be added to the base of the mantle by crystallization of oxides or silicates due to the growth of the inner core (Walker, 2000, 2005), and chemical exchange could be facilitated by the presence of partial melt in the lower few kilometers of the mantle or a basal magma ocean (Labrosse et al., 2007). In this case, the metal–silicate partition coefficients at CMB conditions would have to be orders of magnitude lower than at low *P*–*T* conditions and would need to result in the addition of the HSEs in approximately chondritic proportions.

9.03.3.2.3 Metal–silicate fractionation models

The simplest model of metal–silicate fractionation during core formation involves the ponding of liquid iron at the base of a convecting magma ocean with chemical equilibration occurring at the metal–silicate interface (**Section 9.03.3.2.2.1**, **Figure 8(a)**). An appealing feature of this model is that siderophile element abundances in the mantle can be interpreted directly in terms of magma ocean depth (e.g., Li and Agee, 1996; Righter, 2011; Righter et al., 1997). The timescale required for chemical equilibration across the metal–silicate interface has been investigated by Rubie et al. (2003) assuming that mass transport occurs by chemical diffusion through boundary layers that exist above and below the interface. Assuming that a magma ocean crystallizes from the bottom up, the initial crystallization of silicate minerals at the base of the magma ocean will terminate equilibration between the ponded iron and the overlying magma ocean. Thus, Rubie et al. (2003) also calculated the timescale required for the initial crystallization of the base of a magma ocean. Results are dependent upon the depth of the magma ocean and suggest that equilibration times are almost three orders of magnitude greater than cooling times (**Figure 16**). Such a result is also predicted by considering that rates of conductive heat transfer are much faster than rates of chemical diffusion (Rubie et al., 2003). Therefore, these results appear to rule out simple chemical equilibration at the base of the magma ocean.

The equilibration model of Rubie et al. (2003) is based on the assumption that a dense atmosphere was not present during magma ocean crystallization. The effect of such an insulating atmosphere would be to reduce the rate of heat loss and therefore prolong the lifetime of the magma ocean. However, the rate of convection would also be reduced, which would slow the rate of chemical exchange across the metal–silicate interface. Thus, the presence of an insulating atmosphere is unlikely to affect the conclusions of Rubie et al. (2003). However, as described earlier, there has been a suggestion that a magma ocean adiabat is much steeper than formerly believed with the consequence that terrestrial magma oceans might crystallize from the top down rather than from the bottom up (Mosenfelder et al., 2007, 2009; c.f. Miller et al., 1991). In this case, magma ocean crystallization would be much slower, and the possibility of simple metal–silicate equilibration at its base might need to be reconsidered.

It is currently assumed in core formation models that metal–silicate separation takes place in a magma ocean of global extent and of more or less constant depth (**Figure 8**). As discussed earlier in **Section 9.03.2.3.2**, this assumption requires reconsideration. **Figure 17** shows an alternative model in which the magma ocean that is generated by a large impact is initially a hemispheric body of limited lateral extent. The attainment of isostatic equilibrium eventually results in the formation of a global magma ocean, but metal segregation could already have taken place before this developed. Pressure at the base of the initial hemispheric magma ocean is clearly much higher than at the base of the final global magma ocean,

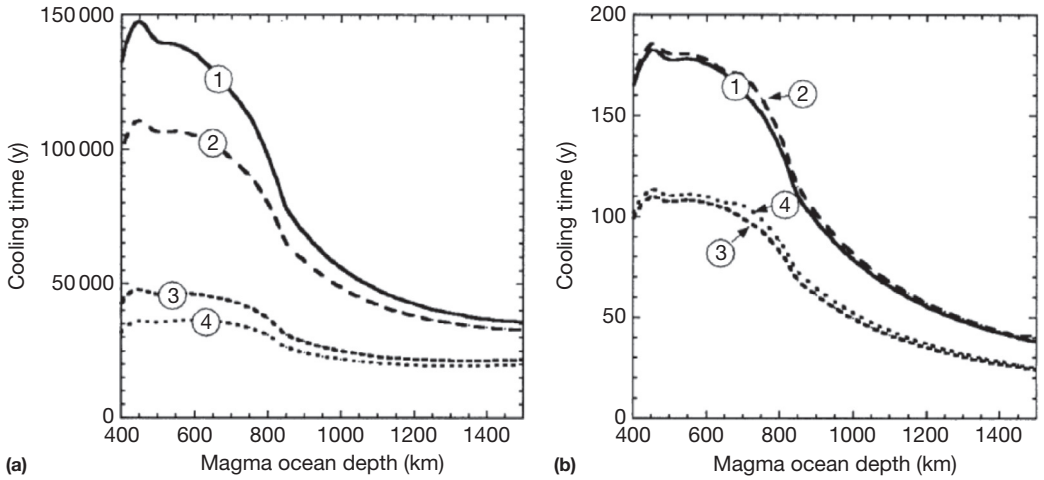

Figure 16 Results of a model in which a layer of segregated (ponded) liquid iron equilibrates with an overlying convecting magma ocean. (a) Time to reach 99% equilibration between metal and silicate as a function of magma ocean depth. (b) Time required for initial crystallization at the base of the magma ocean (thus effectively terminating the equilibration process). The four curves (1–4) are results for a wide range of plausible model parameters. Reproduced from Rubie DC, Melosh HJ, Reid JE, Liebske C, and Righter K (2003) Mechanisms of metal–silicate equilibration in the terrestrial magma ocean. *Earth and Planetary Science Letters* 205: 239–255.

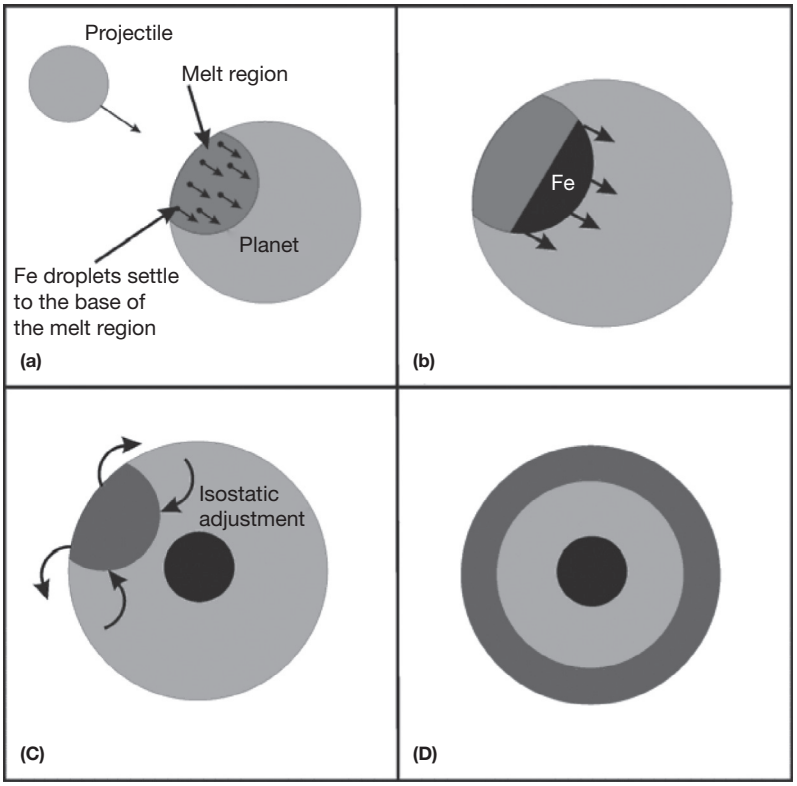

Figure 17 Possible evolution of a deep magma ocean that forms as a consequence of a giant impact. (a) Initially, a hemispheric magma ocean forms that is of limited lateral extent. There is the possibility that iron, emulsified in the form of small dispersed droplets, settles and segregates rapidly to form a protocore at the bottom of this magma ocean (b and c). Subsequent isostatic adjustment causes the magma ocean to evolve into a layer of global extent (d). The relative timing of the processes of metal segregation and isostatic adjustment determines the pressure (and probably also temperature) conditions of metal–silicate equilibration. Reproduced from Tonks WB and Melosh HJ (1992) Core formation by giant impacts. *Icarus* 100: 326–346.

which means that the partitioning of siderophile elements could depend critically on the timing of metal segregation.

As discussed earlier, liquid metal is likely to be present in a magma ocean in the form of small droplets ~1 cm in diameter. Such droplets remain in chemical equilibration with the magma as they settle out and *P*–*T* conditions change because diffusion distances are short (Karato and Murthy, 1997; Rubie et al., 2003). It is necessary to understand the chemical consequences of the settling out of such droplets in order to interpret siderophile element geochemistry in terms of magma ocean depths. Rubie et al. (2003) considered two end-member models for the partitioning of Ni. The models are based on the parameterized Ni partitioning formulation of Righter and Drake (1999), which requires a magma ocean depth of ~800 km for metal–silicate equilibration at its base to produce the estimated core–mantle partition coefficient of ~28. In Model 1 of Rubie et al. (2003), the magma ocean is static (i.e., no convection or mixing) and droplets that are initially uniformly dispersed, settle out, and reequilibrate progressively as they fall. This polybaric equilibration model requires a magma ocean ~1400 km deep (**Figure 18**) because much of the silicate equilibrates at relatively low pressures $D_{\mathrm{M}}^{\mathrm{met-sil}}$ where values are high. Model 2 of Rubie et al. (2003) is based on an assumption of vigorous convection keeping the magma ocean fully mixed and chemically homogeneous. The iron droplets equilibrate finally with silicate liquid at the base of the magma ocean just before segregating into a ponded layer. Because the mass fraction of metal that is available to equilibrate with silicate progressively decreases with time, the effectiveness of metal to remove siderophile elements from the magma ocean also decreases. This model requires a magma ocean ~550 km deep to produce the desired core–mantle partition coefficient of 28 (**Figure 18**).

The two end-member Models 1 and 2 are clearly both physically unrealistic, and a more realistic model must lie somewhere between the two extremes shown in **Figure 18**. In order to investigate the chemical consequences of metal–silicate segregation in a deep magma ocean more rigorously, Höink et al. (2006) have combined two- and three-dimensional numerical convection models with a tracer-based sedimentation method. They found that metal droplets stabilize the magma ocean against convection and that convection only develops in the upper layer of a magma ocean after it has become depleted in iron droplets. The timescale for droplet separation was found to be identical to the Stokes' settling time. Because of the lack of convection in the droplet-dominated layer, the chemical consequences are similar to those of Model 1 of Rubie et al. (2003), although the results of the two- and three-dimensional models of Höink et al. (2006) appear to be very different from each other (see their Figure 20). It must also be noted that, for computational reasons, the Rayleigh numbers in the models

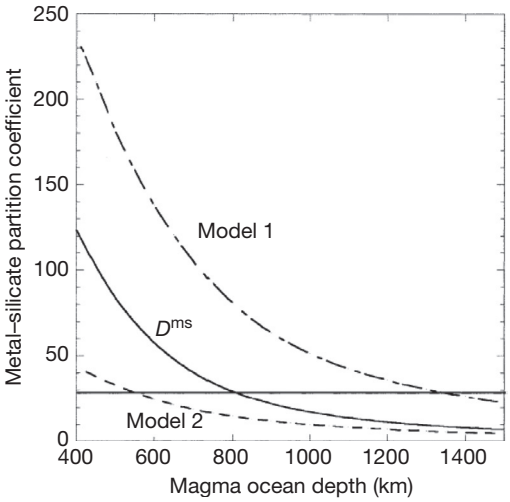

Figure 18 Results of different metal–silicate fractionation models for the siderophile element Ni as a function of magma ocean depth. The core–mantle partition coefficient for this element is estimated to be ~28 (as indicated by the horizontal line). The curve labeled D^{ms} indicates results for simple equilibration between a ponded liquid metal layer and the overlying magma ocean and requires a magma ocean ~800 km deep to obtain the core–mantle value. However, this model is unlikely to be realistic (**Figure 16**). Models 1 and 2 represent extreme end-member cases (see text for details) and require magma ocean depths of ~1400 and ~550 km, respectively. Rubie DC, Melosh HJ, Reid JE, Liebske C, and Righter K (2003). Mechanisms of metal–silicate equilibration in the terrestrial magma ocean. *Earth and Planetary Science Letters* 205: 239–255.

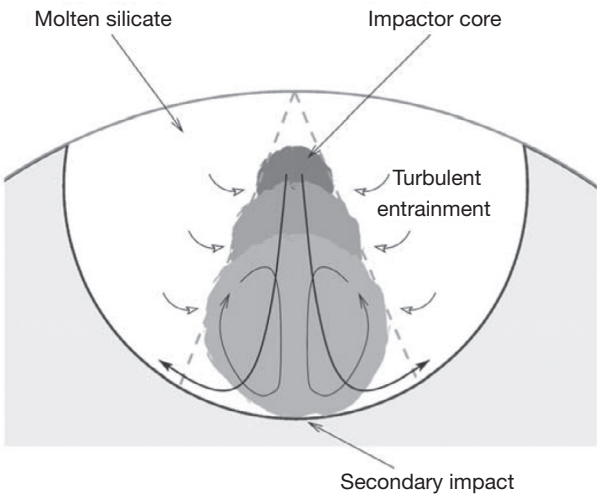

Figure 19 Model of a metallic core of an impactor sinking in a magma ocean. The turbulent entrainment of silicate liquid leads to the descent of a metal–silicate plume. With increasing depth, the plume broadens and an increasing volume of silicate is entrained. Chemical equilibration between metal and the entrained silicate liquid is expected to occur near the base of the magma ocean. Reproduced from Deguen R, Olson P, and Cardin P (2011) Experiments on turbulent metal–silicate mixing in a magma ocean. *Earth and Planetary Science Letters* 310: 303–313.

of Höink et al. (2006) have values of $\leq 10^7$, whereas the Rayleigh number for a deep magma ocean is on the order of 10^{27}–10^{32}, that is, 20–25 orders of magnitude higher (see **Section 9.03.2.3.2**). It is also difficult to understand the lack of composition-driven convection in the Höink et al. model. Only slight variations in the iron/silicate mixture ratio in the lower part of the ocean should create density variations much larger than those induced by thermal variations and thus drive a much more vigorous convection that, while the iron is settling, may overwhelm thermal convection. The Höink et al. models also seem to neglect the very substantial heating that may occur in the lower part of the magma ocean due to the conversion of the gravitational energy of the falling iron droplets into thermal energy, as discussed in **Section 9.03.2.2.3**. Preliminary numerical models of the iron separation process that do include these effects give substantially different results than the Höink et al. models (Melosh and Rubie, 2007). This is a rapidly developing area of research and controversy at the current time.

An alternative and perhaps more realistic physical model for the descent and equilibration of an impactor's core through a magma ocean has been presented by Deguen et al. (2011). This involves the silicate liquid immediately adjacent to the descending mass of metal undergoing turbulent entrainment such that a mixture of metal and silicate descends as an expanding plume or density current (**Figure 19**). The radius of the entrained silicate plume increases linearly with depth so that the volume ratio of metal to silicate in the descending plume decreases with depth and can be determined from

$$\phi = \left(\frac{r_0}{r}\right)^3 = \left(1 + \frac{\alpha z}{r_0}\right)^{-3} \quad [12]$$

where ϕ is the volume fraction of metal in the metal–silicate mixture, r_0 is the original radius of the impacting core, r is the radius of the descending plume, z is depth, and α is a constant with a value ~0.25. An important consequence of this model is that the metal only equilibrates chemically with a small fraction of the total volume of silicate melt in the magma ocean – which, in turn, makes the equilibration pressures required to reproduce mantle siderophile element concentrations higher.

9.03.3.2.4 Concluding remarks

The consistency of MSE abundances with metal–silicate equilibration at high P–T conditions implies that element abundances produced by earlier equilibration in smaller bodies at lower P–T conditions must have been strongly overprinted. This conclusion supports the idea of impactor cores undergoing reequilibration in the magma ocean, presumably as a result of partial or complete emulsification (Rubie et al., 2003). Later events that did not involve reequilibration (e.g., the descent of large iron diapirs through the lower mantle) would leave little or no signature in the observed siderophile element abundances.

9.03.3.3 Light Elements in the Core

The density of the Earth's core is too low, by 5–10%, for it to consist only of Fe and Ni (e.g., Anderson and Isaak, 2002; Birch, 1952). It has therefore been postulated that the core must contain up to ~10 wt% of one or more light elements, with the most likely candidates being S, O, Si, C, P, and H (Poirier, 1994). Knowledge of the identity of the light element(s) is important for constraining the bulk composition

of the Earth and for understanding processes occurring at the CMB and how such processes are affected by crystallization of the inner core (e.g., Buffett et al., 2000; Buffett and Seagle, 2010; Helffrich and Kaneshima, 2004). The main constraints on the identity of the light elements present in the core are based on cosmochemical arguments (McDonough, 2003), experimental data (Badro et al., 2007; Hillgren et al., 2000; Li and Fei, 2003), computational simulations (e.g., Alfe et al., 2002), silicon isotope fractionation (e.g., Fitoussi et al., 2009; Georg et al., 2007; Ziegler et al., 2010), and core formation modeling (Rubie et al., 2011). The topic has been reviewed in part by Hillgren et al. (2000), McDonough (2003), and Li and Fei (2003), and here, we provide only a brief summary of the main arguments and experimental results.

The sulfur content of the core, based on the volatility of this element, is likely to be no more than 1.5–2 wt% (Dreibus and Palme, 1996; McDonough, 2003; McDonough and Sun, 1995). Similarly, cosmochemical constraints suggest that only very small amounts (e.g., $\leq$0.2 wt%) of C and P are present in the core (McDonough, 2003); therefore, these elements are unlikely to contribute significantly to the density deficit.

One of the main controversies concerning the identity of the principal light element(s) in the core involves silicon and oxygen. A high oxygen content is favored by high oxygen fugacity, whereas a high Si content is favored by low oxygen fugacity (Hillgren et al., 2000; Kilburn and Wood, 1997; Li and Fei, 2003; Malavergne et al., 2004). It has therefore been proposed that these two elements are almost mutually exclusive (Figure 10 in O'Neill et al., 1998). Some models of core composition have been based on this exclusivity – that is, it is assumed that the core contains either Si or O but not both of these elements (McDonough, 2003, Table 7). However, the effects of high pressure and temperature are also critical.

Based on experimental results of Gessmann et al. (2001), obtained up to 23 GPa and 2473 K, the solubility of Si in liquid iron increases with both P and T. An extrapolation of their experimental data shows that ~7 wt% Si can be dissolved in liquid Fe at 25–30 GPa, 3100–3300 K, and an f_{O_2} (IW-2), conditions that are often considered to be applicable for core formation (**Figure 20**). This result is in accordance with the geochemical model of the core of Allegre et al. (1995) in which ~7 wt% Si in the core was proposed based on the Mg/Si ratio of the mantle being high compared with CI chondrites. It is also consistent with the results of Si isotope studies (Fitoussi et al., 2009; Georg et al., 2007; Ziegler et al., 2010). Experimental results comparable to those of Gessmann et al. (2001), suggesting a strong effect of temperature and a weak effect of pressure on the metal–silicate partitioning of Si, have been published by Wade and Wood (2005) and Mann et al. (2009).

Oxygen was first proposed as the principal light element in the core more than 30 years ago (e.g., Ohtani and Ringwood, 1984; Ohtani et al., 1984; Ringwood, 1977). Whereas it is clear that the solubility of this element in liquid Fe increases strongly with temperature, the effect of pressure has been controversial. According to studies of phase relations in the Fe–FeO system, solubility increases with pressure (Kato and Ringwood, 1989; Ringwood, 1977). However, investigations of the partitioning of FeO between magnesiowüstite and liquid Fe have indicated that solubility decreases with increasing pressure and, based on a very large extrapolation, would be essentially zero at

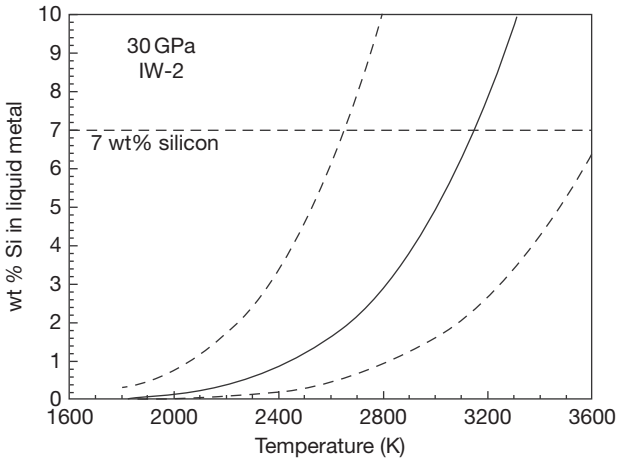

Figure 20 Solubility of Si in liquid Fe alloy at 30 GPa and an oxygen fugacity of IW-2 based on an extrapolation of experimental data. The dashed lines show the extent of the uncertainty envelope based on error propagation. Reproduced from Gessmann CK, Wood BJ, Rubie DC, and Kilburn MR (2001) Solubility of silicon in liquid metal at high pressure: Implications for the composition of the Earth's core, *Earth and Planetary Science Letters* 184: 367–376.

conditions of the CMB (O'Neill et al., 1998; Rubie et al., 2004). Asahara et al. (2007) and Frost et al. (2010) have resolved the controversy by showing that the partitioning of FeO into liquid Fe decreases weakly with pressure up to ~15 GPa and then increases again at high pressures. The reason for the change in pressure dependence is that the Fe–O component dissolved in liquid Fe is more compressible than FeO dissolved in an oxide or silicate phase. Thus, the sign of the volume change (ΔV) of the exchange reaction of oxygen between silicates/oxides and liquid Fe reverses at 10–15 GPa (see also Ohtani et al., 1984; Walker, 2005). As discussed in the succeeding text, the partitioning of oxygen into liquid iron appears to be high enough at core formation conditions for this element to be a significant light element in the Earth's core (Asahara et al., 2007; Rubie et al., 2004; Siebert et al., 2013).

High-pressure studies using the LH-DAC suggest that concentrations of both oxygen and silicon could be significant in the core and could, in combination, account for the density deficit. Takafuji et al. (2005) found 3 wt% Si and 5 wt% O in liquid Fe in equilibrium with (Mg,Fe)SiO3 perovskite at 97 GPa and 3150 K. In similar experiments on liquid Fe coexisting with the postperovskite phase, Sakai et al. (2006) found up to 6.3 wt% O and 4 wt% Si in liquid Fe at 139 GPa and 3000 K. These results should be regarded as preliminary because of the huge temperature gradients and large temperature uncertainties that are characteristic of LH-DAC experiments; in addition, the oxygen fugacity was probably not buffered. In the case of oxygen, the LH-DAC results are mostly consistent with the lower-pressure data of Asahara et al. (2007). However, the silicon results indicate considerably higher solubilities than those predicted by Gessmann et al. (2001). This may be due to Si–O interactions that cause the partitioning of Si into metal to be enhanced by the presence of oxygen in the metal (Tsuno et al., 2013). The high mutual solubilities of O and Si, compared with low P–T results

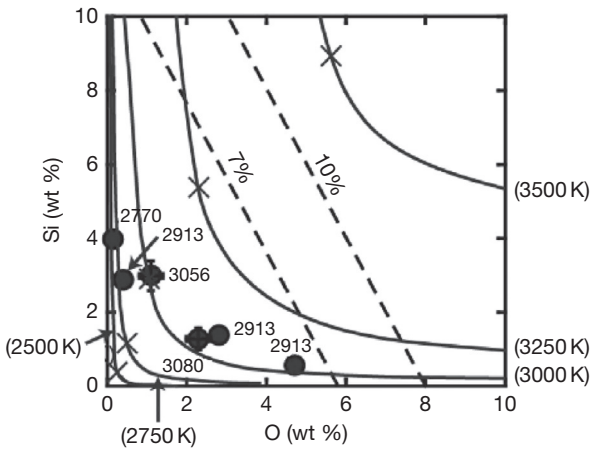

Figure 21 Concentrations of O and Si in liquid iron in equilibrium with silicate liquid at 25 GPa based on experimental data (filled circles) obtained up to 3080 K; the solid lines show a fitted thermodynamic model calculated at temperatures up to 3500 K (Tsuno et al., 2013). (For comparison, see a similar 1 bar plot of O'Neill et al., 1998, **Figure 10**.) Because high O concentrations are favored by high f_{O_2} and high Si concentrations require a low f_{O_2}, the concentrations of these elements in liquid Fe are almost mutually exclusive at low temperatures. At temperatures >3000 K, however, both elements can be present in significant concentrations. The dashed lines indicate concentrations required to account for the 7–10% density deficit of the core, and the crosses indicate concentrations that would result from equilibration with silicate liquid containing 8 wt% FeO. Reproduced from Tsuno K, Frost DJ, and Rubie DC (2013) Simultaneous partitioning of silicon and oxygen into the Earth's core during early Earth differentiation. *Geophysical Research Letters* 40: 66–71.

(O'Neill et al., 1998), are largely the consequence of high temperatures as shown in **Figure 21**.

An additional important observation is that the outer core has a larger density deficit and therefore appears to contain a higher concentration of light element(s) than the inner core (Alfe et al., 2002; Jephcoat and Olson, 1987). This implies that the light element(s) partitions strongly into liquid iron during freezing, which is potentially diagnostic behavior. For instance, Alfe et al. (2002), using molecular dynamics simulations, found that oxygen, due to its small atomic radius, tends to be expelled during the freezing of liquid iron. Conversely, S and Si have atomic radii similar to that of iron at core pressures and thus substitute freely for iron in the solid inner core. Based on the observed density difference between the inner and the outer cores, Alfe et al. (2002) predicted ~8 wt% oxygen in the outer core. These results support the case for O being the main light element and are in agreement with the predictions of Asahara et al. (2007) and Siebert et al. (2013).

The Earth's core is considered not to be in chemical equilibrium with the mantle (Stevenson, 1981), and light element solubilities at core conditions are therefore not necessarily indicative of the actual concentrations of these elements in the core. Instead, the light element content of the core is likely to have been set during core formation, as was the case for the siderophile elements. As discussed earlier, studies of the metal–silicate partitioning of the MSEs indicate that core–mantle partitioning is consistent with metal–silicate equilibration at average conditions of 30–60 GPa and ≤4000 K (**Table 3**). Thus, metal–silicate partitioning of light elements (e.g., O and Si) at such conditions may have determined the light element content of the core. Rubie et al. (2004) investigated this possibility by modeling the partitioning of oxygen (actually the FeO component) between a silicate magma ocean and liquid Fe alloy during core formation as a function of magma ocean depth. Because oxygen solubility in liquid Fe increases strongly with temperature, FeO partitions increasingly into the Fe alloy as the magma ocean depth is increased beyond 1000 km, leaving the silicate depleted in FeO (**Figure 22(a)**). The results of this model are consistent with equilibration in a magma ocean 1200–2000 km deep and with the Earth's core containing 7–8 wt% oxygen.

The Earth's mantle contains ~8 wt% FeO, whereas, based on studies of Martian meteorites, the Martian mantle is considered to contain ~18 wt% FeO. This difference can be explained by oxygen partitioning during core formation so that the possibility that the two planets have similar (or even identical) bulk compositions cannot be excluded (Rubie et al., 2004). Because Mars is a much smaller planet than Earth, temperatures and pressures in a Martian magma ocean are expected to have been relatively low, so that little FeO was extracted from the mantle during core formation (**Figure 21(b)**). This model may also explain why the mass fraction of the Martian core is smaller than that of the Earth's core.

In the model of Rubie et al. (2004), the Earth's mantle starts off in a highly oxidized state and becomes more reduced as FeO partitions into the core. This forms the basis for the model of core formation under oxidizing conditions as proposed by Siebert et al. (2013). In fact, this model is only valid when there is no partitioning of silicon into the core. This is because every mole of silicon that partitions into the core releases two moles of FeO that partition primarily into the mantle (see reaction in **Section 9.03.3.2.2.3**). Thus the initially oxidized mantle cannot be reduced to its present composition when mass balance is taken into account (Rubie et al., 2015).

One advantage of modeling the metal–silicate partitioning of oxygen during core formation, in addition to the siderophile elements, is that assumptions concerning oxygen fugacity are not required. As described earlier in **Section 9.03.3.2.2.3**, this approach was extended by Rubie et al. (2011) by including all major elements when determining the compositions of equilibrated metal and silicate through a mass balance/partitioning approach. Thus, in their model of multistage core formation, the evolution of core composition could be determined as a function of mass accreted (**Figure 16(l)**). According to this model, the Earth's core contains 8 wt% Si, <1 wt% O, and 2 wt% S (but note that these predictions disagree with the arguments of Alfe et al., 2002).

9.03.4 Summary

Theoretical arguments and geochemical observations suggest that the bulk of the mass of the Earth accreted through impacts with smaller bodies (planetesimals and embryos) within about 50 Myr of solar system formation and that at least the larger impacts generated one or more large-scale, if transient, magma oceans. Although many of the impacting bodies were

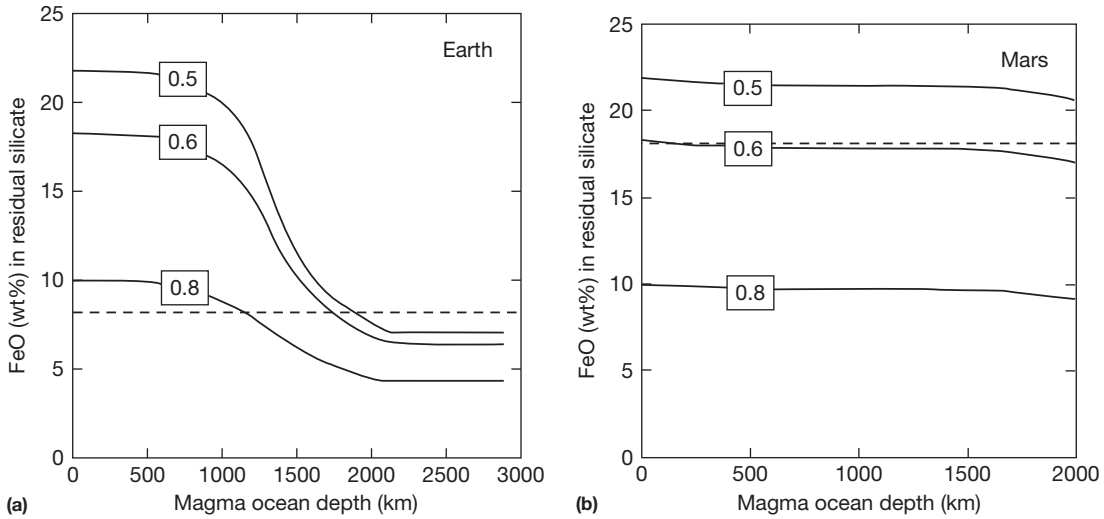

Figure 22 Results of core formation models for Earth (a) and Mars (b), based on metal–silicate partitioning of FeO in a magma ocean. The models are based on a chondritic bulk composition that consists initially of a mixture of metal and silicate components. The bulk oxygen content determines the fraction of metal that is present. The three curves, in each case, show results for different initial bulk oxygen contents, and the labels indicate the weight fraction of Fe that is initially present as metal. The horizontal dashed lines show the current FeO contents of the respective mantles. On Earth, the FeO content of the residual silicate decreases when the magma ocean depth exceeds 1000 km, because, at high temperatures, FeO partitions into the metal phase. On Mars, such an effect is almost absent because magma ocean temperatures are relatively low because of the small size of the planet. These results show that the bulk compositions of Earth and Mars could be similar (e.g., curve labeled '0.6') and that the current FeO content of the Earth's mantle resulted from core formation in a magma ocean around 1800 km deep: in this case, the Earth's core could contain 7–8 wt% oxygen. However, as discussed in the text, this model is only valid when little or no silicon partitions into the core (Reproduced from Rubie DC, Gessmann CK, and Frost DJ (2004) Partitioning of oxygen during core formation on the Earth and Mars. *Nature* 429: 58–61.).

undoubtedly differentiated, preexisting chemical signals appear to have been overprinted by the impact process. Siderophile element concentrations are consistent with magma oceans extending, *on average*, at least to midmantle depths (800–1500 km and 2500–4000 K). The impactor cores underwent partial or complete emulsification as they sank through the magma ocean, resulting in at least some degree of chemical reequilibration, as suggested by both siderophile and Hf–W isotopic observations. This reequilibration ceased as the metal pooled at the base of the magma ocean; subsequent transport of the resulting large-scale iron masses to the growing core was rapid and will have resulted in a significant increase in core temperatures. Following the Moon-forming impact, the initial core temperature was probably at least 6000 K, suggesting that extensive melting occurred in the lowermost mantle.

Unusually, there is broad agreement between the geochemical constraints and geophysical expectations of the core's early history. Nonetheless, several important outstanding questions remain as follows:

(1) The physics of exactly what happens during giant impacts is poorly understood (**Sections 9.03.2.2.2** and **9.03.2.3.2**). In particular, although there are physical and geochemical arguments for impactor emulsification, this process is still poorly understood and has not yet been fully investigated by numerical or laboratory models.
(2) The lifetime of magma oceans is also poorly known (**Section 9.03.2.3.2**). This is in part because complicating factors such as the possible presence of an insulating atmosphere or a foundering crust have a large effect on the outcome. It may be that this is an issue that can only be resolved using radiogenic isotopes with appropriate half-lives, rather than geophysical modeling. In addition, there is a possibility that terrestrial magma oceans may crystallize from the top down rather than from the bottom up (Mosenfelder et al., 2007, 2009) – which might have major implications by greatly extending magma ocean lifetimes.
(3) Geochemical models of core formation are currently hampered by a lack of partitioning data at high pressures and temperatures (i.e., >25 GPa and >3000 K). Even the partitioning of MSEs is poorly known at pressures significantly above 25 GPa and consequently large extrapolations of experimental data are required (e.g., Rubie et al., 2011). Rectifying the latter deficiency requires LH-DAC experiments (e.g., Bouhifd and Jephcoat, 2003; Tschauner et al., 1999), which are difficult to perform successfully because of large temperature gradients (which can drive chemical diffusion), temperature uncertainties, and difficulties in sample analysis. However, recent developments in this area appear very promising (Bouhifd and Jephcoat, 2011; Siebert et al., 2012).
(4) Uncertainties remain concerning the identity of the light element(s) in the core. Based on cosmochemical arguments and recent high-pressure studies, silicon with a lesser amount of oxygen may be the main light elements, together with ~2 wt% S.

(5) Many of the models of accretion and core formation to date have assumed single-stage processes. In practice, of course, accretion and core formation occur as a series of discrete events, under evolving conditions. The effect of these changing conditions on the behavior and chemistry of the core and mantle is just beginning to be addressed (e.g., Halliday, 2004; Rubie et al., 2011, 2012; Wade and Wood, 2005; Wood et al., 2006).

Acknowledgments

We thank Craig Agnor, Dan Frost, Alessandro Morbidelli, David O'Brien, Herbert Palme, Jon Wade, Bernie Wood, and Michael Walter for discussions. Portions of this work were supported by NSF EAR, NASA Origins, the German Science Foundation Priority Programme 1385 'The First 10 Million Years of the Solar System – a Planetary Materials Approach' (Grant Ru1323/2), and European Research Council (ERC) Advanced Grant 'ACCRETE' (contract no. 290568 to DCR).

References

Abe Y (1997) Thermal and chemical evolution of the terrestrial magma ocean. *Physics of the Earth and Planetary Interiors* 100: 27–39.

Agnor C and Asphaug E (2004) Accretion efficiency during planetary collisions. *Astrophysical Journal* 613: L157–L160.

Agnor CB, Canup RM, and Levison HF (1999) On the character and consequences of large impacts in the late stage of terrestrial planet formation. *Icarus* 142: 219–237.

Alfe D, Gillan MJ, and Price GD (2002) Composition and temperature of the Earth's core constrained by combining ab initio calculations and seismic data. *Earth and Planetary Science Letters* 195: 91–98.

Allegre CJ, Poirier J-P, Humler E, and Hofmann AW (1995) The chemical composition of the Earth. *Earth and Planetary Science Letters* 134: 515–526.

Anders E and Grevesse N (1989) Abundances of the elements: Meteoritic and solar. *Geochimica et Cosmochimica Acta* 53: 197–214.

Anderson OL and Isaak DG (2002) Another look at the core density deficit of Earth's outer core. *Physics of the Earth and Planetary Interiors* 131: 19–27.

Andrault D, Bolfan-Casanova N, Lo Nigro G, Bouhifd MA, Garbarino G, and Mezouar M (2011) Solidus and liquidus profiles of chondritic mantle: Implication for melting of the Earth across its history. *Earth and Planetary Science Letters* 304: 251–259.

Asahara Y, Frost DJ, and Rubie DC (2007) Partitioning of FeO between magnesiowüstite and liquid iron at high pressures and temperatures: Implications for the composition of the Earth's outer core. *Earth and Planetary Science Letters* 257: 435–449.

Asphaug E (2010) Similar-sized collisions and the diversity of planets. *Chemie der Erde* 70: 199219.

Asphaug E, Agnor CB, and Williams Q (2006) Hit-and-run planetary collisions. *Nature* 439: 155–160.

Badro J, Fiquet G, Guyot F, et al. (2007) Effect of light elements on the sound velocities in solid iron: Implications for the composition of Earth's core. *Earth and Planetary Science Letters* 254: 233–238.

Bagdassarov N, Golabek GJ, Solferino G, and Schmidt MW (2009a) Constraints on the Fe–S melt connectivity in mantle silicates from electrical impedance measurements. *Physics of the Earth and Planetary Interiors* 177: 139–146.

Bagdassarov N, Solferino G, Golabek GJ, and Schmidt MW (2009b) Centrifuge assisted percolation of Fe–S melts in partially molten peridotite: Time constraints for planetary core formation. *Earth and Planetary Science Letters* 288: 84–95.

Baker J, Bizzarro M, Wittig N, Connelly J, and Haack H (2005) Early planetesimal melting from an age of 4.5662 Gyr for differentiated meteorites. *Nature* 436: 1127–1131.

Ballhaus C and Ellis DJ (1996) Mobility of core melts during Earth's accretion. *Earth and Planetary Science Letters* 143: 137–145.

Benz W, Anic A, Horner J, and Whitby JA (2007) The origin of mercury. *Space Science Reviews* 132: 189202.

Benz W and Cameron AGW (1990) Terrestrial effects of the giant impact. In: Newsom HE and Jones JH (eds.) *Origin of the Earth*, pp. 61–67. Oxford: Oxford University Press.

Birch F (1952) Elasticity and constitution of the Earth's interior. *Journal of Geophysical Research* 69: 227–286.

Blichert-Toft J, Gleason JD, Télouk P, and Albaréde F (1999) The Lu–Hf isotope geochemistry of shergottites and the evolution of the Martian mantle–crust system. *Earth and Planetary Science Letters* 173: 25–39.

Boehler R (2000) High-pressure experiments and the phase diagram of lower mantle and core materials. *Reviews of Geophysics* 38: 221–245.

Borg LE and Draper DS (2003) A petrogenetic model for the origin and compositional variation of the martian basaltic meteorites. *Meteoritics and Planetary Science* 38: 1713–1731.

Bottke WF, Vokrouhlicky D, Minton D, et al. (2012) An Archaean heavy bombardment from a destabilized extension of the asteroid belt. *Nature* 485: 78–81.

Bottke WF, Walker RJ, Day JMD, Nesvorny D, and Elkins-Tanton L (2010) Stochastic late accretion to Earth, the Moon, and Mars. *Science* 330: 1527–1530.

Bouhifd MA and Jephcoat AP (2003) The effect of pressure on the partitioning of Ni and Co between silicate and iron-rich metal liquids: A diamond-anvil cell study. *Earth and Planetary Science Letters* 209: 245–255.

Bouhifd MA and Jephcoat AP (2011) Convergence of Ni and Co metal–silicate partition coefficients in the deep magma-ocean and coupled silicon–oxygen solubility in iron melts at high pressures. *Earth and Planetary Science Letters* 307: 341–348.

Boyet M and Carlson RW (2005) Nd-142 evidence for early (>4.53 Ga) global differentiation of the silicate Earth. *Science* 309: 576–581.

Brandon AD and Walker RJ (2005) The debate over core–mantle interaction. *Earth and Planetary Science Letters* 232: 211–225.

Brenan JM and McDonough WF (2009) Core formation and metal–silicate fractionation of osmium and iridium from gold. *Nature Geoscience* 2: 798–801.

Bruhn D, Groebner N, and Kohlstedt DL (2000) An interconnected network of core-forming melts produced by shear deformation. *Nature* 403: 883–886.

Buffett BA, Garnero EJ, and Jeanloz R (2000) Sediments at the top of Earth's outer core. *Science* 290: 1338–1342.

Buffett BA and Seagle CT (2010) Stratification of the top of the core due to chemical interactions with the mantle. *Journal of Geophysical Research* 115: B04407. http://dx.doi.org/10.1029/2009JB006751.

Busso M, Gallino R, and Wasserburg GJ (1999) Nucleosynthesis in asymptotic giant branch stars: Relevance for galactic enrichment and solar system formation. *Annual Review of Astronomy and Astrophysics* 37: 239–309.

Cameron AGW (2000) High-resolution simulations of the giant impact. In: Canup RM and Righter K (eds.) *Origin of the Earth and Moon*, pp. 133–144. Tucson: University of Arizona Press.

Canup RM (2004) Simulations of a late lunar-forming impact. *Icarus* 168: 433–456.

Canup RM and Asphaug E (2001) Origin of the Moon in a giant impact near the end of the Earth's formation. *Nature* 412: 708–712.

Canup RM and Righter K (eds.) (2000) *Origin of the Earth and Moon*. Tucson: University of Arizona Press.

Canup RM, Ward WR, and Cameron AGW (2001) A scaling relationship for satellite-forming impacts. *Icarus* 150: 288–296.

Caro G, Bourdon B, Halliday AN, and Quitte G (2008) Super-chondritic Sm/Nd ratios in Mars, the Earth and the Moon. *Nature* 452: 336–339.

Caro G, Bourdon B, Wood BJ, and Corgne A (2005) Trace-element fractionation in Hadean mantle generated by melt segregation from a magma ocean. *Nature* 436: 246–249.

Chabot NL and Agee CB (2003) Core formation in the Earth and Moon: New experimental constraints from V, Cr, and Mn. *Geochimica et Cosmochimica Acta* 67: 2077–2091.

Chabot NL, Draper DS, and Agee CB (2005) Conditions of core formation in the Earth: Constraints from nickel and cobalt partitioning. *Geochimica et Cosmochimica Acta* 69: 2141–2151.

Chabot NL and Haack H (2006) Evolution of asteroidal cores. In: Lauretta DS and McSween HY (eds.) *Meteorites and the Early Solar System*, pp. 747–771. Tucson, AZ: University of Arizona Press.

Chamberlin TC (1916) *The Origin of the Earth*, p. 271. Chicago: University of Chicago Press.

Chambers JE (2008) Oligarchic growth with migration and fragmentation. *Icarus* 198: 256–273.

Chambers JE (2009) Planetary migration: What does it mean for planet formation? *Annual Review of Earth and Planetary Sciences* 37: 321–344.

Chambers JE (2010) Terrestrial planet formation. In: Seager S (ed.) *Exoplanets*, pp. 297–318. Tucson: University of Arizona Press.

Chambers JE and Wetherill GW (1998) Making the terrestrial planets: N-body integrations of planetary embryos in three dimensions. *Icarus* 136: 304–327.

Clayton RN and Mayeda TK (1996) Oxygen isotope studies of achondrites. *Geochimica et Cosmochimica Acta* 60: 1999–2017.

Corgne A, Siebert J, and Badro J (2009) Oxygen as a light element: A solution to single-stage core formation. *Earth and Planetary Science Letters* 288: 108–114.

Cottrell E and Walker D (2006) Constraints on core formation from Pt partitioning in mafic silicate liquids at high temperatures. *Geochimica et Cosmochimica Acta* 70: 1565–1580.
Cottrell E, Walter MJ, and Walker D (2009) Metal–silicate partitioning of tungsten at high pressure and temperature: Implications for equilibrium core formation in Earth. *Earth and Planetary Science Letters* 281: 275–287.
Dahl TW and Stevenson DJ (2010) Turbulent mixing of metal and silicate during planet accretion—And interpretation of the Hf–W chronometer. *Earth and Planetary Science Letters* 295: 177–186.
Dalziel SB, Linden PF, and Youngs DL (1999) Self-similarity and internal structure of turbulence induced by Rayleigh–Taylor instability. *Journal of Fluid Mechanics* 399: 1–48.
Dauphas N and Pourmand A (2011) Hf–W–Th evidence for rapid growth of Mars and its status as a planetary embryo. *Nature* 473: 489–492.
Day JMD, Walker RJ, Qin L, et al. (2012) Late accretion as a natural consequence of planetary growth. *Nature Geoscience* 5: 614–617.
Debaille V, Brandon AD, Yin QZ, and Jacobsen B (2007) Coupled ^{142}Nd–^{143}Nd evidence for a protracted magma ocean in Mars. *Nature* 450: 525–528.
Deguen R, Olson P, and Cardin P (2011) Experiments on turbulent metal–silicate mixing in a magma ocean. *Earth and Planetary Science Letters* 310: 303–313.
Drake MJ (2001) The eucrite/Vesta story. *Meteoritics and Planetary Science* 36: 501–513.
Drake MJ and Righter K (2002) Determining the composition of the Earth. *Nature* 416: 39–44.
Dreibus G and Palme H (1996) Cosmochemical constraints on the sulfur content in the Earth's core. *Geochimica et Cosmochimica Acta* 60: 1125–1130.
Dwyer CA, Nimmo F, and Chambers JE (2015) Bulk chemical and Hf-W isotopic consequences of incomplete accretion during planet formation. *Icarus* 245: 145–152.
Elkins-Tanton LT, Burgess S, and Yin Q-Z (2011) The lunar magma ocean: Reconciling the solidification process with lunar petrology and geochemistry. *Earth and Planetary Science Letters* 304: 326–336.
Elkins-Tanton LT, Parmentier EM, and Hess PC (2003) Magma ocean fractional crystallization and cumulate overturn in terrestrial planets: Implications for Mars. *Meteoritics and Planetary Science* 38: 1753–1771.
Elsasser WM (1963) Early history of the earth. In: Geiss J and Goldberg ED (eds.) *Earth Science and Meteoritics*, pp. 1–30. Amsterdam: North-Holland.
Elser S, Meyer MR, and Moore B (2012) On the origin of elemental abundances in the terrestrial planets. *Icarus* 221: 859–874.
Ertel W, O'Neill HStC, Sylvester PJ, and Dingwell DB (1999) Solubilities of Pt and Rh in a haplobasaltic silicate melt at 1300 °C. *Geochimica et Cosmochimica Acta* 63: 2439–2449.
Ertel W, O'Neill HStC, Sylvester PJ, Dingwell DB, and Spettel B (2001) The solubility of rhenium in silicate melts. Implications for the geochemical properties of rhenium at high temperatures. *Geochimica et Cosmochimica Acta* 65: 2161–2170.
Ertel W, Walter MJ, Drake MJ, and Sylvester PJ (2006) Experimental study of platinum solubility in silicate melt to 14 GPa and 2273 K: Implications for accretion and core formation in the Earth. *Geochimica et Cosmochimica Acta* 70: 2591–2602.
Faul UH (1997) Permeability of partially molten upper mantle rocks from experiments and percolation theory. *Journal of Geophysical Research* 102: 10299–10312. http://dx.doi.org/10.1029/96JB03460.
Fiquet G, Auzende AL, Siebert J, et al. (2010) Melting of peridotite to 140 GPa. *Science* 329: 1516–1518.
Fitoussi C, Bourdon B, Kleine T, Oberli F, and Reynolds BC (2009) Si isotope systematics of meteorites and terrestrial peridotites: Implications for Mg/Si fractionation in the solar nebula and for Si in the Earth's core. *Earth and Planetary Science Letters* 287: 77–85.
Fortenfant SS, Dingwell DB, Ertel-Ingrisch W, Capmas F, Birck JL, and Dalpé C (2006) Oxygen fugacity dependence of Os solubility in haplobasaltic melt. *Geochimica et Cosmochimica Acta* 70: 742–756.
Fortenfant SS, Günther D, Dingwell DB, and Rubie DC (2003a) Temperature dependence of Pt and Rh solubilities in a haplobasaltic melt. *Geochimica et Cosmochimica Acta* 67: 123–131.
Fortenfant SS, Rubie DC, Reid J, Dalpé C, and Gessmann CK (2003b) Partitioning of Re and Os between liquid metal and magnesiowüstite at high pressure. *Physics of the Earth and Planetary Interiors* 139: 77–91.
Frost DJ, Asahara Y, Rubie DC, et al. (2010) The partitioning of oxygen between the Earth's mantle and core. *Journal of Geophysical Research* 115: B02202. http://dx.doi.org/10.1029/2009JB006302.
Frost DJ, Liebske C, Langenhorst F, McCammon CA, Tronnes RG, and Rubie DC (2004) Experimental evidence for the existence of iron-rich metal in the Earth's lower mantle. *Nature* 428: 409–412.
Frost DJ, Mann U, Asahara Y, and Rubie DC (2008) The redox state of the mantle during and just after core formation. *Philosophical Transactions of the Royal Society A* 366: 4315–4337. http://dx.doi.org/10.1098/rsta.2008.0147.
Fu RR, Weiss BP, Shuster DL, et al. (2012) An ancient core dynamo in asteroid Vesta. *Science* 338: 238–241.
Gaetani GA and Grove TL (1999) Wetting of mantle olivine by sulfide melt: Implications for Re/Os ratios in mantle peridotite and late-stage core formation. *Earth and Planetary Science Letters* 169: 147–163.
Gancarz AJ and Wasserburg GJ (1977) Initial Pb of the Amîtsoq gneiss, West Greenland, and implications for the age of the Earth. *Geochim. Cosmochim. Acta* 41(9): 1283–1301.
Georg RB, Halliday AN, Schauble EA, and Reynolds BC (2007) Silicon in the Earth's core. *Nature* 447: 1102–1106. http://dx.doi.org/10.1038/nature05927.
Gessmann CK and Rubie DC (1998) The effect of temperature on the partitioning of Ni, Co, Mn, Cr and V at 9 GPa and constraints on formation of the Earth's core. *Geochimica et Cosmochimica Acta* 62: 867–882.
Gessmann CK and Rubie DC (2000) The origin of the depletions of V, Cr and Mn in the mantles of the Earth and Moon. *Earth and Planetary Science Letters* 184: 95–107.
Gessmann CK, Wood BJ, Rubie DC, and Kilburn MR (2001) Solubility of silicon in liquid metal at high pressure: Implications for the composition of the Earth's core. *Earth and Planetary Science Letters* 184: 367–376.
Ghosh A and McSween HY (1998) A thermal model for the differentiation of Asteroid 4 Vesta, based on radiogenic heating. *Icarus* 134: 187–206.
Golabek GJ, Schmeling H, and Tackley PJ (2008) Earth's core formation aided by flow channeling instabilities induced by iron diapirs. *Earth and Planetary Science Letters* 271: 24–33.
Gomes R, Levison HF, Tsiganis K, and Morbidelli A (2005) Origin of the cataclysmic Late Heavy Bombardment period of the terrestrial planets. *Nature* 435: 466–469.
Goossens S, et al. (2011) Lunar gravity field determination using Selene same-beam differential VLBI tracking data. *Journal of Geodesy* 85: 205–228.
Greenwood RC, Franchi IA, Jambon A, and Buchanan PC (2005) Widespread magma oceans on asteroid bodies in the early solar system. *Nature* 435: 916–918. http://dx.doi.org/10.1038/nature03612.
Grimm RE and McSween HY (1993) Heliocentric zoning of the asteroid belt by aluminum-26 heating. *Science* 259: 653–655.
Groebner N and Kohlstedt DL (2006) Deformation-induced metal melt networks in silicates: Implications for core–mantle interactions in planetary bodies. *Earth and Planetary Science Letters* 245: 571–580.
Haisch KE, Lada EA, and Lada CJ (2001) Disk frequencies and lifetimes in young clusters. *Astrophysical Journal* 553: L153–L156.
Halliday AN (2003) The origin and earliest history of the Earth. *Treatise on Geochemistry*, vol. 1, pp. 509–557. Oxford: Elsevier.
Halliday AN (2004) Mixing, volatile loss and compositional change during impact-driven accretion of the Earth. *Nature* 427: 505–509.
Hallworth MA, Phillips JC, Hubbert HE, and Sparks RSJ (1993) Entrainment in turbulent gravity currents. *Nature* 362: 829–831.
Hanks TC and Anderson DL (1969) The early thermal history of the Earth. *Physics of the Earth and Planetary Interiors* 2: 19–29.
Helffrich G and Kaneshima S (2004) Seismological constraints on core composition from Fe–O–S liquid immiscibility. *Science* 306: 2239–2242.
Hillgren VJ, Drake MJ, and Rubie DC (1994) High-pressure and high-temperature experiments on core–mantle segregation in the accreting Earth. *Science* 264: 1442–1445.
Hillgren VJ, Gessmann CK, and Li J (2000) An experimental perspective on the light element in Earth's core. In: Canup RM and Righter K (eds.) *Origin of the Earth and Moon*, pp. 245–264. Tucson: University of Arizona Press.
Höink T, Schmalzl J, and Hansen U (2006) Dynamics of metal–silicate separation in a terrestrial magma ocean. *Geochemistry, Geophysics, Geosystems* 7: Q09008. http://dx.doi.org/10.1029/2006GC001268.
Holzheid A, Schmitz MD, and Grove TL (2000a) Textural equilibria of iron sulphide liquids in partly molten silicate aggregates and their relevance to core formation scenarios. *Journal of Geophysical Research* 105: 13555–13567.
Holzheid A, Sylvester P, O'Neill HStC, Rubie DC, and Palme H (2000b) Evidence for a late chondritic veneer in the Earth's mantle from high-pressure partitioning of palladium and platinum. *Nature* 406: 396–399.
Hustoft JW and Kohlstedt DL (2006) Metal–silicate segregation in deforming dunitic rocks. *Geochemistry, Geophysics, Geosystems* 7: Q02001. http://dx.doi.org/10.1029/2005GC001048.
Iida T and Guthrie RL (1988) *The Physical Properties of Liquid Metals*, pp. 109–146. Oxford: Clarendon.
Jacobsen SB (2005) The Hf–W isotopic system and the origin of the Earth and Moon. *Annual Review of Earth and Planetary Science* 33: 531–570.

Javoy M (1995) The integral enstatite chondrite model of the Earth. *Geophysical Research Letters* 22: 2219–2222.

Jeffreys H (1952) *The Earth*, 3rd ed. Cambridge: Cambridge University Press.

Jephcoat A and Olson P (1987) Is the inner core of the Earth pure iron? *Nature* 325: 332–335.

Jones JH, Capobianco CJ, and Drake MJ (1992) Siderophile elements and the Earth's formation. *Science* 257: 1281–1282.

Jones JH, Neal CR, and Ely JC (2003) Signatures of the siderophile elements in the SNC meteorites and Mars: A review and petrologic synthesis. *Chemical Geology* 196: 21–41.

Kanda R and Stevenson DJ (2006) Suction mechanism for iron entrainment into the lower mantle. *Geophysical Research Letters* 33: L02310. http://dx.doi.org/10.1029/2005GL025009.

Karato S-I and Murthy VR (1997) Core formation and chemical equilibrium in the Earth—I. Physical considerations. *Physics of the Earth and Planetary Interiors* 100: 61–79.

Karki BB and Stixrude LP (2010) Viscosity of $MgSiO_3$ liquid at Earth's mantle conditions: Implications for an early magma ocean. *Science* 328: 740–742.

Kato T and Ringwood AE (1989) Melting relationships in the system Fe–FeO at high pressure: Implications for the composition and formation of the Earth's core. *Physics and Chemistry of Minerals* 16: 524–538.

Kaula WM (1979) Thermal evolution of the Earth and Moon growing by planetesimal impacts. *Journal of Geophysical Research* 84: 999–1008.

Kegler P, Holzheid A, Frost DJ, Rubie DC, Dohmen R, and Palme H (2008) New Ni and Co metal–silicate partitioning data and their relevance for an early terrestrial magma ocean. *Earth and Planetary Science Letters* 268: 28–40.

Kegler P, Holzheid A, Rubie DC, Frost DJ, and Palme H (2005) New results of metal/silicate partitioning of Ni and Co at elevated pressures and temperatures. In: *XXXVI Lunar and Planetary Science Conference,* Abstr. #2030.

Keil K, Stoeffler D, Love SG, and Scott ERD (1997) Constraints on the role of impact heating and melting in asteroids. *Meteoritics and Planetary Science* 32: 349–363.

Kendall JD and Melosh HJ (2012a) Dispersion of iron cores during planetesimal impacts. In: *Meteoritics and Planetary Science Supplement,* Abstract 5302.

Kendall JD and Melosh HJ (2012b) Fate of iron cores during planetesimal impacts. In: *LPSC Conference, 43,* Abstract #2699.

Keppler H and Rubie DC (1993) Pressure-induced coordination changes of transition-metal ions in silicate melts. *Nature* 364: 54–55.

Kilburn MR and Wood BJ (1997) Metal–silicate partitioning and the incompatibility of S and Si during core formation. *Earth and Planetary Science Letters* 152: 139–148.

Kimura K, Lewis RS, and Anders E (1974) Distribution of gold between nickel–iron and silicate melts: Implications for the abundances of siderophile elements on the Earth and Moon. *Geochimica et Cosmochimica Acta* 38: 683–701.

Kleine T, Palme H, Mezger M, and Halliday AN (2005) Hf–W chronometry of lunar metals and the age and early differentiation of the Moon. *Science* 310: 1671–1673.

Kleine T, Touboul M, Bourdon B, et al. (2009) Hf–W chronometry and the accretion and early evolution of asteroids and terrestrial planets. *Geochimica et Cosmochimica Acta* 73: 5150–5188.

Kokubo E and Genda H (2010) Formation of terrestrial planets from protoplanets under a realistic accretion condition. *Astrophysical Journal Letters* 714: L21–L25.

Kokubo E and Ida S (1998) Oligarchic growth of protoplanets. *Icarus* 131: 171–178.

Kominami J, Tanaka H, and Ida S (2005) Orbital evolution and accretion of protoplanets tidally interacting with a gas disk I. Effects of interaction with planetesimals and other protoplanets. *Icarus* 178: 540–552.

Kong P, Ebihara M, and Palme H (1999) Siderophile elements in Martian meteorites and implications for core formation in Mars. *Geochimica et Cosmochimica Acta* 63: 1865–1875.

Kyte FT (1998) A meteorite from the Cretaceous/Tertiary boundary. *Nature* 396: 237–239.

Labrosse S, Hernlund JW, and Coltice N (2007) A crystallizing dense magma ocean at the base of the Earth's mantle. *Nature* 450: 866–869. http://dx.doi.org/10.1038/nature06355.

Laporte D and Watson EB (1995) Experimental and theoretical constraints on melt distribution in crustal sources: The effect of crystalline anisotropy on melt interconnectivity. *Chemical Geology* 124: 161–184.

Leinhardt ZM and Richardson DC (2005) Planetesimals to protoplanets 1. Effect of fragmentation on terrestrial planet formation. *Astrophysical Journal* 625: 427–440.

Li J and Agee CB (1996) Geochemistry of mantle–core differentiation at high pressure. *Nature* 381: 686–689.

Li J and Agee CB (2001) The effect of pressure, temperature, oxygen fugacity and composition on partitioning of nickel and cobalt between liquid Fe–Ni–S alloy and liquid silicate: Implications for the Earth's core formation. *Geochimica et Cosmochimica Acta* 65: 1821–1832.

Li J and Fei Y (2003) Experimental constraints on core composition. In: Holland HD and Turekian KK (eds.) Carlson RW (ed.) *The Mantle and Core. Treatise on Geochemistry*, vol. 2, pp. 521–546. Oxford: Elsevier-Pergamon.

Liebske C and Frost DJ (2012) Melting phase relations in the MgO–$MgSiO_3$ system between 16 and 26 GPa: Implications for melting in Earth's deep interior. *Earth and Planetary Science Letters* 345–348: 159–170.

Liebske C, Schmickler B, Terasai H, et al. (2005) Viscosity of peridotite liquid up to 13 GPa: Implications for magma ocean viscosities. *Earth and Planetary Science Letters* 240: 589–604.

Lin J-R, Gerya TV, Tackley PJ, Yuen DA, and Golabek GJ (2009) Numerical modeling of protocore destabilization during planetary accretion: Methodology and results. *Icarus* 204: 732–748.

Lin J-R, Gerya TV, Tackley PJ, Yuen DA, and Golabek GJ (2011) Protocore destabilization in planetary embryos formed by cold accretion: Feedbacks from non-Newtonian rheology and energy dissipation. *Icarus* 213: 24–42.

Lindstrom DJ and Jones JH (1996) Neutron activation analysis of multiple 10–100 μg glass samples from siderophile element partitioning experiments. *Geochimica et Cosmochimica Acta* 60: 1195–1203.

Lodders K (2003) Solar System abundances and condensation temperatures of the elements. *The Astrophysical Journal* 591: 1220–1247.

Lodders K and Fegley B (1998) *The Planetary Scientist's Companion*. Oxford: Oxford University Press.

Ma Z (2001) Thermodynamic description for concentrated metallic solutions using interaction parameters. *Metallurgical and Materials Transactions B* 32: 87–103.

Maier WD, Andreoli MAG, McDonald I, et al. (2006) Discovery of a 25 cm asteroid clast in the giant Morokweng impact crater, South Africa. *Nature* 441: 203–206.

Malavergne V, Siebert J, Guyot F, et al. (2004) Si in the core? New high-pressure and high-temperature experimental data. *Geochimica et Cosmochimica Acta* 68: 4201–4211.

Mann U, Frost DJ, and Rubie DC (2009) Evidence for high-pressure core–mantle differentiation from the metal–silicate partitioning of lithophile and weakly-siderophile elements. *Geochimica et Cosmochimica Acta* 73: 7360–7386.

Mann U, Frost DJ, Rubie DC, Becker H, and Audétat A (2012) Partitioning of Ru, Rh, Pd, Re, Ir and Pt between liquid metal and silicate at high pressures and high temperatures – Implications for the origin of highly siderophile element concentrations in the Earth's mantle. *Geochimica et Cosmochimica Acta* 84: 593–613. http://dx.doi.org/10.1016/j.gca.2012.01.026.

Margot JL, Peale SJ, and Solomon SC (2012) Mercury's moment of inertia from spin and gravity data. *Journal of Geophysical Research* 117: E00109.

Matsui T and Abe Y (1986) Impact-induced atmospheres and oceans on Earth and Venus. *Nature* 322: 526–528.

McDonough WF (2003) Compositional model for the Earth's core. *Treatise on Geochemistry,* pp. 517–568. Amsterdam: Elsevier.

McDonough WF and Sun S-s (1995) The composition of the Earth. *Chemical Geology* 120: 223–253.

McSween HY (1999) *Meteorites and Their Parent Planets*. Cambridge, UK: Cambridge University Press.

Médard E, Schmidt MW, Wälle M, Keller NS, and Günther D (2010) Pt in silicate melts: Centrifuging nanonuggets to decipher core formation processes. *41st Lunar and Planetary Science Conference,* Abstract #2639.

Melosh HJ (1990) Giant impacts and the thermal state of the early Earth. In: Newsom HE and Jones JE (eds.) *Origin of the Earth*, pp. 69–83. Oxford: Oxford University Press.

Melosh HJ and Rubie DC (2007) Ni partitioning in the terrestrial magma ocean: A polybaric numerical model. In: *Lunar and Planetary Science XXXVIII,* Abstract #1593.

Miller GH, Stolper EM, and Ahrens TJ (1991) The equation of state of a molten komatiite 2. Application to komatiite petrogenesis and the Hadean mantle. *Journal of Geophysical Research* 96: 11849–11864.

Minarik WG, Ryerson FJ, and Watson EB (1996) Textural entrapment of core-forming melts. *Science* 272: 530–533.

Monteux J, Ricard Y, Coltice N, Dubuffet F, and Ulvrova M (2009) A model of metal–silicate separation on growing planets. *Earth and Planetary Science Letters* 287: 353–362.

Morbidelli A, Chambers J, Lunine JI, et al. (2000) Source regions and timescales for the delivery of water to the Earth. *Meteoritics and Planetary Science* 35: 1309–1320.

Morgan JW (1986) Ultramafic xenoliths: Clues to Earth's late accretionary history. *Journal of Geophysical Research* 91: 12375–12387.

Morishima R, Stadel J, and Moore B (2010) From planetesimals to terrestrial planets: N-body simulations including the effects of nebular gas and giant planets. *Icarus* 207: 517–535.

Mosenfelder JL, Asimow PD, and Ahrens TJ (2007) Thermodynamic properties of Mg_2SiO_4 liquid at ultra-high pressures from shock measurements to 200 GPa on

forsterite and wadsleyite. *Journal of Geophysical Research* 112: B06208. http://dx.doi.org/10.1029/2006JB004364.

Mosenfelder JL, Asimow PD, Frost DJ, Rubie DC, and Ahrens TJ (2009) The $MgSiO_3$ system at high pressure: Thermodynamic properties of perovskite, postperovskite, and melt from global inversion of shock and static compression data. *Journal of Geophysical Research* 114: B01203. http://dx.doi.org/10.1029/2008JB005900.

Mukhopadhyay S (2012) Early differentiation and volatile accretion recorded in deep-mantle neon and xenon. *Nature* 486: 101–124.

Murthy VR (1991) Early differentiation of the Earth and the problem of mantle siderophile elements – A new approach. *Science* 253: 303–306.

Newsom HE (1990) Accretion and core formation in the Earth: Evidence from siderophile elements. In: Newsom HE and Jones JH (eds.) *Origin of the Earth*, pp. 273–288. New York: Oxford University Press.

Nimmo F, O'Brien DP, and Kleine T (2010) Tungsten isotopic evolution during late-stage accretion: Constraints on Earth–Moon equilibration. *Earth and Planetary Science Letters* 292: 363–370.

O'Neill HStC (1991) The origin of the Moon and the early history of the Earth – A chemical model. Part 2: The Earth. *Geochimica et Cosmochimica Acta* 55: 1159–1172.

O'Neill HStC (1992) Siderophile elements and the Earth's formation. *Science* 257: 1282–1284.

O'Neill HStC and Palme H (1998) Composition of the silicate Earth: Implications for accretion and core formation. In: Jackson I (ed.) *The Earth's Mantle*, pp. 3–126. Cambridge, UK: Cambridge University Press.

O'Brien DP, Morbidelli A, and Levison HF (2006) Terrestrial planet formation with strong dynamical friction. *Icarus* 184: 39–58.

Ohtani E and Ringwood AE (1984) Composition of the core. I. Solubility of oxygen in molten iron at high temperatures. *Earth and Planetary Science Letters* 71: 85–93.

Ohtani E, Ringwood AE, and Hibberson W (1984) Composition of the core. II. Effect of high pressure on solubility of FeO in molten iron. *Earth and Planetary Science Letters* 71: 94–103.

Ohtani E and Yurimoto H (1996) Element partitioning between metallic liquid, magnesiowüstite, and silicate liquid at 20 GPa and 2500 °C: A secondary ion mass spectrometric study. *Geophysical Research Letters* 23: 1993–1996.

O'Neill HSC, Canil D, and Rubie DC (1998) Oxide–metal equilibria to 2500 °C and 25 GPa: Implications for core formation and the light component in the Earth's core. *Journal of Geophysical Research* 103: 12239–12260.

O'Neill HSC and Palme H (2008) Collisional erosion and the non-chondritic composition of the terrestrial planets. *Philosophical Transactions of the Royal Society of London A* 366: 4205–4238.

Palme H and O'Neill HStC (2003) Cosmochemical estimates of mantle composition. In: Carlson RW (ed.) and Holland HD and Turekian KK (series eds.) *The Mantle and Core. Treatise on Geochemistry*, vol. 2, pp. 1–38. Oxford: Elsevier-Pergamon.

Pierazzo E, Vickery AM, and Melosh HJ (1997) A re-evaluation of impact melt production. *Icarus* 127: 408–432.

Poirier J-P (1994) Light elements in the Earth's outer core: A critical review. *Physics of the Earth and Planetary Interiors* 85: 319–337.

Poirier J-P, Malavergne V, and Le Mouël JL (1998) Is there a thin electrically conducting layer at the base of the mantle? In: Gurnis M, Wysession ME, Knittle E, and Buffett BA (eds.) *The Core–Mantle Boundary Region*. *Geodynamics*, vol. 28, pp. 131–137. Washington, DC: American Geophysical Union.

Porcelli D, Woolum D, and Cassen P (2001) Deep Earth rare gases: Initial inventories, capture from the solar nebula, and losses during Moon formation. *Earth and Planetary Science Letters* 193: 237–251.

Pritchard ME and Stevenson DJ (2000) Thermal aspects of a lunar origin by giant impact. In: Canup RM and Righter K (eds.) *Origin of the Earth and Moon*, pp. 179–196. Tucson: University of Arizona Press.

Quitté G, Latkoczy C, Halliday AN, Schönbächler M, and Günther D (2005) Iron-60 in the Eucrite parent body and the initial $^{60}Fe/^{56}Fe$ of the solar system. In: *LPSC-XXXVI*, Abstract 1827.

Raymond SN, Quinn T, and Lunine JI (2007) High resolution simulations of the final assembly of Earth-like planets 2. Water delivery and planetary habitability. *Astrobiology* 7: 66–84.

Reid JE, Suzuki A, Funakoshi K, et al. (2003) The viscosity of $CaMgSi_2O_6$ liquid at pressures up to 13 GPa. *Physics of the Earth and Planetary Interiors* 139: 45–54.

Righter K (2003) Metal–silicate partitioning of siderophile elements and core formation in the early Earth. *Annual Review of Earth and Planetary Sciences* 31: 135–174.

Righter K (2005) Highly siderophile elements: Constraints on Earth accretion and early differentiation. In: van der Hilst RD, Bass JD, Matas J, and Trampert J (eds.) *Earth's Deep Mantle: Structure, Composition and Evolution*. *Geophysical Monograph*, vol. 160, pp. 201–218. Washington: American Geophysical Union.

Righter K (2011) Prediction of metal–silicate partition coefficients for siderophile elements: An update and assessment of PT conditions for metal–silicate equilibrium during accretion of the Earth. *Earth and Planetary Science Letters* 304: 158–167.

Righter K and Drake MJ (1996) Core formation in Earth's Moon, Mars, and Vesta. *Icarus* 124: 513–529.

Righter K and Drake MJ (1997) Metal–silicate equilibrium in a homogeneously accreting earth: New results for Re. *Earth and Planetary Science Letters* 146: 541–553.

Righter K and Drake MJ (1999) Effect of water on metal–silicate partitioning of siderophile elements: A high pressure and temperature terrestrial magma ocean and core formation. *Earth and Planetary Science Letters* 171: 383–399.

Righter K and Drake MJ (2000) Metal–silicate equilibration in the early Earth: New constraints from volatile moderately siderophile elements Ga, Sn, Cu and P. *Geochimica et Cosmochimica Acta* 64: 3581–3597.

Righter K and Drake MJ (2001) Constraints on the depth of an early terrestrial magma ocean. *Meteoritics & Planetary Science* 36: A173.

Righter K and Drake MJ (2003) Partition coefficients at high pressure and temperature. *Treatise on Geochemistry*, vol. 2, pp. 425–449. Amsterdam: Elsevier.

Righter K, Drake MJ, and Yaxley G (1997) Prediction of siderophile element metal–silicate partition coefficients to 20 GPa and 2800 °C: The effects of pressure, temperature, oxygen fugacity, and silicate and metallic melt compositions. *Physics of the Earth and Planetary Interiors* 100: 115–134.

Righter K, Humayun M, and Danielson L (2008) Partitioning of palladium at high pressures and temperatures during core formation. *Nature Geoscience* 1: 321–323.

Righter K, Pando KM, Danielson L, and Lee C-T (2010) Partitioning of Mo, P and other siderophile elements (Cu, Ga, Sn, Ni, Co, Cr, Mn, V, and W) between metal and silicate melt as a function of temperature and silicate melt composition. *Earth and Planetary Science Letters* 291: 1–9.

Ringwood AE (1977) Composition of the core and implications for the origin of the Earth. *Geochemical Journal* 11: 111–135.

Rose LA and Brenan JM (2001) Wetting properties of Fe–Ni–Co–Cu–O–S melts against olivine: Implications for sulfide melt mobility. *Economic Geology and the Bulletin of the Society of Economic Geologists* 96: 145–157.

Rubie DC, Jacobson SA, Morbidelli A, et al. (2015) Accretion and differentiation of the terrestrial planets with implications for the compositions of early-formed Solar System bodies and accretion of water. *Icarus* 248: 89–108.

Rubie DC, Frost DJ, Mann U, et al. (2011) Heterogeneous accretion, composition and core–mantle differentiation of the Earth. *Earth and Planetary Science Letters* 301: 31–42. http://dx.doi.org/10.1016/j.epsl.2010.11.030.

Rubie DC, Gessmann CK, and Frost DJ (2004) Partitioning of oxygen during core formation on the Earth and Mars. *Nature* 429: 58–61.

Rubie DC, Melosh HJ, Reid JE, Liebske C, and Righter K (2003) Mechanisms of metal–silicate equilibration in the terrestrial magma ocean. *Earth and Planetary Science Letters* 205: 239–255.

Rubin AM (1993) Dikes vs. diapirs in viscoelastic rock. *Earth and Planetary Science Letters* 119: 641–659.

Rubin AM (1995) Propagation of magma-filled cracks. *Annual Review of Earth and Planetary Sciences* 23: 287–336.

Rudge JF, Kleine T, and Bourdon B (2010) Broad bounds on Earth's accretion and core formation constrained by geochemical models. *Nature Geoscience* 3: 439–443.

Rushmer T, Minarik WG, and Taylor GJ (2000) Physical processes of core formation. In: Canup RM and Righter K (eds.) *Origin of the Earth and Moon*, pp. 227–244. Tucson: University of Arizona Press.

Rushmer T, Petford N, Humayun M, and Campbell AJ (2005) Fe-liquid segregation in deforming planetesimals: Coupling core-forming compositions with transport phenomena. *Earth and Planetary Science Letters* 239: 185–202.

Russell CT and Luhmann JG (1997) Mercury: Magnetic field and magnetosphere. In: Shirley JH and Fairbridge RW (eds.) *Encyclopedia of Planetary Sciences*, pp. 476–478. New York: Chapman and Hall.

Safronov VS (1978) The heating of the Earth during its formation. *Icarus* 33: 1–12.

Sakai T, Kanto T, Ohtani E, et al. (2006) Interaction between iron and post-perovskite at core–mantle boundary and core signature in plume source region. *Geophysical Research Letters* 33: L15317. http://dx.doi.org/10.1029/2006GL026868.

Samuel H (2012) A re-evaluation of metal diapir breakup and equilibration in terrestrial magma oceans. *Earth and Planetary Science Letters* 313–314: 105–114.

Samuel H, Tackley PJ, and Evonuk M (2010) Heat partitioning in terrestrial planets during core formation by negative diapirism. *Earth and Planetary Science Letters* 290: 13–19.

Sanloup C, van Westrenen W, Dasgupta R, Maynard-Casely H, and Perrillat J-P (2011) Compressibility change in iron-rich melt and implications for core formation models. *Earth and Planetary Science Letters* 306: 118–121.

Scherstén A, Elliott T, Hawkesworth C, Russell S, and Massarik J (2006) Hf–W evidence for rapid differentiation of iron meteorite parent bodies. *Earth and Planetary Science Letters* 241: 530–542.

Schmickler B, Liebske C, Holzapfel C, and Rubie DC (2005) Viscosity of peridotite liquid up to 24 GPa: Predictions from self-diffusion coefficients. *Fall Meeting Suppl., Abstr. MR11A-06*, *EOS Transactions American Geophysical Union* 86(52).

Schönbächler M, Carlson RW, Horan MF, Mock TD, and Hauri EH (2010) Heterogeneous accretion and the moderately volatile element budget of the Earth. *Science* 328: 884–887.

Schramm DN, Tera F, and Wasserburg GJ (1970) The isotopic abundance of ^{26}Mg and limits on ^{26}Al in the early solar system. *Earth and Planetary Science Letters* 10: 44–59.

Schubert G, Anderson JD, Spohn T, and McKinnon WB (2004) Interior composition, structure and dynamics of the Galilean satellites. In: Bagenal F, Dowling T, and McKinnon WB (eds.) *Jupiter: The Planet, Satellites and Magnetosphere*, pp. 281–306. Cambridge: Cambridge University Press.

Shannon MC and Agee CB (1996) High pressure constraints on percolative core formation. *Geophysical Research Letters* 23: 2717–2720.

Shannon MC and Agee CB (1998) Percolation of core melts at lower mantle conditions. *Science* 280: 1059–1061.

Siebert J, Badro J, Antonangeli D, and Ryerson FJ (2012) Metal–silicate partitioning of Ni and Co in a deep magma ocean. *Earth and Planetary Science Letters* 321–322: 189–197.

Siebert J, Badro J, Antonangeli D, and Ryerson FJ (2013) Terrestrial accretion under oxidizing conditions. *Science* 339: 1194–1197.

Siebert J, Corgne A, and Ryerson FJ (2011) Systematics of metal–silicate partitioning for many siderophile elements applied to Earth's core formation. *Geochimica et Cosmochimica Acta* 75: 1451–1489.

Snow JE and Schmidt G (1998) Constraints on Earth accretion deduced from noble metals in the oceanic mantle. *Nature* 391: 166–169.

Solomatov VS (2000) Fluid dynamics of a terrestrial magma ocean. In: Canup RM and Righter K (eds.) *Origin of the Earth and Moon*, pp. 323–338. Tucson: University of Arizona Press.

Solomon S (1979) Formation, history and energetics of cores in the terrestrial planets. *Physics of the Earth and Planetary Interiors* 19: 168–182.

Spohn T and Schubert G (1991) Thermal equilibration of the Earth following a giant impact. *Geophysical Journal International* 107: 163–170.

Stevenson DJ (1981) Models of the Earth's core. *Science* 214: 611–619.

Stevenson DJ (1989) Formation and early evolution of the Earth. In: Peltier WR (ed.) *Mantle Convection Plate Tectonics and Global Dynamics*. New York: Gordon and Breach.

Stevenson DJ (1990) Fluid dynamics of core formation. In: Newsom HE and Jones JH (eds.) *Origin of the Earth*. Oxford: Oxford University Press.

Stevenson DJ (2003) Mission to the Earth's core—A modest proposal. *Nature* 423: 239–240.

Stixrude L and Karki B (2005) Structure and freezing of $MgSiO_3$ liquid in Earth's lower mantle. *Science* 310: 297–299.

Tachibana S, Huss GR, Kita NT, Shimoda G, and Morishita Y (2006) Fe-60 in chondrites: Debris from a nearby supernova in the early solar system? *Astrophysical Journal* 639: L87–L90.

Takafuji N, Hirose K, Mitome M, and Bando Y (2005) Solubilities of O and Si in liquid iron in equilibrium with $(Mg,Fe)SiO_3$ perovskite and the light elements in the core. *Geophysical Research Letters* 32: L06313. http://dx.doi.org/10.1029/2005GL022773.

Takafuji N, Hirose K, Ono S, Xu F, Mitome M, and Bando Y (2004) Segregation of core melts by permeable flow in the lower mantle. *Earth and Planetary Science Letters* 224: 249–257.

Tang H and Dauphas N (2012) Abundance, distribution, and origin of 60Fe in the solar protoplanetary disk. *Earth and Planetary Science Letters* 359–360: 248–263.

Tarduno JA, Cottrell RD, Nimmo F, et al. (2012) Evidence for a dynamo in the main group pallasite parent body. *Science* 338: 93–95.

Taylor SR and Norman MD (1990) Accretion of differentiated planetesimals to the Earth. In: Newsom HE and Jones JH (eds.) *Origin of the Earth*, pp. 29–43. New York: Oxford University Press.

Terasaki H, Frost DJ, Rubie DC, and Langenhorst F (2005) The effect of oxygen and sulphur on the dihedral angle between Fe–O–S melt and silicate minerals at high pressure: Implications for Martian core formation. *Earth and Planetary Science Letters* 232: 379–392. http://dx.doi.org/10.1016/j.epsl.2005.01.030.

Terasaki H, Frost DJ, Rubie DC, and Langenhorst F (2007) The interconnectivity of Fe–O–S liquid in polycrystalline silicate perovskite at lower mantle conditions. *Physics of the Earth and Planetary Interiors* 161: 170–176.

Terasaki H, Frost DJ, Rubie DC, and Langenhorst F (2008) Percolative core formation in planetesimals. *Earth and Planetary Science Letters* 273: 132–137.

Terasaki H, Urakawa S, Funakoshi K, et al. (2009) In situ measurement of interfacial tension of Fe–S and Fe–P liquids under high pressure using X-ray radiography and tomography techniques. *Physics of the Earth and Planetary Interiors* 174: 220–226.

Terasaki H, Urakawa S, Rubie DC, et al. (2012) Interfacial tension of Fe–Si liquid at high pressure: Implications for liquid Fe-alloy droplet size in magma oceans. *Physics of the Earth and Planetary Interiors* 174: 220–226.

Thibault Y and Walter MJ (1995) The influence of pressure and temperature on the metal–silicate partition coefficients of nickel and cobalt in a model C1 chondrite and implications for metal segregation in a deep magma ocean. *Geochimica et Cosmochimica Acta* 59: 991–1002.

Thomas PC, Parker JW, McFadden LA, et al. (2005) Differentiation of the asteroid Ceres as revealed by its shape. *Nature* 437: 224–226.

Thomson W and Tait PG (1883) *Treatise on Natural Philosophy*. Cambridge: Cambridge University Press, p. 527.

Tonks WB and Melosh HJ (1992) Core formation by giant impacts. *Icarus* 100: 326–346.

Tonks WB and Melosh HJ (1993) Magma ocean formation due to giant impacts. *Journal of Geophysical Research* 98: 5319–5333.

Touboul M, Kleine T, Bourdon B, Palme H, and Wieler R (2007) Late formation and prolonged differentiation of the Moon inferred from W isotopes in lunar metals. *Nature* 450: 1206–1209.

Treiman AH, Jones JH, and Drake MJ (1987) Core formation in the Shergottite parent body and comparison with the Earth. *Journal of Geophysical Research* 92: E627–E632.

Tschauner O, Zerr A, Specht S, Rocholl A, Boehler R, and Palme H (1999) Partitioning of nickel and cobalt between silicate perovskite and metal at pressures up to 80 GPa. *Nature* 398: 604–607. http://dx.doi.org/10.1038/19287.

Tsuno K, Frost DJ, and Rubie DC (2013) Simultaneous partitioning of silicon and oxygen into the Earth's core during early Earth differentiation. *Geophysical Research Letters* 40: 66–71.

Tucker JM and Mukhopadhyay S (2014) Evidence for multiple magma ocean outgassing and atmospheric loss episodes from mantle noble gases. *Earth and Planetary Science Letters* 393: 254–265.

Tuff J, Wood BJ, and Wade J (2011) The effect of Si on metal–silicate partitioning of siderophile elements and implications for the conditions of core formation. *Geochimica et Cosmochimica Acta* 75: 673–690.

Turan JW (1984) Nucleosynthesis. *Annual Review of Nuclear and Particle Science* 34: 53–97.

Turcotte DL and Schubert G (2002) *Geodynamics*. Cambridge: Cambridge University Press.

Urey HC (1952) *The Planets: Their Origin and Development*, p. 245. New Haven: Yale University Press.

von Bargen N and Waff HS (1986) Permeabilities, interfacial areas and curvatures of partially molten systems: Results of numerical computations of equilibrium microstructures. *Journal of Geophysical Research* 91: 9261–9276.

Wade J and Wood BJ (2005) Core formation and the oxidation state of the Earth. *Earth and Planetary Science Letters* 236: 78–95.

Wade J, Wood BJ, and Tuff J (2012) Metal–silicate partitioning of Mo and W at high pressures and temperatures: Evidence for late accretion of sulphur to the Earth. *Geochimica et Cosmochimica Acta* 85: 58–74.

Wagner C (1962) *Thermodynamics of Alloys*. Reading, MA: Addison-Wesley.

Walker D (2000) Core participation in mantle geochemistry: Geochemical Society Ingerson Lecture. *Geochimica et Cosmochimica Acta* 64: 2897–2911.

Walker D (2005) Core–mantle chemical issues. *Canadian Mineralogist* 43: 1553–1564.

Walker RJ (2009) Highly siderophile elements in the Earth, Moon and Mars: Update and implications for planetary accretion and differentiation. *Chemie der Erde-Geochemistry* 69: 101–125.

Walker D, Norby L, and Jones JH (1993) Superheating effects on metal–silicate partitioning of siderophile elements. *Science* 262: 1858–1861.

Walsh KJ, Morbidelli A, Raymond SN, O'Brien DP, and Mandell AM (2011) A low mass for Mars from Jupiter's early gas-driven migration. *Nature* 475: 206–209.

Walte NP, Becker JK, Bons PD, Rubie DC, and Frost DJ (2007) Liquid distribution and attainment of textural equilibrium in a partially-molten crystalline system with a high-dihedral-angle liquid phase. *Earth and Planetary Science Letters* 262: 517–532.

Walte NP, Rubie DC, Bons PD, and Frost DJ (2011) Deformation of a crystalline aggregate with a small percentage of high-dihedral-angle liquid: Implications for

core–mantle differentiation during planetary formation. *Earth and Planetary Science Letters* 305: 124–134.
Walter MJ, Newsom HE, Ertel W, and Holzheid A (2000) Siderophile elements in the Earth and Moon: Metal/silicate partitioning and implications for core formation. In: Canup RM and Righter K (eds.) *Origin of the Earth and Moon*, pp. 265–290. Tucson: University of Arizona Press.
Walter MJ and Thibault Y (1995) Partitioning of tungsten and molybdenum between metallic liquid and silicate melt. *Science* 270: 1186–1189.
Walter MJ and Tronnes RG (2004) Early Earth differentiation. *Earth and Planetary Science Letters* 225: 253–269.
Wänke H (1981) Constitution of terrestrial planets. *Philosophical Transactions of the Royal Society* 303: 287–302.
Warren PH (1985) The magma ocean concept and lunar evolution. *Annual Review of Earth and Planetary Sciences* 13: 201–240.
Warren PH (1993) A concise compilation of petrologic information on possible pristine nonmare Moon rocks. *American Mineralogist* 78: 360–376.
Warren PH, Kallemeyn GW, and Kyte FT (1999) Origin of planetary cores: Evidence from highly siderophile elements in Martian meteorites. *Geochimica et Cosmochimica Acta* 63: 2105–2122.
Wasson JT (1985) *Meteorites: Their Record of Early Solar-System History*, p. 267. New York: W.H. Freeman.
Weber RC, Lin PY, Garnero EJ, Williams Q, and Lognonne P (2011) Seismic detection of the lunar core. *Science* 331: 309–312.
Weidenschilling SJ, Spaute D, Davis DR, Marzari F, and Ohtsuki K (1997) Accretional evolution of a planetesimal swarm. 2. The terrestrial zone. *Icarus* 128: 429–455.
Wetherill GW (1985) Occurrence of giant impacts during the growth of the terrestrial planets. *Science* 228: 877–879.
Wetherill GW and Stewart GR (1993) Formation of planetary embryos – Effects of fragmentation, low relative velocity, and independent variation of eccentricity and inclination. *Icarus* 106: 190–209.
Williams Q and Hemley RJ (2001) Hydrogen in the deep Earth. *Annual Review of Earth and Planetary Sciences* 29: 365418.
Wood BJ and Halliday AN (2005) Cooling of the Earth and core formation after the giant impact. *Nature* 437: 1345–1348.
Wood BJ and Halliday AN (2010) The lead isotopic age of the Earth can be explained by core formation alone. *Nature* 465: 767–770.
Wood BJ, Walter MJ, and Wade J (2006) Accretion of the Earth and segregation of its core. *Nature* 441: 825–833. http://dx.doi.org/10.1038/nature04763.
Yoder CF (1995) Astrometric and geodetic properties of Earth and the solar system. In: Ahrens TJ (ed.) *Global Earth Physics*, pp. 1–31. Washington, DC: American Geophysical Union.
Yoshino T, Price JD, Wark DA, and Watson EB (2006) Effect of faceting on pore geometry in texturally equilibrated rocks: Implications for low permeability at low porosity. *Contributions to Mineralogy and Petrology* 152: 169–186. http://dx.doi.org/10.1007/s00410-006-0099-y.
Yoshino T, Walter MJ, and Katsura T (2003) Core formation in planetesimals triggered by permeable flow. *Nature* 422: 154–157.
Young GA (1965) *The Physics of the Base Surge*. White Oak, MD: U.S. Naval Ordnance Laboratory. http://www.nature.com/nature/journal/v259/n5540/abs/259190a0.html.
Ziegler K, Young ED, Schauble EA, and Wasson JT (2010) Metal–silicate silicon isotope fractionation in enstatite meteorites and constraints on Earth's core formation. *Earth and Planetary Science Letters* 295: 487–496.